



ACADEMIC STUDIES IN SCIENCE AND MATHEMATICS - II

Editor :
PROF. DR. HASAN AKGÜL

İmtiyaz Sahibi / Publisher • Yaşar Hız
Genel Yayın Yönetmeni / Editor in Chief • Eda Altunel
Editör / Editor • Prof. Dr. Hasan Akgül
Kapak & İç Tasarım / Cover & Interior Design • Karaf Ajans

Birinci Basım / First Edition • © Haziran 2020

ISBN • 978-625-7884-61-7

© copyright

Bu kitabın yayın hakkı Gece Kitaplığı'na aittir.
Kaynak gösterilmeden alıntı yapılamaz, izin
almadan hiçbir yolla çoğaltılamaz.

The right to publish this book belongs to Gece Kitaplığı.
Citation can not be shown without the source, reproduced in any way
without permission.

Gece Kitaplığı / Gece Publishing
Türkiye Adres / Turkey Address: Kızılay Mah. Fevzi Çakmak 1. Sokak
Ümit Apt. No: 22/A Çankaya / Ankara / TR
Telefon / Phone: +90 312 384 80 40
web: www.gecekitapligi.com
e-mail: gecekitapligi@gmail.com



Baskı & Cilt / Printing & Volume

Sertifika / Certificate No: 47083

Academic Studies in Science and Mathematics - II

Editor

Prof. Dr. Hasan Akgül

TABLE OF CONTENTS

Chapter 1

ON ISATIN THIOSEMICARBAZONES, THEIR DERIVATIVES, AND COMPLEX FORMATION

Barbaros AKKURT 1

Chapter 2

METHODS FOR DEVELOPING SOFT SET STRUCTURES IN SOFT DITOPOLOGICAL SPACES

Güzide ŞENEL..... 21

Chapter 3

N-ENGEL LEİBNİZ ALGEBRAS

Nil MANSUROĞLU 29

Chapter 4

C SEGMENT AUTOMOBILE SELECTION BY USING ELECTRE METHOD

Nuray GIRGINER, Lokman DAL..... 37

Chapter 5

PROPERTIES AND HEALTH BENEFITS OF PROBIOTIC AND PREBIOTIC KEFIR

Songul CETİK YILDIZ 59

Chapter 6

EFFECT OF DIFFERENT PRE-TREATMENTS ON SEED GERMINATION OF SALVIA FRUTICOSA MILL., SATUREJA THYMBRA L. AND THYMBRA SPICATA L.

Ummahan ÖZ..... 69

Chapter 7

THE RECENT ELECTROCHROMIC STUDIES BASED ON NICKEL OXIDE-CONDUCTING POLYMER HYBRID MATERIALS

Esin EREN 101

Chapter 8

ANALYSIS OF SELF-ASSEMBLED MULTILAYERS: MONITORING AND CHARACTERIZATION

Nejla CINI..... 121

Chapter 9

WHAT PURPOSE DO THE GREAT MATHEMATICAL PROBLEMS
SERVE?

Güzide ŞENEL..... 141



ON ISATIN THIOSEMICARBAZONES, THEIR DERIVATIVES, AND COMPLEX FORMATION

Barbaros AKKURT¹

¹ PhD, Istanbul Technical University, Faculty of Science and Letters, Department of Chemistry,
akkurtb@itu.edu.tr

INTRODUCTION

Isatin is a biologically active indole derivative, with a ketone group at 3-position. Ketones and aldehydes can react with amines, hydrazines, and (thio)semicarbazide to yield Schiff's bases, hydrazones, and (thio)semicarbazones respectively, frequently with high yields with the elimination of at least one molecule of water. The resulting molecule most probably has high biological activity, and we have covered some examples for them. As an additional reaction, these compounds react with metal salts, like Cu(II), Zn(II), and ClFe(III), and some of these structures present biological activity, too. In this treatise, we introduce the readers to the biological activity of isatin thiosemicarbazones, substituted at various positions (N1, N3, and N4) with literature coverage.

LITERATURE REVIEW

In work by Ali *et al.* (2014), they prepared six novel copper(II) complexes from the N-phenylthiosemicarbazone of isatin (See **Figure 1**). Along with standard methods of characterization, they have grown single crystals of Cu-2 and Cu-3 complexes and studied with XRD. Calf thymus DNA (ct-DNA) interaction showed that the high intercalative binding constant, in the range of 0.16 to $1.46 \times 10^6 \text{ M}^{-1}$, indicates the intercalative ability of the complexes. Electrophoretic studies of the five complexes revealed that Cu-1 and Cu-2 behaved as oxidative DNA-cleaving agents, whereas the others are oxidative and hydrolytic DNA cleaving agents. The possible anti-cancer potential of the complexes against human colorectal carcinoma cell line is available from the *in vitro* antiproliferative study (Ali *et al.*, 2014).

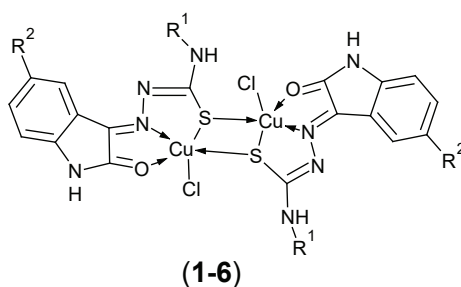
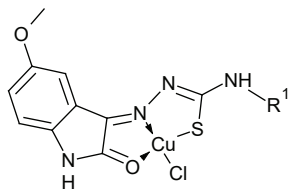


Figure 1: The structures of the complexes (1-6). 5-H (1), 5-CH₃ (2), 5-F (3), 5-NO₂ (4), N-Me-5-CH₃ (5), and N-Et-5-CH₃ (6).

Aneesrahman and co-workers showed three novel 5-methoxyisatin thiosemicarbazone molecules and their copper(II) complexes, and their spectral characterization revealed that the ligands bind to the copper(II) ion via an ONS donor set in a square planar fashion (see **Figure 2**). The researchers also reported single-crystalline X-ray diffraction studies. The

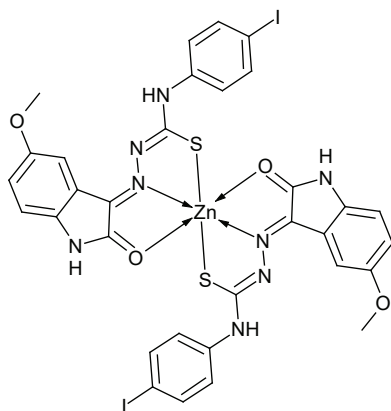
complexes were able to interact with BSA/DNA with an excellent binding constant. The researchers studied the complexes in antimicrobial activity, radical scavenging activity, and antiproliferative activity, and the results were reported (Aneesrahman *et al.*, 2019).



(7-9)

Figure 2: The structure of 5-methoxyisatin thiosemicarbazone-copper(II) complex. The R groups are pyrrolidin-1-yl (7), morpholin-1-yl (8), and cyclohexanamin-1-yl (9).

Bakır and co-workers studied linoleic acid peroxidation in the presence of copper(II) ions only or butylated hydroxytoluene (BHT), gallic acid, and BHT/GA pair. They also added 5-methoxyisatin-3-(4-chlorophenyl) thiosemicarbazone or 5-methoxyisatin-3-(4-phenyl)thiosemicarbazone into the medium. They aerated or incubated the medium at physiological conditions. DPPH (1,1-diphenylpicrylhydrazyl) radical scavenging method yielded IC_{50} values like 69.60 μ M (BHT), 11.87 μ M (GA), 88.71 μ M (isatin-3-chlorophenyl thiosemicarbazone), 73.62 μ M (isatin-3-phenyl thiosemicarbazone), and 430.11 μ M bis(isatin-3-(4-iodophenyl) thiosemicarbazonato)zinc(II) (see **Figure 3**). They also applied detailed computational methods to obtain valuable data (Bakır *et al.*, 2018).



(10)

Figure 3: A representation of zinc(II) chelate of isatin N-(4-iodophenyl)thiosemicarbazone.

Using N-substituted isatin derivatives with nickel(II) ions, a group of researchers synthesized a total of eight complexes in which three of them are novel; they included the others for comparison. Complex **11** bis(1-allylisatin-3-phenylthiosemicarbazonato)nickel(II) (see **Figure 4**) showed impressive results against human cancer lines (acute monocytic leukemia MOLM-14, histiocytic lymphoma U937, and myeloma IM-9). The complex also enhanced the apoptotic cell line and induced the cell cycle arrest at the G1 phase. This complex was not toxic to the Vero cell line (IC_{50} higher than 300 μ M). They also studied the concentration-dependent cleavage of supercoiled (SC) DNA by complex **11** to the corresponding nicked circular (NC) form (Balachandran *et al.*, 2018).

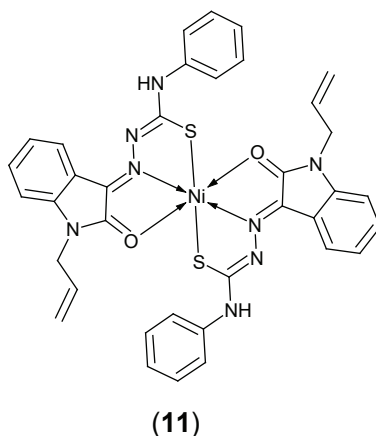


Figure 4: The molecular structure of complex 11.

Casas *et al.* reacted dimethylthallium(III) acetate and isatin-3-thiosemicarbazone to give a monomeric complex. Upon recrystallization from dimethylsulfoxide, the complex dimerizes to $[TlMe_2(isaTSC)DMSO]_2$ (**12**) (see **Figure 5**). The dimeric structure has a weak bonding, and the geometry was distorted pentagonal bipyramidal (Casas *et al.*, 2000).

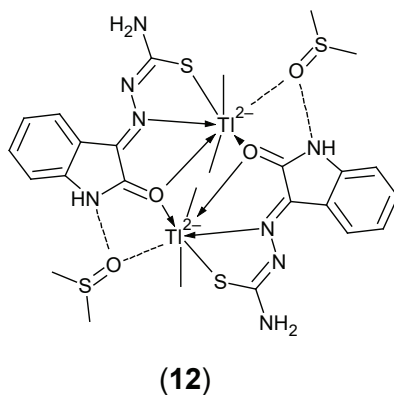
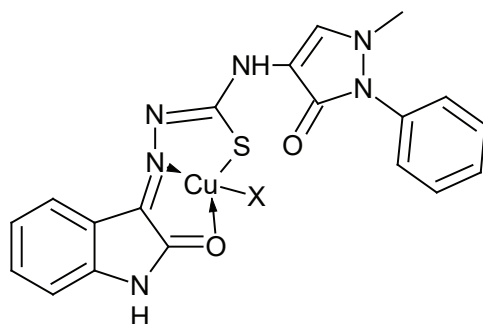


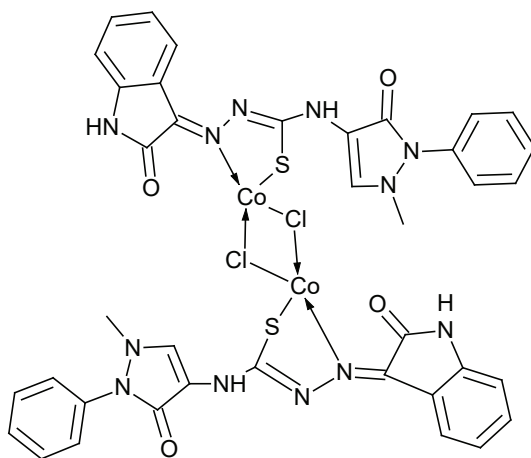
Figure 5: The structure of the complex 12.

In a research conducted by El-Saied and co-workers, they condensed isatin and 4-aminoantipyrine thiosemicarbazone to give a ligand and prepared its corresponding Cu(II) (**13-17**; see **Figure 6**), Co(II) (see **Figures 7 (18)** and **8 (19)**), Ni(II) (**(20)**, see **Figure 9**), Zn(II) (**(21)**, see Figure 10), and Fe(III) complexes (**(22)**, see Figure 11). They tested the ligand and several complexes against solid tumors. The research group has concluded that complex **20** extraordinarily reduced the volume of the tumor, inhibited the expression of vascular endothelial growth factor (VEGF), and induced the expression of cysteine aspartyl specific protease-7 (caspase-7). The AST, ALT, albumin, and glucose levels restored to their typical values. They report that the complexes are potent anti-cancer agents against solid tumors induced by EAC cells (El-Saied *et al.*, 2019).



X = Cl, 13; Br, 14; NO₃, 15; OAc, 16; ClO₄, 17

Figure 6: Structures of complexes (13-17).



(18)

Figure 7: The structure of complex (18).

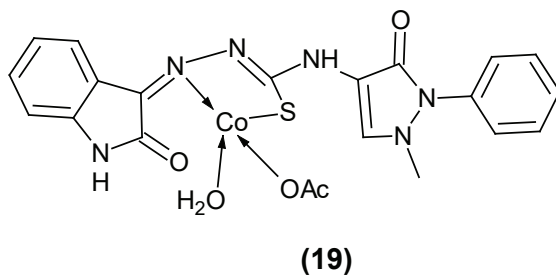


Figure 8: The structure of complex (19).

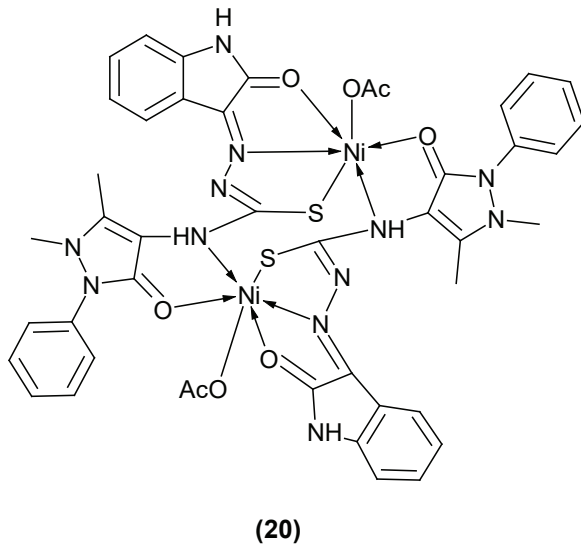


Figure 9: The structure of the Ni complex (20).

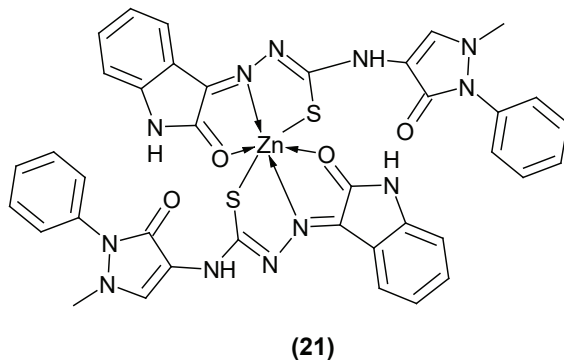


Figure 10: Structure of the Zn complex (21).

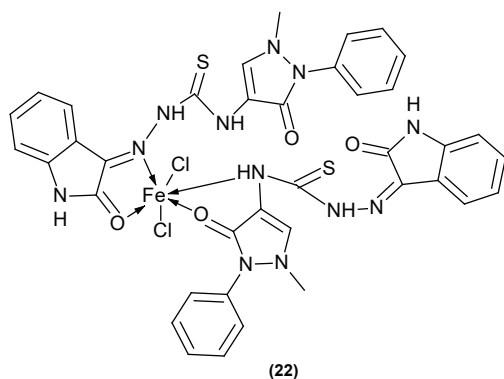


Figure 11: Structure of the Fe complex (22).

El-Sawaf and his co-workers described a new, N4-morpholinylthiosemicarbazone of isatin. This ligand in the HL form formed Co(II), Cu(II), and Pd(II) complexes in a $[M(L)X]$ fashion, where X is chloride, bromide, and acetate (23). With Zn(II) ion, the complex uses a neutral bidentate NS donor set (24). $NiCl_2$ yielded an octahedral complex with the ligand's ONS donors ((25), see Figure 12). All complexes resulted in higher biological activities than the parent ligand. The researchers conclude that the copper bromide complex acted as a superior antimicrobial agent than the other complexes and the ligand (El-Sawaf *et al.*, 2018).

A review investigates recent advances on isatin-azole, isatin-quinoline/quinolone, isatin-furan/coumarin, isatin hydrazone/(thio)semicarbazone, isatin dimers, and isatin-indole hybrids to be potential anti-bacterial agents (see Figures 13-18). SAR studies provide broad-spectrum, high potency, low toxicity, and multiple mechanisms of action (Guo, 2019).

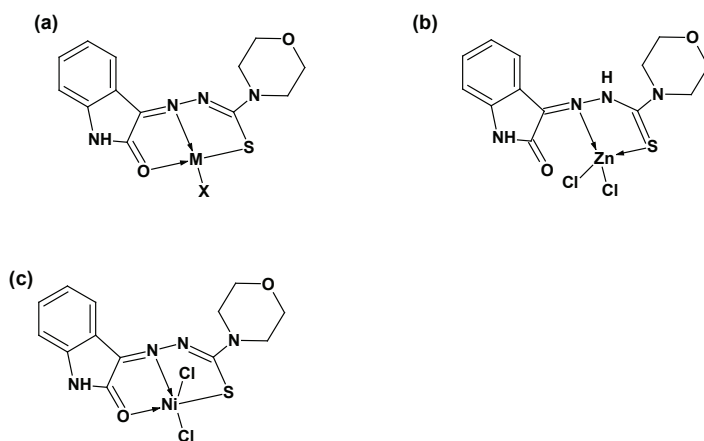
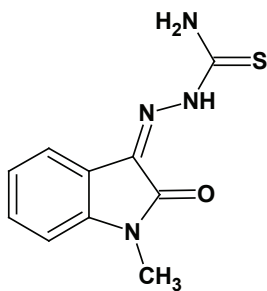
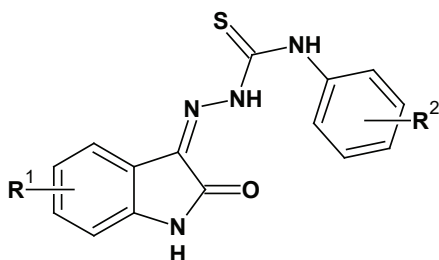


Figure 12: Metal complexes with ONS donor set, (a) $M = Co(II), Cu(II), Pd(II)$, $X = Cl, Br, OAc, ClO_4$ (23). (b) The structure of the zinc(II) complex; the ligand behaves as an NS donor (24). (c) The structure of the nickel(II) complex (25).



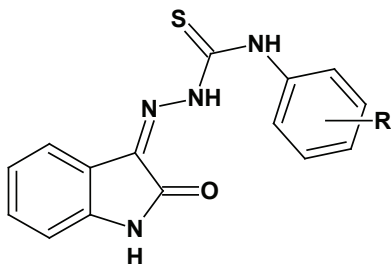
(26)

Figure 13: Methisazone, a well-known drug (26).



(27)

Figure 14: 28 compounds fit in this generic structure (27).



(28)

Figure 15: The authors reviewed 15 compounds with compound (28).

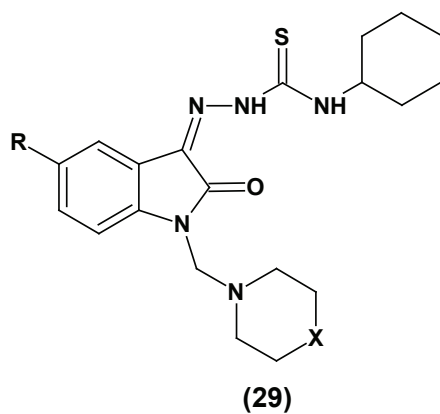


Figure 16: Compound family (29). 7 compounds fit into this generic formula.

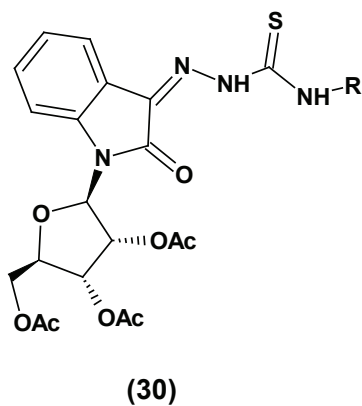


Figure 17: Three compounds fit this generic compound formula (30).

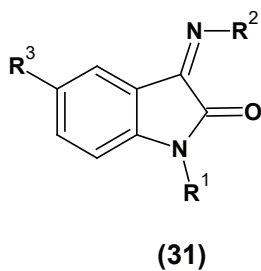


Figure 18: Generic formula (31). For R_1 , there are two, for R_2 , there are seven, and for R_3 , there are five possibilities.

A group of isatin thiosemicarbazones are considered for tuberculosis treatment (Jiang *et al.*, 2018; see **Figures 19-22**).

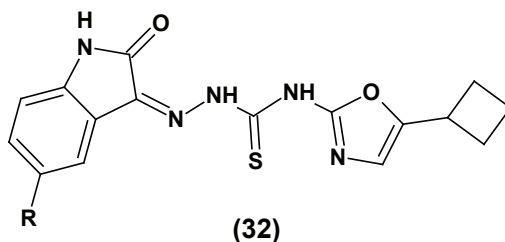


Figure 19: Some isatin thiosemicarbazones for tuberculosis treatment; for (32), $R = H$ or F .

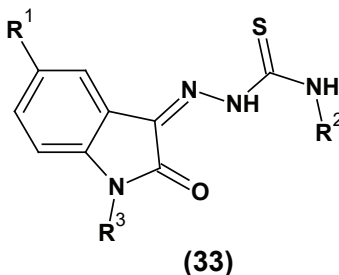


Figure 20: Compound (33); $R^1 = Me, OCF_3$, $R^2 =$ allyl, H , methyl, ethyl, butyl, benzyl, cyclohexyl, substituted phenyl; $R^3 = H$, methyl, methylmorpholinyl.

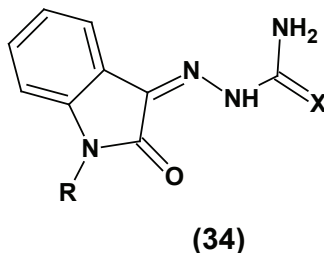


Figure 21: Generic structure depicted as (34). $X = S$, $R = H$; $X = S$, $R = OAc$.

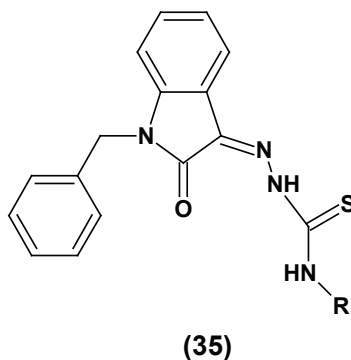
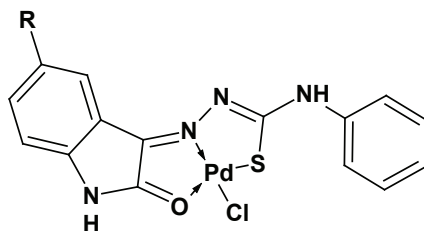


Figure 22: $R = H$; $R = Me$; $R = Et$; $R =$ phenyl; $R =$ cyclohexyl.

Munikumari and co-workers have prepared the N-phenylthiosemicarbazones of substituted isatin derivatives (see **Figure 23**) and investigated

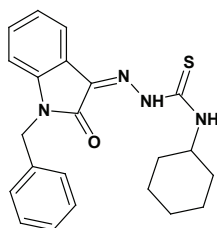
their antimicrobial (R=bromo and chloro), anti-fungal (R=bromo), antioxidant (R=nitro) activities. The nitro-substituted complex was highly active against HeLa cells with the standard compound (Munikumari *et al.*, 2019).



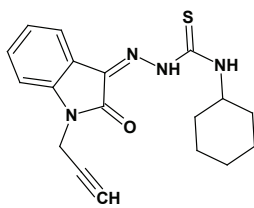
(36)

Figure 23: Palladium(II) complex of N4-phenyl-substituted isatin-3-thiosemicarbazone (36). R is chloro, bromo, or nitro.

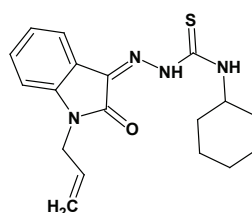
Muralisankar and co-workers have prepared a thiosemicarbazone from hexyl isothiocyanate and hydrazine, then synthesized the copper complexes with two different structures (mononuclear and dinuclear) according to the radical bound to the N1 position of isatin (see **Figures 24-25**). They investigated the binding affinity against calf thymus DNA (ct-DNA) and bovine serum albumin (BSA) with ultraviolet-visible and fluorescent spectrophotometry. Cu complexes showed an intercalative mode of DNA binding. All complexes provided pUC19 plasmid DNA cleavage without an external agent. 1-Benzylisatin-derived thiosemicarbazone showed good activity against human breast cancer (MCF7) and lung cancer (A549) cell lines (Muralisankar *et al.*, 2016).



(37)



(38)



(39)

Figure 24: The structures of the thiosemicarbazones (37-39).

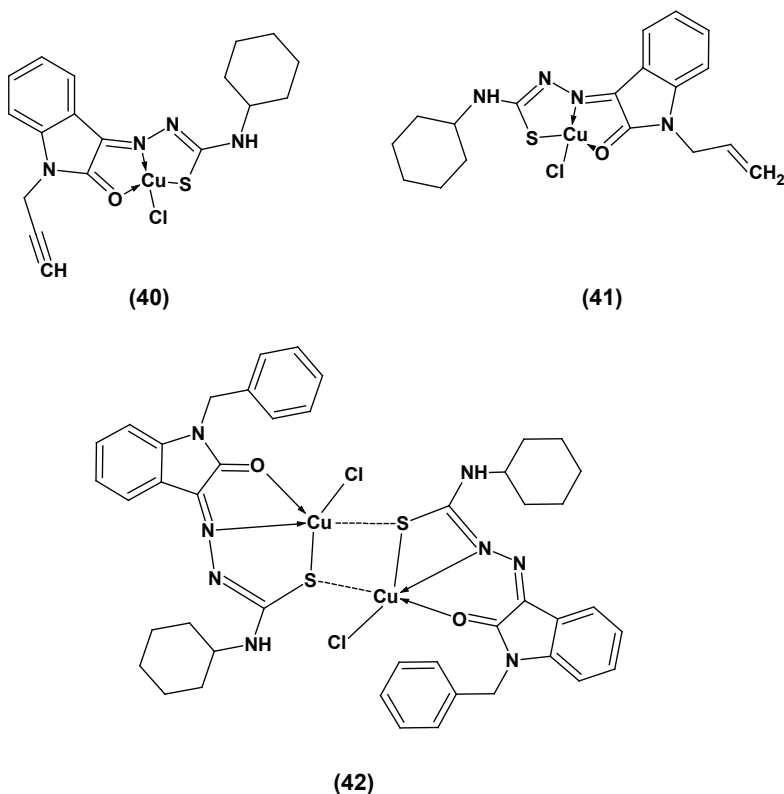


Figure 25: The structures of copper complexes from (37-39).

Pati and co-workers studied multifunctional isatin derivatives, especially substituted at N1 position and some methyl substitution at N4 position (see **Figure 26**). They researched the anti-cancer activity for pancreatic tumor lines (Pati *et al.*, 2018).

Saranya and co-workers prepared ten isatin thiosemicarbazone compounds (47-56) and characterized them with well-known techniques (see **Figure 27**). They then investigated *in vitro* antioxidant behavior and cytotoxicity against MCF-7 (breast cancer cell line), and according to the results, four compounds showed significant antioxidant behavior, and one compound exhibited higher cytotoxicity than the others. With *in vitro* PLA2 inhibition assay and *in silico* molecular docking study, they found anti-inflammatory activity, and all compounds showed promising results (Saranya *et al.*, 2019).

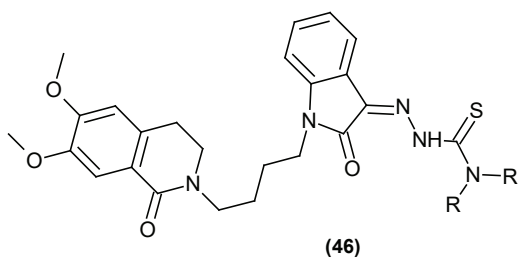
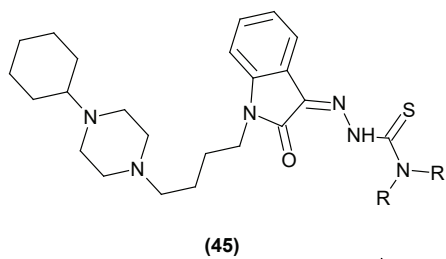
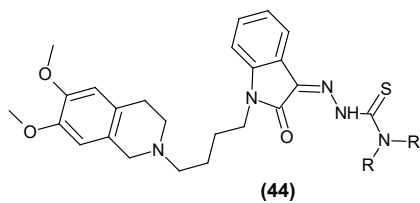
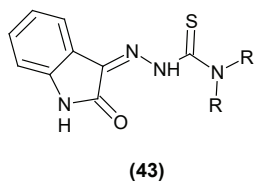


Figure 26: Multifunctional isatin thiosemicarbazones (43-46).

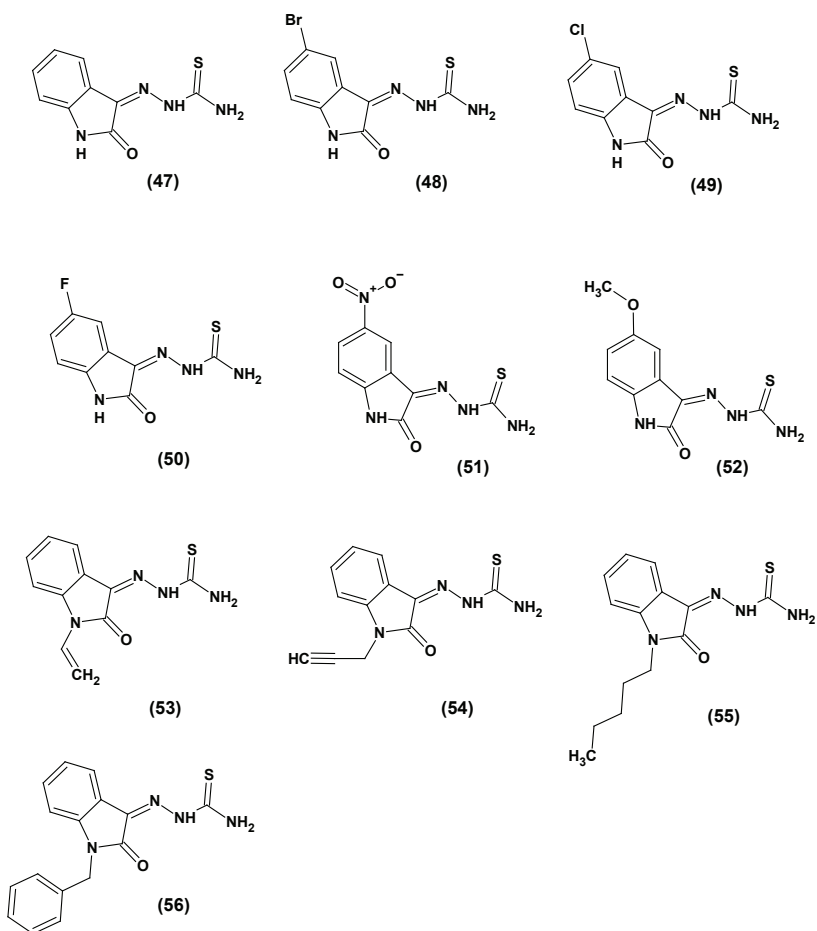


Figure 27: Compound numbers and substitution patterns. (47): Isatin-3-thiosemicarbazone, (48): 5-Bromoisatin-3-thiosemicarbazone, (49): 5-Chloroisatin-3-thiosemicarbazone, (50): 5-Fluoroisatin-3-thiosemicarbazone, (51): 5-Nitroisatin-3-thiosemicarbazone, (52): 5-Methoxyisatin-3-thiosemicarbazone, (53): 1-Vinylisatin-3-thiosemicarbazone, (54): 1-Propargylisatin-3-thiosemicarbazone, (55): 1-Pentylisatin-3-thiosemicarbazone, (56): 1-Benzylisatin-3-thiosemicarbazone.

A Serbian group of investigators has examined the effect of isatin-3-thiosemicarbazone and its Mn(II), Fe(II), Ni(II), and Zn(II) complexes (see **Figure 28**) showed good results in the production of antibiotics. Ni(II), Fe(II), and Mn(II) complexes were octahedral, whereas Zn(II) complex was tetrahedral. Iron(II) complex was the most successful one, having the highest Hexaene H-85 and Azalomycine B concentrations 306 $\mu\text{g cm}^{-3}$ and 127 $\mu\text{g cm}^{-3}$, respectively. The bacterium studied was *Streptomyces hygroscopicus* CH-7, synthesizing the antibiotics (Ilić *et al.*, 2019).

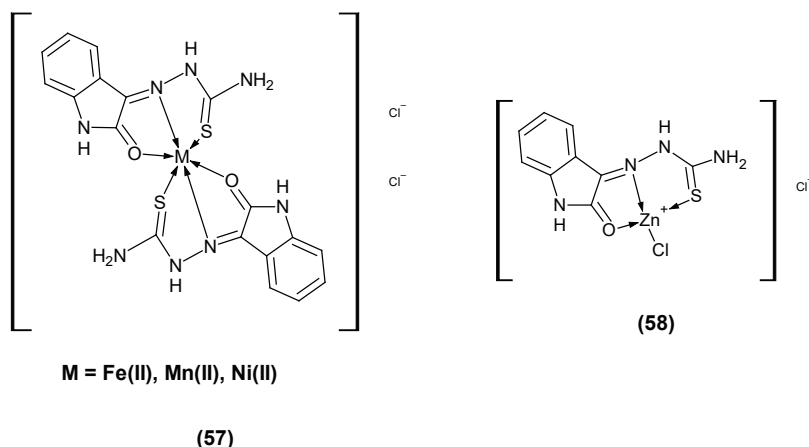


Figure 28: The chemical structures of isatin-3-thiosemicarbazone-metal complexes (57-58).

Khan *et al.* have studied the effect of isatin thiosemicarbazone N4-methyl or ethyl substitution on the nuclearity of copper(I) complexes containing halogen atom and triphenylphosphine as co-ligands (see **Figure 29**). The results showed that the complexes had 1:1:1 stoichiometry of halogen:triphenylphosphine:isatin-3-thiosemicarbazone-N-methyl/ethyl (Khan *et al.*, 2016).

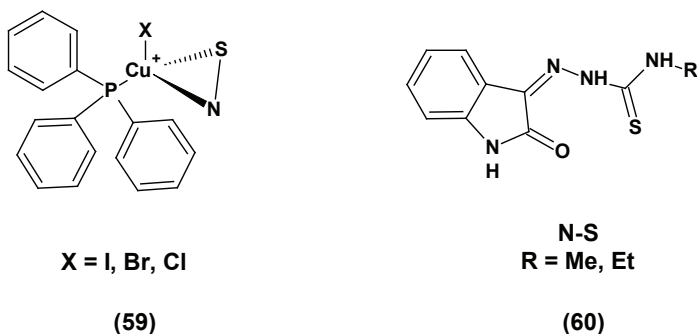


Figure 29: Cu(I) complexes of N4-methyl or ethyl isatin thiosemicarbazone (59-60).

A group of researchers from Russia has synthesized N1-(3,5-bis(tert-butyl)-4-hydroxyphenylmethyl) substituted isatin-3-thiosemicarbazone and prepared complexes with cobalt(II) acetate salt (**Figure 30**) to give an octahedral complex with 1:2 (M:L) stoichiometry (Zvereva *et al.*, 2012).

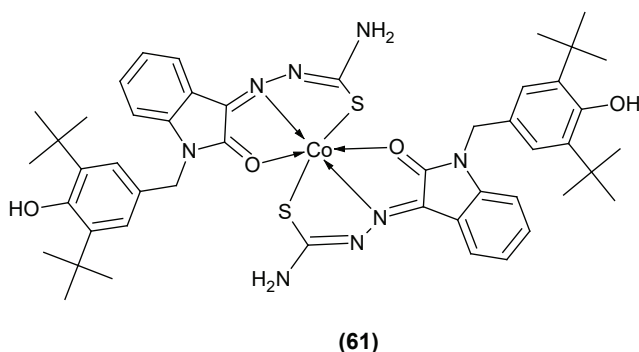


Figure 30: The structure of CoL_2 -type complex (61).

CONCLUSION

It is a fact that isatin thiosemicarbazones, especially when substituted at the N4, N1 of the thiosemicarbazide moiety, and 5-position of the isatin ring, show exceptionally high biological activities. A detailed study with variable substitutions at the positions above might reveal a high activity, yielding anti-bacterial, anti-fungal, anti-inflammatory, and anti-cancer/anti-tumor activities. Metal complexes, on the other hand, might show a surprising amount of activity and might even be better than the parent ligand. Changing the metal ion and, if possible, the oxidation state of it might indicate different and exciting outcomes.

ACKNOWLEDGMENTS

The author is indebted to Prof. Dr. Yasemin DAŞDEMİR and Prof. Dr. Mehmet ALTUN for their fruitful discussions.

BIBLIOGRAPHY

- Ali, A. Q., Teoh, S. G., Eltayeb, N. E., Khadeer Ahamed, M. B., & Abdul Majid, A. M. S. (2014). Synthesis of copper(II) complexes of isatin thiosemicarbazone derivatives: In vitro anti-cancer, DNA binding, and cleavage activities. *Polyhedron*, 74, 6–15. <https://doi.org/10.1016/j.poly.2014.02.025>
- Aneesrahman, K. N., Ramaiah, K., Rohini, G., Stefy, G. P., Bhuvanesh, N. S. P., & Sreekanth, A. (2019). Synthesis and characterisations of copper(II) complexes of 5-methoxyisatin thiosemicarbazones: Effect of N-terminal substitution on DNA/protein binding and biological activities. *Inorganica Chimica Acta*, 492, 131–141. <https://doi.org/10.1016/j.ica.2019.04.019>
- Bakır, T., Sayiner, H. S., & Kandemirli, F. (2018). Experimental and theoretical investigation of antioxidant activity and capacity of

- thiosemicarbazones based on isatin derivatives. *Phosphorus, Sulfur, and Silicon and the Related Elements*, 193(8), 493–499. <https://doi.org/10.1080/10426507.2018.1452232>
- Balachandran, C., Haribabu, J., Jeyalakshmi, K., Bhuvanesh, N. S. P., Karvembu, R., Emi, N., & Awale, S. (2018). Nickel(II) bis(isatin thiosemicarbazone) complexes induced apoptosis through mitochondrial signaling pathway and G0/G1 cell cycle arrest in IM-9 cells. *Journal of Inorganic Biochemistry*, 182, 208–221. <https://doi.org/10.1016/j.jinorgbio.2018.02.014>
- Casas, J., Castellano, E., Garcia Tasende, M., Sánchez, A., & Sordo, J. (2000). Reaction of dimethylthallium(III) acetate and isatin-3-thiosemicarbazone. Crystal and molecular structure of dimethyl(dimethylsulfoxide)(isatin-3-thiosemicarbazonato) thallium(III). *Inorganica Chimica Acta*, 304, 283–287.
- El-Saied, F., El-Aarag, B., Salem, T., Said, G., Khalifa, S., & El-Seedi, H. (2019). Synthesis, Characterization, and In Vivo Anti-Cancer Activity of New Metal Complexes Derived from Isatin-N(4) antipyrinethiosemicarbazone Ligand Against Ehrlich Ascites Carcinoma Cells. *Molecules*, 24(18), 3313. <https://doi.org/10.3390/molecules24183313>
- El-Sawaf, A. K., El-Essawy, F., Nassar, A. A., & El-Samanody, E.-S. A. (2018). Synthesis, spectral, thermal and antimicrobial studies on cobalt(II), nickel(II), copper(II), zinc(II) and palladium(II) complexes containing thiosemicarbazone ligand. *Journal of Molecular Structure*, 1157, 381–394. <https://doi.org/10.1016/j.molstruc.2017.12.075>
- Guo, H. (2019). Isatin derivatives and their anti-bacterial activities. *European Journal of Medicinal Chemistry*, 164, 678–688. <https://doi.org/10.1016/j.ejmech.2018.12.017>
- Ilić, S., Konstantinović, S., Gojgić Cvijović, G., & Veljković, V. (2019). Antibiotic production by *Streptomyces hygroscopicus* CH-7 in medium containing Schiff base complexes. *Hem. Ind.*, 73(2), 93–101.
- Jiang, D., Wang, G.-Q., Liu, X., Zhang, Z., Feng, L.-S., & Liu, M.-L. (2018). Isatin Derivatives with Potential Antitubercular Activities: Isatin Derivatives with Potential Antitubercular Activities. *Journal of Heterocyclic Chemistry*, 55(6), 1263–1279. <https://doi.org/10.1002/jhet.3189>
- Khan, A., Jasinski, J. P., Smoleaski, V. A., Paul, K., Singh, G., & Sharma, R. (2016). Synthesis, structure and cytotoxicity evaluation of complexes of N1-substituted-isatin-3-thiosemicarbazone with copper(I) halides. *Inorganica Chimica Acta*, 449, 119–126. <https://doi.org/10.1016/j.ica.2016.05.013>
- Munikumari, G., Konakanchi, R., Nishtala, V. B., Ramesh, G., Kotha, L. R., Chandrasekhar, K. B., & Ramachandraiah, C. (2019). Palladium(II)

complexes of 5-substituted isatin thiosemicarbazones: Synthesis, spectroscopic characterization, biological evaluation and *in silico* docking studies. *Synthetic Communications*, 49(1), 146–158. <https://doi.org/10.1080/00397911.2018.1546400>

- Muralisankar, M., Sujith, S., Bhuvanesh, N. S. P., & Sreekanth, A. (2016). Synthesis and crystal structure of new monometallic and bimetallic copper(II) complexes with N-substituted isatin thiosemicarbazone ligands: Effects of the complexes on DNA/protein-binding property, DNA cleavage study and *in vitro* anti-cancer activity. *Polyhedron*, 118, 103–117. <https://doi.org/10.1016/j.poly.2016.06.017>
- Pati, M. L., Niso, M., Spitzer, D., Berardi, F., Contino, M., Riganti, C., Hawkins, W. G., & Abate, C. (2018). Multifunctional thiosemicarbazones and deconstructed analogues as a strategy to study the involvement of metal chelation, Sigma-2 (σ_2) receptor and P-gp protein in the cytotoxic action: *In vitro* and *in vivo* activity in pancreatic tumors. *European Journal of Medicinal Chemistry*, 144, 359–371. <https://doi.org/10.1016/j.ejmech.2017.12.024>
- Saranya, S., Haribabu, J., Vadakkedathu Palakkeezhillam, V. N., Jerome, P., Gomathi, K., Rao, K. K., Hara Surendra Babu, V. H., Karvembu, R., & Gayathri, D. (2019). Molecular structures, Hirshfeld analysis and biological investigations of isatin based thiosemicarbazones. *Journal of Molecular Structure*, 1198, 126904. <https://doi.org/10.1016/j.molstruc.2019.126904>
- Zvereva, E. E., Gubaidullin, A. T., Katsyuba, S. A., Vandyukov, A. E., Tagasheva, R. G., Bukharov, S. V., Nugumanova, G. N., & Mukmeneva, N. A. (2012). A cobalt(ii) acetate complex with 1-(3,5-di-tert-butyl-4-hydroxybenzyl)-1H-indole-2,3-dione 3-thiosemicarbazone: Synthesis and structure. *Russian Chemical Bulletin*, 61(10), 1909–1916. <https://doi.org/10.1007/s11172-012-0265-5>



Chapter 2

METHODS FOR DEVELOPING SOFT SET STRUCTURES IN SOFT DITOPOLOGICAL SPACES

Güzide ŞENEL¹

¹ Dr. Öğr. Üyesi, Amasya Üniversitesi, g.senel@amasya.edu.tr

1. Introduction

Textures were introduced as a point-based setting for the study of fuzzy sets. It was proved that textures were an appropriate setting for the development of complement-free mathematical concepts. Within years, authors lay the foundation for a theory of ditopology imposed on textures and introduced ditopological texture. Ditopological texture spaces were introduced by L.M. Brown (Brown & Diker, 1998) as a point-based setting for the study of fuzzy sets. In this study texture spaces characterized which arise in the lattice of intuitionistic sets on a set X and gave some topological results. In (Yıldız & Özçağ, 2013) it is shown that if the complemented discrete ditopological texture space is bi-submaximal, then dcompactness implies strong dcompactness. This result remains an open problem to determine conditions for general ditopological texture spaces. In this work the general information about ditopological space is given based on the study (Yıldız & Özçağ, 2013).

In 1999, Molodtsov introduced soft set theory and showed that the soft set theory can be applied to several areas successfully; for example, the smoothness of functions, game theory, Riemann-integration, Perron-integration, etc. He also showed that soft set theory is free from the parametrization inadequacy syndrome of other theories developed for vagueness (Yuksel et al., 2013). By using the operations of soft sets, the theory of soft topological space determined by Shabir and Naz in 2011 over the initial universe. As a continuation of topological results, it is ingenious to investigate the behavior of soft topological structures in any extra topology. Consequently, soft bitopological (Ittanagi, 2014) and soft ditopological (SDT) space (Dizman, T. S., 2016) on a soft set was introduced. In perspective on the significance of topological structure in growing delicate set hypothesis, Senel, G. introduced new soft sets in soft ditopological spaces and showed them with the operator $\tilde{\delta}$. In this study I aim to discuss how SDT-spaces theory can be developed by using new $\tilde{\delta}$ sets which were firstly mentioned in the works of Senel, G. Also, in this study, the main threshold definitions which are sufficient to analyse the structure of all defined $\tilde{\delta}$ -soft sets have been presented.

In this study, I study $\tilde{\delta}$ soft sets in consideration of the studies of (Senel, G.) that are given in the references. Also, I should note that this is a compilation work that's main works are given in the references.

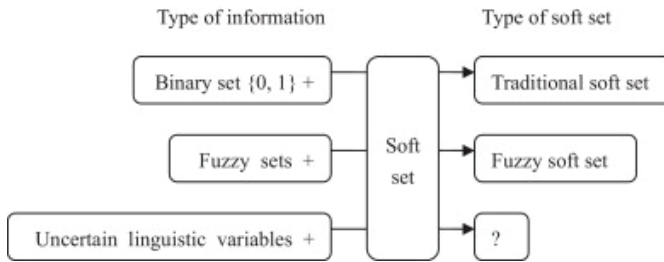
2. Analyzing The Concept of Soft Set

A pair (F, E) is called a soft set (over U) if and only if F is a mapping of E into the set of all subsets of the set U . In other words, the soft set is a parameterized family of subsets of the set U . Every set $F(e)$, $e \in E$, from this family may be considered as the set of e -approximate elements of the soft set (Molodtsov, 1999). Let us consider the following example is given in [Pal & Mondal, 2011].

Example 2.1: A soft set (F, E) describes the attractiveness of the bikes which Mr. X is going to buy. U is the set of bikes under consideration. E is the set of parameters. Each parameter is a word or a sentence. $E = (e_1 = \text{stylish}; e_2 = \text{heavy duty}; e_3 = \text{light}; e_4 = \text{steel body}; e_5 = \text{cheap}; e_6 = \text{good mileage}; e_7 = \text{easily Started}; e_8 = \text{long driven}; e_9 = \text{costly}; e_{10} = \text{fibre body})$.

In this case, to define a soft set means to point out stylish bikes, heavy duty bikes, and so on (Pal & Mondal, 2011).

Soft set is a parametrized general mathematical tool which deal with a collection of approximate descriptions of objects. Each approximate description has two parts; a predicate and an approximate value set. In classical mathematics, a mathematical model of an object is constructed and define the notion of exact solution of this model. (Ibrahim&Yusuf, 2012).



(Saraf, 2013)

This table explains the transformation of the information to the soft sets.

Suppose a binary operation denoted by $*$, is defined for all subsets of the set U . Let (F, A) and (G, B) be two soft sets over U . Then the operation $*$ for the soft sets is defined in the following way:

$(F, A) * (G, B) = (H, A \times B)$, where $H(\alpha, \beta) = F(\alpha) * G(\beta)$, $\alpha \in A$, $\beta \in B$ and $A \times B$ is the Cartesian product of the sets A and B (Saraf, 2013).

$$\begin{array}{ccccccc}
 \text{central soft sets:} & (f_A, A) & \sqcup & (g_B, B) & = & (h_C, C) \\
 & \updownarrow & & \updownarrow & & \updownarrow \\
 \text{soft sets:} & F_A & \sqcup & G_B & = & H_C
 \end{array}$$

3. Analyzing The Structure of Soft Ditopological Spaces (SDT – Spaces)

Definition: (Senel, G., 2016) Let f be a nonempty soft set over the universe U , $g \subseteq f$, $\tilde{\tau}$ be a soft topology on f and $\tilde{\tau}_g$ be a soft subspace topology on g . Then, $(f, \tilde{\tau}, \tilde{\tau}_g)$ is called a soft ditopological space which is abbreviated as SDT-space.

A pair $\tilde{\delta} = (\tilde{\tau}, \tilde{\tau}_g)$ is called a soft ditopology over f and the members of $\tilde{\delta}$ are said to be $\tilde{\delta}$ -soft unclosed in f .

The complement of $\tilde{\delta}$ -soft unclosed set is called $\tilde{\delta}$ -soft closed soft set.

Definition: (Senel, G., 2016) Let $h \subseteq f$. Then, $\tilde{\delta}$ -soft interior ($\tilde{\delta}$ -int) of h , indicated by $(h)_{\tilde{\delta}}^{\circ}$, is determined by

$$(h)_{\tilde{\delta}}^{\circ} = \bigcup \{h : k \subseteq h, k \text{ is } \tilde{\delta}\text{-soft open}\}$$

The $\tilde{\delta}$ -soft closure ($\tilde{\delta}$ -cl) of h , indicated by $(\bar{h})_{\tilde{\delta}}$, is determined by

$$(\bar{h})_{\tilde{\delta}} = \bigcap \{k : h \subseteq k, k \text{ is } \tilde{\delta}\text{-soft closed}\}$$

Note that $(h)_{\tilde{\delta}}^{\circ}$ is the biggest $\tilde{\delta}$ -soft unclosed set that contained in h and $(\bar{h})_{\tilde{\delta}}$ is the smallest $\tilde{\delta}$ -soft closed set that containing h

4. New $\tilde{\delta}$ - Soft Sets in SDT-Spaces

Definition: (Şenel, n.d.) Let $(f, \tilde{\delta})$ be an SDT-space and $h \subseteq f$. Then,

i. h is $\tilde{\delta}$ -soft regular open ($\tilde{\delta}$ -sr-open) set if

$$h = \tilde{\delta}\text{-int}(\tilde{\delta}\text{-cl}(h))$$

ii. and $\tilde{\delta}$ -soft regular closed ($\tilde{\delta}$ -sr-closed) set if

$$h = \tilde{\delta}\text{-cl}(\tilde{\delta}\text{-int}(h)).$$

iii. h is $\tilde{\delta}$ -soft α -open ($\tilde{\delta}$ -s α -open) set if

$$h \subseteq \tilde{\delta}\text{-int}(\tilde{\delta}\text{-cl}(\tilde{\delta}\text{-int}(h)))$$

iv. and h is $\tilde{\delta}$ -soft α -closed ($\tilde{\delta}$ -s α -closed) set if

$$h \subseteq \tilde{\delta}\text{-cl}(\tilde{\delta}\text{-int}(\tilde{\delta}\text{-cl}(h))).$$

v. h is $\tilde{\delta}$ -soft preopen ($\tilde{\delta}$ -sp-open) set if

$$h \subseteq \tilde{\delta}\text{-int}(\tilde{\delta}\text{-cl}(h))$$

vi. and h is $\tilde{\delta}$ -soft preclosed ($\tilde{\delta}$ -sp-closed) set if

$$h \subseteq \tilde{\delta}\text{-cl}(\tilde{\delta}\text{-int}(h)).$$

vii. h is $\tilde{\delta}$ -soft semi open ($\tilde{\delta}$ -ss-open) set if

$$h \subseteq \tilde{\delta}\text{-cl}(\tilde{\delta}\text{-int}(h))$$

viii. and h is $\tilde{\delta}$ -soft semi closed ($\tilde{\delta}$ -ss-closed) set if

$$h \subseteq \tilde{\delta}\text{-int}(\tilde{\delta}\text{-cl}(h)).$$

ix. h is $\tilde{\delta}$ -soft β -open ($\tilde{\delta}$ -s β -open) set if

$$h \subseteq \tilde{\delta}\text{-cl}(\tilde{\delta}\text{-int}(\tilde{\delta}\text{-cl}(h)))$$

x. and h is $\tilde{\delta}$ -soft β -closed ($\tilde{\delta}$ -s β -closed) set if

$$h \subseteq \tilde{\delta}\text{-int}(\tilde{\delta}\text{-cl}(\tilde{\delta}\text{-int}(h))).$$

Theorem: (Şenel, n.d.) Let $(f, \tilde{\delta})$ be an SDT-space. Then, the $\tilde{\delta}$ -soft sets have the following properties:

- i. Every $\tilde{\delta}$ -soft preopen set is $\tilde{\delta}$ -soft β -open.
- ii. Every $\tilde{\delta}$ -soft semi open set is $\tilde{\delta}$ -soft β -open.
- iii. Every $\tilde{\delta}$ -soft α open set is $\tilde{\delta}$ -soft preopen.

Theorem: (Şenel, n.d.) Let $(f, \tilde{\delta})$ be an SDT-space. Then,

- i. Every $\tilde{\delta}$ -soft preopen set is $\tilde{\delta}$ -soft b-open set.
- ii. Every $\tilde{\delta}$ -soft b-open set is $\tilde{\delta}$ -soft β -open set.
- iii. Every $\tilde{\delta}$ -soft semi open set is $\tilde{\delta}$ -soft b-open set.

Theorem: (Şenel, n.d.) Let $(f, \tilde{\delta})$ be an SDT-space, $h \subseteq f$ and h is a $\tilde{\delta}$ -sb-open set. Then,

- i. If $\tilde{\delta}\text{-cl}(h) = \phi$ then h is a $\tilde{\delta}$ -ss-open set.
- ii. If $\tilde{\delta}\text{-int}(h) = \phi$ then h is a $\tilde{\delta}$ -sp-open set.

Theorem: (Şenel, n.d.) Let $(f, \tilde{\delta})$ be an SDT-space, $h \subseteq f$ and h is a $\tilde{\delta}$ -sb-open set. Then,

- (i) If h is a $\tilde{\delta}$ -sr-closed set, then h is a $\tilde{\delta}$ -sp-open set.
- (ii) If h is a $\tilde{\delta}$ -sp-open set, then h is a $\tilde{\delta}$ -ss-open set.

Theorem: (Şenel, n.d.) Let $(f, \tilde{\delta})$ be an SDT-space, $h \subseteq f$. Then,

- i. $\tilde{\delta}\text{-sbcl}(h) = h \cup [\tilde{\delta}\text{-int}(\tilde{\delta}\text{-cl}(h)) \tilde{\cap} \tilde{\delta}\text{-cl}(\tilde{\delta}\text{-int}(h))]$.
- ii. $\tilde{\delta}\text{-sbint}(h) = h \tilde{\cap} [\tilde{\delta}\text{-int}(\tilde{\delta}\text{-cl}(h)) \cup \tilde{\delta}\text{-cl}(\tilde{\delta}\text{-int}(h))]$.

5. Conclusion

The mathematical prerequisite for this text is a working knowledge of new $\tilde{\delta}$ -soft sets in SDT-Spaces. This work is a literature review research and presents the new developments.

6. Declarations

Acknowledgements: The author gratefully acknowledge the comments of the editorial board which led to the improvement of this paper.

Funding: There is no source of funding for the research.

Availability of data and materials: The datasets used or analyzed during the current study are available from the corresponding author on reasonable request.

References

- Yıldız, F., & Özçağ, S. (2013). The ditopology generated by pre-open and pre-closed sets, and submaximality in textures. *Filomat*, 27(1), 95–107.
- Brown, L. M., & Diker, M. (1998). Ditopological texture spaces and intuitionistic sets. *Fuzzy Sets and Systems*, 98(2), 217–224.
- Brown, L. M., Ertürk, R., & Dost, Ş. (2004). Ditopological texture spaces and fuzzy topology, I. Basic Concepts. *Fuzzy Sets and Systems*, 147(2), 171–199.
- A. Kharal and B. Ahmad. Mappings on soft classes, Inf. Sci., INS-D-08-1231 by ESS, pp. 1-11, 2010.
- A. M. Ibrahim and A. O. Yusuf. Development of Soft Set Theory, American International Journal of Contemporary Research 2(9), 205-210, 2012.
- D. A. Molodtsov. Soft set theory- First results, Computers Math. Appl. 37 (4/5),19-31, 1999.
- Dizman, T. S., Šostak, A., Yuksel, Ş., 2016. Soft Ditopological Spaces, *Filomat*, 30(1): 209-222.
- Şenel, G., The Theory of Soft Ditopological Spaces, *International Journal of Computer Applications*, 150(4), September (2016), 1-5.
- Şenel, G., (n.d.). An Approach to Generate New Soft Sets and Spaces in Soft Ditopological Spaces, Submitted.
- Şenel, G., (n.d.). Sufficient and Necessary Conditions to Analyse the Structure of δ -soft sets, submitted.
- Şenel, G., Examination of Multi Structures on Topological Spaces and Ditopological Spaces, *Academic Studies in Mathematic and Natural Sciences*, First Edition February 2019, Cetinje-Montenegro, ISBN • 978-9940-540-72-2, pp. 53-60.
- Senel, G., A Survey On The Historical Perspective of Soft Set Theory, Research & Reviews in Science and Mathematics, Gece Publishing, First Edition March 2019, ISBN 978-605-7631-45-9, pp. 85-93.
- Shabir, M., Naz, M., On soft topological spaces, *Computers and Mathematics with Applications* 61, (2011), 1786-1799.
- Basavaraj M. Ittanagi, Soft Bitopological Spaces, *International Journal of Computer Applications*, 107(7), (2014), 1-4.
- S. Saraf. Survey or Review on Soft Set Theory and Development, The SIJ Transactions on Computer Science Engineering & its Applications (CSEA), 1 (3), 59-66, 2013.
- S. Mondal and M. Pal, Soft matrices, *Afr. J. Math. Comput. Sci. Res.* 4 (13), 379–388, 2011.



Chapter 3

N-ENGEL LEİBNİZ ALGEBRAS

Nil MANSUROĞLU¹

¹ Dr. Öğretim Üyesi, Kırşehir Ahi Evran Üniversitesi, Fen-Edebiyat Fakültesi, Matematik Bölümü, nil.mansuroglu@ahievran.edu.tr; nilmansuroglu@hotmail.com

1. Introduction

In 1993, Leibniz algebras were firstly described by Loday as a non-(anti)commutative generalization of Lie algebras. In paper (Loday and Pirashvili, (1993)) by the point of view of homological algebras, these algebras were investigated by Loday and Pirashvili. Leibniz algebras are natural generalizations of Lie algebras. In literature there have been various studies which were draw attention to results natural and to results showing the differences and the analogs between Leibniz algebras and Lie algebras. In (Frolova, 2011), Frolova proved that any Leibniz algebra over a field of characteristic zero with the Engel identity is nilpotent. In this note, our main goal is to commence the systematic study of n -Engel Leibniz algebras. We give a description of n -Engel Leibniz algebras. The main result of the paper is a generalization of the result of E.I. Zelmanov (Zelmanov, 1987) concerning the nilpotency of an n -Engel Lie algebras over a field of characteristic zero to the case of Leibniz algebras. Throughout of the paper we fix a field F of characteristic zero.

We organized this paper as follows. In Section 2 we gives some basic properties of Leibniz algebras to be used throughout this work. In Section 3 we describe n -Engel Leibniz algebras. Then in Section 4 we focus on 3 -Engel Leibniz algebras and we provide the sufficient conditions to show that an algebra L is 3 -Engel Leibniz algebra.

2. Preliminaries

Firstly, we begin to recall some basic definitions and some basic conclusions which we need for our aims. Leibniz algebras have many properties analogs to those of Lie algebras. We refer to (Bloh, 1965), (Demir et al, 2014), (Gorbatsevich), (Kurdachenko and Chupordia, 2017), (Jacobson, 1979) for more details.

Suppose that L is a non-associative algebra with multiplication $(,): L \times L \rightarrow L$ over the field F of characteristic zero. If L satisfies the Leibniz identity

$$a(bc) = (ab)c + b(ac)$$

for all $a, b, c \in L$, then L is sid to be (left) Leibniz algebra. The Leibniz identity is equivalent to the Jacobi identity when the multiplication $(,)$ is anti-commutative. For $a \in L$ we denote L_a the left multiplication

operator $L_a: L \rightarrow L$ by $L_a(x) = ax$ for all $x \in L$. The set $A(L)$ of all left multiplication operators of L is a Lie algebra.

Throughout this paper we use left normed notation, that is, for $a_1, a_2, \dots, a_n \in L$

$$a_1 a_2 \dots a_n = a_1 (a_2 (\dots (a_{n-1} a_n))).$$

This means that

$${}_n b a = \underbrace{b(b(\dots(b a)))}_{n \text{ times}}.$$

If ${}_n b a = 0$, then this is called Engel identity. If for all $a, b \in L$, the Engel identity ${}_n b a = 0$ is satisfied, L is called n -Engel algebra. For any element $a \in L$ and $n \in \mathbb{Z}^+$ we define $a^n \in L$ by $a^1 = a$ and $a^{n+1} = (a, a^n)$.

It is clear to show that any Lie algebra is a Leibniz algebra. If a Leibniz algebra L with the condition that $aa = a^2 = 0$ for all $a \in L$, then L becomes a Lie algebra. For the subspaces U and V of a Leibniz algebra L , (U, V) is a subspace which is generated by the elements (u, v) where $u \in U$ and $v \in V$.

A subspace I of L is called a subalgebra if $(I, I) \subseteq I$, I is left (respectively right) ideal if $(L, I) \subseteq I$ (respectively $(I, L) \subseteq I$). If I is both left ideal and right ideal, I is an ideal of L . We define L^n by $L^1 = L$ and $L^{n+1} = (L, L^n)$ inductively. If $L^2 = 0$, then the Leibniz algebra L is called abelian.

For any Leibniz algebra L , we define the Leibniz kernel ideal of L by $Leib(L) = Span\{a^2 \mid a \in L\}$.

We also define L^k inductively by defining $L^1 = L$ and $L^{k+1} = (L, L^k)$ for $k \geq 1$. Then the series of ideals

$$L = L^1 \supseteq L^2 \supseteq \dots \supseteq L^k \supseteq \dots$$

is said to be the lower central series of L . If there is a positive integer k such that $L^{k+1} = 0$ but $L^k \neq 0$, a Leibniz algebra L is called a nilpotent Leibniz algebra of class k .

Now, we define the series of ideals

$$L = L^{(0)} \supseteq L^{(1)} \supseteq \dots \supseteq L^{(n)} \supseteq \dots$$

where $L^{(0)} = L$, $L^{(1)} = (L^{(0)}, L^{(0)})$, ..., $L^{(n+1)} = (L^{(n)}, L^{(n)})$ for $n \geq 0$ is called the derived series of L . For some positive integer n , if we have $L^{(n)} = 0$, L is called a solvable Leibniz algebra.

Theorem 2.1. (Barnes, 2018) If L_a is nilpotent, then L is nilpotent.

Theorem 2.2. (Barnes, 2018) Let A be a Leibniz algebra and $a \in A$. Let b a product of $n \geq 1$ a 's. Then $L_b = 0$, however the product is associated.

Corollary 2.3. (Barnes, 2018) Let $b \neq 0$ be power of a . Then b has the form $b = a(a(\dots(aa)))$.

3. n -Engel Leibniz algebras

For all $a, b \in L$, if L satisfies ${}_nba = 0$ for some n ; namely $L_b^n(a) = 0$, then L is said to be n -Engel Leibniz algebra.

Proposition 3.1. Let L be an n -Engel Leibniz algebra over a field F . Then the Engel identity is equivalent to

$$\sum_{\sigma \in \text{Sym}(n)} (b_{\sigma(n)} b_{\sigma(n-1)} \dots b_{\sigma(1)} a) = 0.$$

Proof. Suppose that $b_{\sigma(n)} = b_{\sigma(n-1)} = \dots = b_{\sigma(1)} = b$. Then we have $n! ({}_nba) = 0$. Since $\text{char} F$ is not divisible by $n!$, we obtain ${}_nba = 0$. This implies the Engel identity. Now we consider

$$S = ({}_n(\alpha_1 b_{\sigma(1)} + \alpha_2 b_{\sigma(2)} + \dots + \alpha_n b_{\sigma(n)})a)$$

for $\alpha_1, \alpha_2, \dots, \alpha_n \in F$. By using bilinear property, we get

$$S = S_0 + \alpha_1 S_1 + \alpha_1 \alpha_2 S_2 + \cdots + \alpha_1 \alpha_2 \cdots \alpha_n \sum_{\sigma \in \text{Sym}(n)} (b_{\sigma(n)} b_{\sigma(n-1)} \cdots b_{\sigma(1)} a)$$

where S_0 is the sum of the monomials not divisible by α_1 , $\alpha_1 S_1$ is the sum of the monomials from $S - S_0$ not divisible by α_2 and so on. By taking $\alpha_1 = 0$ we obtain $S_0 = 0$. By taking $\alpha_1 = \alpha_2 = 0$ we obtain $S_1 = 0$. Continuing this process, we finally have that

$$\sum_{\sigma \in \text{Sym}(n)} (b_{\sigma(n)} b_{\sigma(n-1)} \cdots b_{\sigma(1)} a) = 0. \quad \square$$

In this note, in particular, we focus on the case $n = 3$. In a 3 -Engel Leibniz algebra

$$\begin{aligned} 0 &= {}_3(ab+c)a \\ &= \alpha({}_2cba + cbca + b{}_2ca) + \alpha^2(c{}_2ba + bcba \\ &\quad + {}_2bca) \end{aligned} \quad (3.1)$$

and

$$\begin{aligned} 0 &= \alpha{}_3(b+c)a = \alpha({}_2cba + cbca + b{}_2ca) + \alpha(c{}_2ba + bcba \\ &\quad + {}_2bca) \end{aligned} \quad (3.2)$$

By subtracting (3.2) from (3.1), we obtain

$$(\alpha^2 - \alpha)(c{}_2ba + bcba + {}_2bca) = 0.$$

If $\alpha \neq 0, 1$, we have

$$c{}_2ba + bcba + {}_2bca = 0.$$

4. 3 -Engel Leibniz algebras

In this section we investigate 3 -Engel Leibniz algebras. To show that an algebra L is 3 -Engel Leibniz algebra, we need to show that for all $a, b, c, b_1, b_2, b_3 \in L$

- (i) $a(bc) = (ab)c + b(ac)$
- (ii) ${}_3ba = 0$
- (iii) ${}_2cba + cbca + b{}_2ca = 0$
- (iv) $\sum_{\sigma \in \text{Sym}(n)} (b_{\sigma(3)} b_{\sigma(2)} b_{\sigma(1)} a) = 0.$

By (ii), (iii) and (iv), the algebra satisfies the 3 -Engel identity.

Theorem 4.1. Suppose that L is a finite dimensional Leibniz algebra and $A(L)$ is nilpotent of class n . Then L is n -Engel Leibniz algebra.

Proof. $A^n(L) = 0$, namely for all $L_a \in A(L)$, $L_a^n = 0$. Hence $L_a^n(x) = {}_n a x = 0$ for $x \in L$. This implies the Engel identity. Therefore, L is n -Engel Leibniz algebra. \square

The main result of this paper is the following.

Theorem 4.3. If L is nilpotent, then L is n -Engel Leibniz algebra.

Proof. Suppose that L is nilpotent and n is the nilpotency class of L . Therefore, $L^n \neq 0$ and $L^{n+1} = 0$. For all $y_n, y_{n-1}, \dots, y_2, y_1, x \in L$

$$y_n y_{n-1} \dots y_2 y_1 x = 0$$

so that if $y_1 = y_2 = \dots = y_{n-1}$, $y_n = y$, then ${}_n y x = 0$. This implies n -Engel identity. Thus L becomes n -Engel Leibniz algebra. \square

5. References

- Barnes, D., Engel subalgebras of Leibniz algebras, arXiv:0810.2849v1.
- Bloh, A.M., 1965. A generalization of the concept of Lie algebra, *Dokl. Akad. Nauk SSSR*, 165, 471-473.
- Bloh, A.M., 1971. A certain generalization of the concept of Lie algebra, *Algebra and Number Theory, Moskow. Gos. Ped. Inst. U^cen.* 375, 9-20.
- Demir, I., Misra C.K. and Ernie, S., 2014. On some structures of Leibniz algebras, in *Recent Advances in Representation Theory, Quantum Groups, Algebraic Geometry, and Related Topics*, Contemporary Mathematics, vol. 623, *Amer. Math. Soc.*, Providence, RI, pp. 41-54.
- Frolova, Y.Y., 2011. The Nilpotency of Leibniz Algebras with Engel condition, *Moscow University Mathematics Bulletin*, 66, 3, 136-138.
- Loday, J.L., 1993. Une version non commutative des algebres de Lie: les algebres de Leibniz, *Enseign. Math.*, 39, 269-293.
- Gorbatsevich, V., On some basic properties of Leibniz algebras, arXiv:1302.3345v2.
- Loday J.L. and Pirashvili, T., 1993. Universal enveloping algebras of Leibniz algebras and (co)homology, *Math. Ann.*, 269, (1), 139-158.

- Kurdachenko, L.A. and Chupordia, V.A., 2017. On some minimal Leibniz algebras, *Journal of Algebra and Its App.*, 16, no.2, 1-16.
- Jacobson, N., 1979. Lie Algebras, Dover.
- Zelmanov, E.I., 1987. Engel Lie Algebras, *Dokl. Akad. Nauk SSSR*, 292, 2, 265.



Chapter 4

C SEGMENT AUTOMOBILE SELECTION BY USING ELECTRE METHOD¹

Nuray GIRGINER², Lokman DAL³

¹ This study is derived from the paper presented at the 4th International GAP Business Sciences and Economics Congress held at Harran University between 29 November and 01 December 2019.

² Prof.Dr., Eskisehir Osmangazi University, Faculty of Economics and Administrative Sciences, Business Administration Department, ngirginer@gmail.com, ORCID: 0000-0003-1228-5800

³ Ph.D. Student, Eskisehir Osmangazi University, Social Sciences Institute, Business Administration Division, lokmandal1986@gmail.com, ORCID: 0000-0002-8932-8744

1. INTRODUCTION

Decision making may be defined as making the most appropriate choice among the multiple choices that any person encounters. People or institutions may face many problems in daily life. In these cases, it may often be the problem of which of the multiple solutions can give the most appropriate answer to the need. Criteria, value judgments, needs, standards, etc. that form the basis of the choice of person or institutions can make the problem even more complicated and cause the decision maker to falter. Human beings can often be intuitive in their multi-criteria choice. However, researches have shown that heuristic behavior is not sufficient for complex and vital decisions, although it is sufficient for making everyday decisions (Saaty, 1994).

Multi-Criteria Decision Making (MCDM) techniques are analytical methods that consist of more than one criterion and that systematically solve the problem of people in line with the importance they attach to the criteria. These methods began to be developed in the 1960s, when a number of tools were needed to assist decision making (Saaty, 1980).

Multi-Criteria Decision Making techniques are examined under 4 sub-titles: basic methods, single synthesis criterion methods, sorting methods and interactive methods. Under these subtitles, there are many methods like AHP, TOPSIS, PROMETHEE, MACHBETH, VIKOR, STEM etc.. One of these methods is the ELECTRE method, which is one of the ranking methods.

It is understood from the current literature that there are many studies done with the ELECTRE method. These studies are classified and summarized in Table 1.

Table 1. Some Studies On ELECTRE Method

Title	Source
Company/Supplier Selection	Birgun and Cihan, 2010
	Kılıcogullari et al., 2012
	Yavuz, 2013
	Arslan and Uysal, 2017
	Wan et al., 2017
	Shojaie et al., 2018
	Ji et al., 2018
	Nasution et al., 2020
	Arslankaya, 2020

Performance Evaluation	Karacasu, 2007 Sonmez et al., 2010 Urfalioglu and Genc, 2013 Ozbek, 2015 Dash, 2016 Gunay and Kaya, 2017 Allegro and Giambalvo, 2019
Service Quality Assessment	Celik and Ustasuleyman, 2015 Uludag and Dogan, 2016
Location Selection Problems	Yucel and Ulutas, 2009 Akyuz and Soba, 2013 Soba, 2014 Ghoseiri and Lessan, 2014 Keles and Tunca, 2015 Turan and Turan, 2016 Kumar et al., 2016 Pereira et al., 2019

In the literature, there are also studies on tool/equipment selection problems which are used Multi Criteria Decision Making methods. Some of these studies can be summarized as follows: Ballı et al. (2007) addressed the automobile selection problem according to the criteria expressed in linguistic values and used the Fuzzy PROMETHEE method. Yurekli (2008) was solved the most suitable attack helicopter problem to meet the needs of the Turkish Armed Forces with five ELECTRE methods under specified criteria within the scope of ATAK project. Ertuğrul and Karakasoglu (2010) discussed the laptop selection problem in a business by using ELECTRE and Fuzzy Analytical Hierarchy Process methods together. Athawale and Chakraborty (2011) used the ELECTRE II method to determine the most suitable material handling equipment. Chatterjee et al. (2014) discussed the issue of automatic medical examination device selection by using ELECTRE methods.

In this study, it was tried to solve a specific person's C segment automobile selection problem. 9 different brands of C segment automobiles determined by a specific consumer were compared by means of ELECTRE method. Weights and scale ranges were determined according to the order of importance of the criteria decided by the consumer. The most important 7 features of the automobiles were scored by making internet research. As a result of matrixes and calculations, the most suitable options for the criteria were sorted to the consumer.

2. ELECTRE

ELECTRE (Elimination and Choice Translating Reality), introduced

first by Roy, Beneyoun et al. in 1966, is widely used in many real-life decision making issues like appropriate location selection, device/equipment selection, water management strategy selection, recruitment for companies etc. (Figueira et al. 2012:61). ELECTRE has the meaning of “*elimination and choice that reflects the truth*” (Turan and Turan, 2016:20) and is based on bilateral superiority comparisons between alternatives for each evaluation factor. In ELECTRE method process, there are 8 steps for solving any problem.

2.1. ELECTRE Method Process Steps

ELECTRE method process steps are briefly described below.

2.1.1. The First Step: Creating The Decision Matrix (A)

The first step in decision making with ELECTRE method is to create the Decision Matrix (A) by the decision maker. The Decision Matrix is also known as initial matrix. Alternatives belonging to the advantages to be lined up in the lines of the matrix and the evaluation factors to be used in decision making are written in the columns and shown as below.

$$A_j = \begin{bmatrix} a_{11} & a_{12} & \dots & a_{1n} \\ a_{21} & a_{22} & \dots & a_{2n} \\ \vdots & \vdots & \ddots & \vdots \\ a_{m1} & a_{m2} & \dots & a_{mn} \end{bmatrix}$$

In the A_{ij} matrix, m shows the number of alternatives and n shows the number of evaluation factors.

2.1.2. The Second Step: Creating The Standard Decision Matrix (X)

The Standard Decision Matrix is calculated by using the matrix A elements. The formula below is used for the calculation.

$$x_{ij} = \frac{a_{ij}}{\sqrt{\sum_{k=1}^m a_{jk}^2}}$$

After calculations, the X matrix is created as follows:

$$X_j = \begin{bmatrix} x_1 & x_2 & \dots & x_{1n} \\ x_2 & x_2 & \dots & x_{2n} \\ \cdot & & & \cdot \\ \cdot & & & \cdot \\ \cdot & & & \cdot \\ x_{m1} & x_{m2} & \dots & x_m \end{bmatrix}$$

2.1.3. The Third Step: Creating the Weighted Standard Decision Matrix (Y)

Evaluation factors may differ in importance for the decision maker. In order to reflect these differences to the solution, Y matrix is calculated. The decision maker should first determine the weights (w_i) of the evaluation factors.

$$\left(\sum_{i=1}^n w_i = 1 \right)$$

Then, the Y matrix is created by multiplying the elements in each column of the X matrix by the corresponding w_i value. The Y matrix is shown below:

$$Y_j = \begin{bmatrix} w_1 x_1 & w_2 x_2 & \dots & w_n x_{1n} \\ w_1 x_2 & w_2 x_2 & \dots & w_n x_{2n} \\ \cdot & & & \cdot \\ \cdot & & & \cdot \\ \cdot & & & \cdot \\ w_1 x_{m1} & w_2 x_{m2} & \dots & w_n x_m \end{bmatrix}$$

2.1.4. The Fourth Step: Determining Concordance (C_{kl}) and Discordance (D_{kl}) Sets

In this step, Concordance (C_{kl}) and Discordance (D_{kl}) values are determined based on the Y matrix. When determining the Concordance (C_{kl}) and the Discordance (D_{kl}) sets these formulas are used below.

$$C_k = \{j, y_k \geq y_j\}$$

$$D_k = \{j, y_k < y_j\} = j - C_k$$

2.1.5. The Fifth Step: Creating Concordance (C) and Discordance (D) Matrices

The elements of the Concordance Matrix (C) are calculated via the following formula:

$$C_k = \sum_{j \in C_k} w_j$$

After calculations, C matrix is found and it is $m \times m$ in size as seen below.

$$C = \begin{bmatrix} - & c_2 & c_3 & \dots & c_{1m} \\ c_2 & - & c_3 & \dots & c_{2m} \\ \cdot & & & & \cdot \\ \cdot & & & & \cdot \\ \cdot & & & & \cdot \\ c_{m1} & c_{m2} & c_{m3} & \dots & - \end{bmatrix}$$

The elements of the Discordance Matrix (D) are calculated via the following formula:

$$D_k = \frac{\max_{j \in D_k} |y_k - y_j|}{\max_j |y_k - y_j|}$$

Like the C matrix, the D matrix is $m \times m$ in size and does not take values for $k=1$. The D matrix is shown below:

$$D = \begin{bmatrix} - & d_2 & d_3 & \dots & d_{1m} \\ d_2 & - & d_3 & \dots & d_{2m} \\ \cdot & & & & \cdot \\ \cdot & & & & \cdot \\ \cdot & & & & \cdot \\ d_{m1} & d_{m2} & d_{m3} & \dots & - \end{bmatrix}$$

2.1.6. The Sixth Step: Creating Concordance Superiority (F) and Discordance Superiority (G) Matrices

The Concordance Superiority Matrix (F) is $m \times m$ in size. The concordance threshold value (\underline{c}) is found via following formula:

$$\underline{c} = \frac{1}{m(m-1)} \sum_{k=1}^m \sum_{l=1}^m c_k$$

m in the formula shows the number of decision points. More specifically, the value of \underline{c} equals to the product of the sum of the elements forming $\frac{1}{m(m-1)}$ and matrix C .

The elements of matrix $F (f_{kl})$ take either 1 or 0 values and there is no value as it indicates the same alternatives on the diagonal of the matrix. If,

$$c_k \geq \underline{c} \Rightarrow f_k = 1 \text{ and } c_k < \underline{c} \Rightarrow f_k = 0$$

The Discordance Superiority Matrix (G) is also $m \times m$ in size and it is created similarly to the F matrix. The discordance threshold value (\underline{d}) is found via the following formula:

$$\underline{d} = \frac{1}{m(m-1)} \sum_{k=1}^m \sum_{l=1}^m d_k$$

The value of \underline{d} equals to the product of the sum of the elements forming $\frac{1}{m(m-1)}$ and matrix D .

The elements of the matrix $G (g_{kl})$ take either 1 or 0 values, and there is no value since it shows the same decision points on the diagonal of the matrix. If,

$$d_k \geq \underline{d} \Rightarrow g_k = 1 \text{ and } d_k < \underline{d} \Rightarrow g_k = 0$$

2.1.7. The Seventh Step: Creating Total Dominance (E) Matrix

The elements of the Total Dominance Matrix $E (e_{kl})$ are mutual product of the f_{kl} and g_{kl} elements. The matrix E is $m \times m$ -sized depending on the matrices C and D , and again consists of either 1 or 0 values.

2.1.8. The Eighth Step: Determining the Importance Order of Decision Points

Rows and columns of matrix E show decision points. For example, if the matrix E is calculated as follows,

$$E = \begin{bmatrix} - & 0 & 0 \\ 1 & - & 0 \\ 1 & 1 & - \end{bmatrix} \quad e_{21} = 1, e_{31} = 1 \text{ and } e_{32} = 1$$

This shows the absolute superiority of the 2nd decision point to the 1st decision point, the 3rd decision point to the 1st decision point and the 3rd decision point to the 2nd decision point. In this case, if the decision points are expressed with the symbol $A_i (i=1,2,\dots,m)$, the order of importance of the decision points will be A_3, A_2 and A_1 .

3. CASE STUDY

Many people consider quite a lot of criteria when they want to buy an automobile. Many factors like vehicle's body type, color, price, performance, consumer satisfaction, warranty, service quality, safety, fuel consumption, design, second-hand market etc. are some criterias that decision makers consider. In this study, 9 different brands of automobiles determined in line with the basic needs of a specific person were compared with ELECTRE method in the context of the consumer's criteria. The best options that meet the needs of the consumer's problem were listed.

The person planned to buy a brand-new C segment automobile with diesel, between 1.499 cc. and 1.600 cc. engine cylinder capacity, hatchback (5 doors), automatic transmission and equipped with the highest package. Although there were many cars with these features, the person couldn't make a decision, but finally assigned 9 options below as a result of his research and appreciation. These options were:

1. Opel Astra-K Excellence
2. Volkswagen Golf Highline
3. Seat Leon Xcellence
4. Audi A3 Design
5. Honda Civic Executive
6. Ford Focus Titanium
7. Peugeot 308 Allure
8. Fiat Egea Lounge

9. Hyundai i30 Elite

The criteria that determine the importance of 9 different models are listed by the consumer as follows.

Price: The person thought to buy a car that he desire with the most affordable price; and for this, he preferred the lowest price as a first criteria. While scoring process, it was assigned that any car with the highest score would be the car with the lowest price. Therefore, the brand-new prices of the cars included in the options were found from related websites and scoring was made.

Safety: It was preferred that the vehicle to be purchased has the highest level of safety compared to it's peers. Accordingly, scoring was made by taking into account the test scores of the latest version of the cars in options, which entered the Euro NCAP test. For calculating the test scores, the arithmetic mean of the *adult passenger*, *child passenger*, *pedestrian* and *safety assistant* percentage scores, in which the models were evaluated in Euro NCAP tests, were taken into account.

Performance: The option was expected to have the highest performance compared to its peers. The criterion to be considered in performance scoring would be 0-100 km. values (the speed up time) of the cars. For this, the technical information of each model about 0-100 km. speed reaching values were determined from the websites. The vehicle with the lowest duration was given the highest score.

Fuel Consumption: The average amount of fuel that each car consumes in every 100 km. in urban and intercity distances varies. The car was required to have the lowest fuel consumption in both urban and intercity use. For this, the average amount of mixed fuel consumed by each model in every 100 km. was found on related websites. Afterwards, scoring was made accordingly and the car with the lowest consumption was given the highest score.

Second-Hand Market: The person wanted to sell his car in a short time when he thought of the possibility of not being satisfied with the car or extraordinary situations such as needing urgent money. For this, he wanted the car to be the best in the second-hand market relatively to other 8 cars. For this purpose, the numbers of 9 cars for sale in a popular vehicle trading website in Turkey have been found. The highest rating was made for the car with a high amount of sales on the website.

Customer Satisfaction: Customer satisfaction of the cars' brands in the options was important for the person. In order to evaluate the level of people's satisfaction from the 9 different brands, data was collected from a widely used complaint website which was very popular in Turkey. In the

website, there were customer representatives of member brands and they can respond to complaints as soon as possible. Accordingly, the scoring was made by taking into consideration the number of complaints and appreciations of customers for the brands and the percentage of general brand satisfaction.

Warranty Period: The person wanted the vehicle to be the brand that provides the longest warranty period in year (or warranty in km.), as the vehicle had an automatic gearbox and he had to take into account the costs of possible malfunctions. Accordingly, the highest rating was made for the car brand, which gave the highest warranty period in years or km.

4. APPLICATION AND FINDINGS

For the implementation of the ELECTRE method, each of the criteria must have a numerical weight and scale value. The scale length can be chosen arbitrarily when determining the scale ranges of the criteria. However, considering the importance order of the criteria, it is useful to give the largest scale value to the criterion with the highest severity. Similar situation is valid for weights. The criterion with the highest severity has the highest weight (Yucel and Ulutas, 2009:337).

Table 2 shows the options and criteria. The scale values of the criteria with the same weights are based on the same. This is because it provides ease of process. *Safety* and *Performance* criteria have the same importance. For this reason, the same scale and weight are taken into account.

Table 2. Options and Criteria Table

Criteria	Options	Opel Astra-K Excellence	Volkswagen Golf Highline	Seat Leon Xcellence	Audi A3 Design	Honda Civic Executive	Ford Focus Titanium	Peugeot 308 Allure	Fiat Egea Lounge	Hyundai i30 Elite	Weight	Scale
PRICE		8	4	9	3	5	6	7	8	10	7	(3-10)
SAFETY		8	7	8	9	8	7	7	2	6	6	(1-9)
PERFORMANCE		8	5	8	5	4	4	9	6	6	6	(1-9)
FUEL CONSUMPTION		1	2	3	3	3	2	5	4	3	1	(1-5)
SECOND-HAND MARKET		5	7	4	6	2	4	3	5	3	4	(1-7)

CUSTOMER SATISFACTION	2	2	2	2	1	3	6	2	3	2	(2-6)
WARRANTY PERIOD	6	6	6	6	7	5	6	8	5	5	(5-8)

4.1. Creating Matrices

In ELECTRE method, three types of matrices are used: Concordance Matrix, First Discordance Matrix and Second Discordance Matrix.

4.1.1. Creating The Concordance Matrix

Situations where the options are dominant or equal in relation to each other are taken into consideration when creating the concordance matrix. For example, when compared the dominance and equality between Opel Astra-K Excellence and Volkswagen Golf Highline options in Table 1, it is understood that Opel Astra-K Excellence option is dominant on Volkswagen Golf Highline in terms of *price*, *safety*, *performance* criteria. On the other hand, they are equal in *customer satisfaction* and *warranty period* criteria. For this reason, the criteria of Opel Astra-K Excellence option higher or equal than Volkswagen Golf Highline option are take into consideration and divided by the total weight value. Opel Astra-K Excellence's concordance superiority to Volkswagen Golf Highline is calculated as; $= (7+6+6+2+5)/31=0,84$. This value is written in the area where the Opel Astra-K Excellence column coincides with the Volkswagen Golf Highline line. All options are compared with each other in this way, and the concordance matrix is created. The Concordance Matrix is shown in Table 3.

Table 3: The Concordance Matrix

	Opel Astra-K Excellence	Volkswagen Golf Highline	Seat Leon Xcellence	Audi A3 Design	Honda Civic Executive	Ford Focus Titanium	Peugeot 308 Allure	Fiat Egea Lounge	Hyundai i30 Elite
Opel Astra-K Excellence		0,39	0,87	0,58	0,39	0,10	0,45	0,61	0,32
Volkswagen Golf Highline	0,84		0,87	0,65	0,61	0,52	0,87	0,68	0,52
Seat Leon Xcellence	0,74	0,35		0,58	0,39	0,19	0,45	0,39	0,32
Audi A3 Design	0,65	0,77	0,68		0,42	0,29	0,68	0,68	0,52
Honda Civic Executive	0,81	0,39	0,84	0,61		0,61	0,65	0,81	0,65
Ford Focus Titanium	0,90	0,71	0,94	0,71	0,58		0,87	0,74	0,68

Peugeot 308 Allure	0,71	0,48	0,71	0,48	0,35	0,32		0,52	0,35
Fiat Egea Lounge	0,69	0,39	0,68	0,39	0,19	0,26	0,48		0,68
Hyundai i30 Elite	0,58	0,48	0,71	0,52	0,39	0,55	0,77	0,52	

4.1.2. Creating The First Discordance Matrix

In order to create the First Discordance Matrix, the criteria where the options are dominant are selected and the criterion with the highest score difference for the options is determined. The difference value is divided by the largest scale length and the first number of incompatibilities is found. For example, the criteria that Opel Astra-K Excellence dominates the Volkswagen Golf Highline are *price*, *safety* and *performance*. The criterion with the highest score difference among these criteria is;

$\max [(8-4=4), (8-7=1), (8-5=3)]=4$, that is, it seems to be the *price*.

Since the highest value in the scale is 8, it is found as $4/8 = 0.50$. This value is the first discordance (biggest discordance) number of the Volkswagen Golf Highline option compared to the Opel Astra-K Excellence option. It is written in the area where the Volkswagen Golf Highline column and the Opel Astra-K Excellence row overlap. These processes are performed for all options and the First Discordance Matrix is created. Table 4 shows the First Discordance Matrix.

Table 4. The First Discordance Matrix

	Opel Astra-K Excellence	Volkswagen Golf Highline	Seat Leon Xcellence	Audi A3 Design	Honda Civic Executive	Ford Focus Titanium	Peugeot 308 Allure	Fiat Egea Lounge	Hyundai i30 Elite
Opel Astra-K Excellence		0,50	0,11	0,56	0,50	0,50	0,22	0,75	0,20
Volkswagen Golf Highline	0,25		0,33	0,11	0,63	0,43	0,44	0,63	0,40
Seat Leon Xcellence	0,11	0,56		0,67	0,44	0,44	0,22	0,67	0,20
Audi A3 Design	0,22	0,22	0,22		0,44	0,22	0,33	0,78	0,30
Honda Civic Executive	0,25	0,13	0,11	0,22		0,25	0,11	0,75	0,20
Ford Focus Titanium	0,13	0,29	0,11	0,33	0,25		0,11	0,63	0,10

Peugeot 308 Allure	0,44	0,44	0,44	0,44	0,56	0,56		0,56	0,30
Fiat Egea Lounge	0,38	0,50	0,22	0,56	0,38	0,38	0,22		0,30
Hyundai i30 Elite	0,20	0,60	0,10	0,70	0,50	0,40	0,30	0,40	

4.1.3. Creating The Second Discordance Matrix

In determining the Second Discordance Matrix, the process for determining the First Discordance Matrix is applied. However, the criterion with the second highest score difference for the options is determined. The difference value found is divided by the largest scale length to find the Second Discordance Number. As it was remembered, we determined the criteria in which Opel Astra-K Excellence is dominant on Volkswagen Golf Highline to create the first mismatch matrix in terms of price, safety and performance. The criterion with the second highest score differences among these criteria;

$\max [(8-4=4), (8-7=1), (8-5=3)]=3$, that is, it seems to be the *performance*.

Since the highest value in the scale is 8, it is found as $3/8 = 0.38$. This value is the second discordance number of the Volkswagen Golf Highline option compared to the Opel Astra-K Excellence option. The result is written in the area where the Volkswagen Golf Highline column and the Opel Astra-K Excellence row overlap. These processes are also performed for all options and the Second Discordance Matrix is created. Table 5 shows the Second Discordance Matrix.

Table 5. The Second Discordance Matrix

	Opel Astra-K Excellence	Volkswagen Golf Highline	Seat Leon Xcellence	Audi A3 Design	Honda Civic Executive	Ford Focus Titanium	Peugeot 308 Allure	Fiat Egea Lounge	Hyundai i30 Elite
Opel Astra-K Excellence		0,38	0,00	0,33	0,38	0,13	0,11	0,25	0,20
Volkswagen Golf Highline	0,13		0,00	0,11	0,13	0,14	0,00	0,25	0,10
Seat Leon Xcellence	0,22	0,33		0,33	0,44	0,33	0,11	0,22	0,20
Audi A3 Design	0,11	0,11	0,11		0,11	0,22	0,22	0,11	0,30

Honda Civic Executive	0,13	0,13	0,00	0,11		0,13	0,11	0,00	0,20
Ford Focus Titanium	0,13	0,14	0,00	0,11	0,25		0,00	0,13	0,10
Peugeot 308 Allure	0,44	0,44	0,22	0,44	0,56	0,33		0,44	0,30
Fiat Egea Lounge	0,25	0,25	0,11	0,22	0,38	0,25	0,22		0,20
Hyundai i30 Elite	0,20	0,10	0,10	0,10	0,20	0,20	0,00	0,20	

4.2. Finding The Threshold Value and Creating The Threshold Matrix

The Threshold Value is the numbers required to reach the solution from the matrices. These numbers are;

- ***p***: Indicates The Concordance Matrix, boxes that are greater than or equal to this value are selected.
- ***q***: Indicates The Discordance Matrix, boxes that are less than or equal to this value are are selected.
- ***s***: Indicates whether The Discordance Matrix is first or second.

If the same field is filled in both matrices, that field is crossed out by typing “X”. Since it is a middle value compared to other values, ***p*** value was chosen as 0,6 for The Concordance Matrix. It was determined as ***s***=1. In other words, The First Discordance Matrix will be taken into consideration first. If the result is not found here, it will be passed to The Second Discordance Matrix and the ***q*** value can be changed.

Because it is considered to be an average value, the ***q*** value was chosen as 0,3 for The First Discordance Matrix,

Values greater than or equal to 0,6 are marked with yellow color in the The Concordance Matrix and values less than or equal to 0,3 are also marked yellow color in The First Discordance Matrix. The table regarding all of these markings is shown in Table 6.

Table 6. The Concordance Matrix Markings

The Concordance Matrix ($p \geq 0,6$)	Opel Astra-K Excellence	Volkswagen Golf Highline	Seat Leon Xcellence	Audi A3 Design	Honda Civic Executive	Ford Focus Titanium	Peugeot 308 Allure	Fiat Egea Lounge	Hyundai i30 Elite
Opel Astra-K Excellence		0,39	0,87	0,58	0,39	0,10	0,45	0,61	0,32

Volkswagen Golf Highline	0,84		0,87	0,65	0,61	0,52	0,87	0,68	0,52
Seat Leon Xcellence	0,74	0,35		0,58	0,39	0,19	0,45	0,39	0,32
Audi A3 Design	0,65	0,77	0,68		0,42	0,29	0,68	0,68	0,52
Honda Civic Executive	0,81	0,39	0,84	0,61		0,61	0,65	0,81	0,65
Ford Focus Titanium	0,90	0,71	0,94	0,71	0,58		0,87	0,74	0,68
Peugeot 308 Allure	0,71	0,48	0,71	0,48	0,35	0,32		0,52	0,35
Fiat Egea Lounge	0,69	0,39	0,68	0,39	0,19	0,26	0,48		0,68
Hyundai i30 Elite	0,58	0,48	0,71	0,52	0,39	0,55	0,77	0,52	
The First Discordance Matrix ($q \leq 0,3$)	Opel Astra-K Excellence	Volkswagen Golf Highline	Seat Leon Xcellence	Audi A3 Design	Honda Civic Executive	Ford Focus Titanium	Peugeot 308 Allure	Fiat Egea Lounge	Hyundai i30 Elite
Opel Astra-K Excellence		0,50	0,11	0,56	0,50	0,50	0,22	0,75	0,20
Volkswagen Golf Highline	0,25		0,33	0,11	0,63	0,43	0,44	0,63	0,40
Seat Leon Xcellence	0,11	0,56		0,67	0,44	0,44	0,22	0,67	0,20
Audi A3 Design	0,22	0,22	0,22		0,44	0,22	0,33	0,78	0,30
Honda Civic Executive	0,25	0,13	0,11	0,22		0,25	0,11	0,75	0,20
Ford Focus Titanium	0,13	0,29	0,11	0,33	0,25		0,11	0,63	0,10
Peugeot 308 Allure	0,44	0,44	0,44	0,44	0,56	0,56		0,56	0,30
Fiat Egea Lounge	0,38	0,50	0,22	0,56	0,38	0,38	0,22		0,30
Hyundai i30 Elite	0,20	0,60	0,10	0,70	0,50	0,40	0,30	0,40	

After markings in Table 6, the matrices are placed on top of each other and a cross is placed in the boxes where the signs intersect, and The Threshold Matrix is created and shown in Table 7.

Table 7. The Threshold Matrix

	Opel Astra-K Excellence	Volkswagen Golf Highline	Seat Leon Xcellence	Audi A3 Design	Honda Civic Executive	Ford Focus Titanium	Peugeot 308 Allure	Fiat Egea Lounge	Hyundai i30 Elite
Opel Astra-K Excellence			X						
Volkswagen Golf Highline	X			X					
Seat Leon Xcellence	X								
Audi A3 Design	X	X	X						
Honda Civic Executive	X		X	X		X	X		X
Ford Focus Titanium	X	X	X				X		X
Peugeot 308 Allure									
Fiat Egea Lounge			X						X
Hyundai i30 Elite			X				X		

“X” signs indicate that the option in the column is superior to the option in the row.

5. CONCLUSION

In this study, where a C segment automobile selection problem was addressed, 9 cars were sorted using the ELECTRE method in line with the main criteria determined by a specific person. The criteria that constitute the basis for the selection of the cars were *price, safety, performance, fuel consumption, second-hand market, customer satisfaction and warranty period*. Weighting was made in line with the mentioned criteria and the importance placed by the person (decision maker) on the criteria, and the information collected about the alternatives was scored.

Concordance and discordance matrices were calculated by using ELECTRE method. Since the First Discordance Matrix responds to the

solution, there was no need to use the Second Discordance Matrix. According to the markings made as a result of the analysis, the following options for the solution of the C segment automobile selection problem were determined to be the best solution, respectively.

1. Peugeot 308 Allure,
2. Opel Astra-K Excellence, Seat Leon Xcellence,
3. Volkswagen Golf Highline, Hyundai i30 Elite, Fiat Egea Lounge,
4. Audi A3 Design,
5. Ford Focus Titanium,
6. Honda Civic Executive.

The results which were found by using ELECTRE method and listed above were subjective. In the application of the ELECTRE method, the aim is not to find the best or the worst, but to determine the most suitable options for the criteria determined by any decision maker. If the importance given to the criteria and scoring changes, then the results may also change. ELECTRE method only sorts the options according to criteria. The final decision belongs to decision maker. ELECTRE is a useful method for sorting alternatives to decision makers for problem solving.

6. REFERENCES

- Akyuz, Y., Soba, M. (2013). *“Optimal Location Choice In Textile Sector By Using Electre Method: A Case Of Usak”*, Int. Journal of Management Economics and Business, Vol.: 9, No.: 19, pp.: 185-198
- Allegro, R., Giambalvo, O. (2019). *“University Performance Before And During Economic Crises An Analysis Of Graduate Characteristics”*, UNIPA Springer Series, e-book ISBN 978-3-030-36142-6
- Arslan, H. M., Uysal, H. T. (2017). *“The Determination Of The Most Convenient Supplier By Method Of Electre I: The Application Of Wood Sector”*, Duzce University Journal of Social Sciences Institute, Year: 7, No: 1
- Arslankaya, S. (2020). *“Catering Company Selection With Fuzzy Ahp, Electre And Vikor Method For A Company Producing Trailer”*, European Journal of Science and Technology, Vol.: 18, pp.: 413-423.
- Athawale, V. M., Chakraborty, S. (2011). *“Decision Making For Material Handling Equipment Selection Using Electre II Method”*, Journal of the Institution of Engineers (India), Part PR: Production Engineering Division, Vol.: 91
- Ballı, S., Karasulu, B., Korukoglu, S. (2007). *“An Application Of Fuzzy Promethee Method For Selecting Optimal Car Problem”*, Dokuz

- Eylul University, Faculty of Economics and Administrative Sciences Journal, Vol.: 22, Iss.: 1, pp.: 139-147
- Birgun, S., Cihan, E. (2010). "*Supplier Selection Process Using Electre Method*", 2010 IEEE International Conference on Intelligent Systems and Knowledge Engineering. 15-16 November 2010, Hangzhou, China
- Chatterjee, P., Mondal, S., Chakraborty, Sh. (2014). "*A Comprehensive Solution To Automated Inspection Device Selection Problems Using Electre Methods*", International Journal of Technology, Vol.: 5, No: 2
- Celik, P., Ustasuleyman, T. (2015). "*Assessing The Service Quality Of GSM Operators By Electre I And Promethee Methods*", International Journal of Economic and Administrative Studies, Vol.: 6, Iss.: 12, pp.: 137-160
- Dash, M. (2016). "*Banking Performance Measurement Using Multi-Criteria Decision Models Electre And Promethee: The Case Of Indian Banks*", International Journal of Operations and Quantitative Management, Vol.: 22, No: 1
- Ertugrul, I., Karakasoglu, N. (2010). "*Computer Selection For A Company With Electre And Fuzzy Ahp Method*", Dokuz Eylul University Faculty of Economics and Administrative Sciences Journal, Vol.: 25, Iss.: 2, pp.: 23-41
- Figueira, J. R. Greco, S., Roy, B., Slowinski, R. (2012). "*An Overview Of Electre Methods And Their Recent Extensions*", Journal Of Multi-Criteria Decision Analysis, pp.: 61-85
- Ghoseiri, K., Lessan, J. (2014). "*Waste Disposal Site Selection Using An Analytic Hierarchal Pairwise Comparison And Electre Approaches Under Fuzzy Environment*", Journal of Intelligent and Fuzzy Systems, Vol.: 26, No: 2
- Gunay, B., Kaya, I. (2017). "*The Performance Measurement Of The Intermediary Institutions Traded In Borsa Istanbul With Multi Criteria Decision Making Methods*", Manisa Celal Bayar University Journal of Social Sciences, Vol.: 15, Iss.: 2, pp. 141-164
- Ji, P., Zhang, H., Wang, J. (2018). "*Selecting An Outsourcing Provider Based On The Combined Mabac–Electre Method Using Single-Valued Neutrosophic Linguistic Sets*", Computers & Industrial Engineering, Vol.: 120
- Karacasu, M. (2007). "*Use Of Decision Support Model (Electre Method) In The Evaluation Of Urban Public Transport Investments*", 7th Transportation Congress, Congress Symposium Proceedings Book, pp. 155-165
- Keles, M. K., Tunca, M. Z. (2015). "*A Study On Technopark Decision By Using Hierarchical Electre Method*", Suleyman Demirel University, Faculty of Economics and Administrative Sciences Journal, Vol.: 20,

Iss.: 1, pp.: 199-223

- Kılıcogulları, P., Özcan, B., Ertug, B. (2012). *"Using Electre Method In Choosing A Fuel Station"*, Operations Research and 29th National Congress of Industrial Engineering
- Kumar, P., Singh, R. K., Sinha, P. (2016). *"Optimal Site Selection For A Hospital Using A Fuzzy Extended Electre Approach"*, Journal of Management Analytics, Vol.: 3, No: 2
- Nasution, N., Febriad, B., Mahalisa, G., Hijriana, N., Rasyidan, M., Sinaga, D. M., Dewi, S. M., Windarto, A. P., Aswan, N., Raharjo, M. R. (2020). *"Application Of Electre Algorithm In Skincare Product Selection"*, 1st Bukittinggi International Conference on Education
- Ozbek, A. (2015). *"Assessment Of Voluntary Workers In Non-Governmental Organisations According To The Electre Method"*, Electronic Journal of Social Sciences, Vol.: 14, No: 54, pp.: 219-232
- Pereira, J., Oliveira, Elaine C. B., Gomes, Luiz F. A. M., Araújo, Renato M. (2019). *"Sorting Retail Locations In A Large Urban City By Using ELECTRE TRI-C And Trapezoidal Fuzzy Numbers"*, Soft Computing, Vol.: 23, No: 12
- Shojaie, A. A., Babaie, S., Sayah, E., Mohammaditabar, D. (2018). *"Analysis And Prioritization of Green Health Suppliers Using Fuzzy ELECTRE Method With A Case Study"*, Global Journal of Flexible Systems Management, Vol.: 19, No: 1
- Soba, M. (2014). *"Determining Of The Selection Of The Bank Location Through Analytical Hierarchy Process And Electre Methods: The Case Of The Towns Usak"*, Mustafa Kemal University Journal of Social Sciences Institute, Vol.: 11, No: 25, pp.: 459-473
- Sonmez, A., Buyuksaatçı, S., Tuncbilek, N., Gencyılmaz, G., (2010). *"Evaluation of the Performance of Banks Traded in ISE"*, 10th National Production Research Symposium, pp. 99-114, Girne, Cyprus (TRNC)
- Turan, H., Turan, G. (2016). *"Using Electre Method In The Plant Location Selection"*, International Refereed Journal of Research on Economics Management, Iss.: 7, pp.: 18-28
- Uludag, A. S., Dogan, H. (2016). *"A Service Quality Application Focusing On The Comparison Of Multi-Criteria Decision Making Method"*, Cankırı Karatekin University, Faculty of Economics and Administrative Sciences Journal, Vol.: 6, Iss.: 2, pp.: 17-47
- Urfalioglu, F., Genc, T. (2013). *"Comparison Of The Economic Performance Between Turkey And The European Union Members With Multi Criteria Decision Making Methods"*, Marmara University Faculty of Economics and Administrative Sciences Journal, Vol.: XXXV, Iss.: II, pp.: 329-360
- Wan, S., Xu, G., Dong, J. (2017). *"Supplier Selection Using ANP And ELECTRE II In Interval 2-Tuple Linguistic Environment"*, Information

Sciences, Vol.: 385-386, pp.: 19-38

- Yavuz, O. (2013). "*Supplier Selection Process Using Electre I Decision Model And An Application In The Retail Sector*", Journal of Business Research, Vol.: 5, Iss.: 4, pp.: 210-226
- Yucel, M., Ulutas, A. (2009). "*Choosing A Place For A Cargo Company In Malatya By Using Electre Method In Multi-Criteria Decision Methods*", Selcuk University, Journal of Social and Economic Research, Vol.: 11, Iss.: 17, pp.: 327-344
- Yurekli, H. (2008). "*Use Of The Electre Methods In The Selection Of Attack Helicopters*", Istanbul University, Social Sciences Institute, Ph.D. Thesis



Chapter 5

PROPERTIES AND HEALTH BENEFITS OF PROBIOTIC AND PREBIOTIC KEFIR

Songul CETIK YILDIZ¹

¹ Asst.Prof.Dr., Mardin Artuklu University, Vocational Higher School of Health Services, Department of Medical Services and Techniques, songulcetik@gmail.com

1. Introduction

The demand for probiotic and prebiotic products is gradually increasing [1,2]. Probiotic microorganisms can reinforce immune response and the intestinal barrier while preventing the negative effects of pathogens [3,4]. Prebiotics, on the other hand, are short-chain carbohydrates that selectively enrich the activity of certain beneficial bacteria groups and they cannot be digested by digestive enzymes in humans [5]. Kefir contains plenty of probiotics and prebiotics [6]. Many potential health studies were conducted on fermented cow, sheep and goat milk in addition to kefir, which is known as the main source of probiotics [7,8].

0.1. Properties of Kefir

Kefir is a foamy, dense and slightly sour beverage that has been produced in the Caucasus region since old times and commercially manufactured in Europe and America today [9]. It was originally an acidic-alcoholic fermented milk product made in the Balkans, Eastern Europe and the Caucasus Region [10].

Kefir grains have an irregular shape with miscellaneous dimensions and a diameter ranging between 0.3 and 2 cm. Kefir grains have an indented and elastic surface that can be white or slightly yellowish. The grains consist of microbial cells, metabolic products of microbial cells, coagulated milk proteins and carbohydrates [11]. Kefir grains are a community where bacteria and yeast exist together and it has a similar appearance to cauliflower [12]. These grains swell when placed in milk and become whiter. After the fermentation of the milk is completed and the slightly sour, dense, refreshing and foamy (due to the CO₂ it contains) kefir is produced, the grains can be percolated and reused many times [13].

Various traditional and industrial methods are used for the production of Kefir. While the traditional production method of Kefir involves adding kefir grains to milk directly, different methods can be used in the industrial process [6]. Traditional kefir can be obtained at home using kefir grains with fresh or pasteurized cow, goat, sheep, coconut, rice or soy milk [14].

Kefir is a fermented product that is known for its potential health benefits related to the microbial species it contains and kefir fermentation [15]. Kefir grains contain a rich microbial community consisting of yeast and bacterial microflora responsible for Kefir fermentation [16]. 65-80% of the microbial structure in kefir consists of lactobacilli while 20% consists of streptococci and 5% consists of yeast [17]. Previous studies have revealed that the regular consumption of kefir has antioxidant, anticarcinogenic, antiallergic, antidiabetic and antibacterial effects, regulates the immune system and cholesterol, and reduces lactose tolerance and blood pressure [18-21].

0.2. Nutritional Content

Kefir contains all of the nutrients in milk. Additionally, it has been reported that kefir includes certain fatty acids and aminoacids, which are very important for the human body and can only be taken through nutrients [20]. Kefir includes vitamins such as B1, B2, B6, B12, folic acid, vitamin K and biotin (vit H). It also contains microminerals such as calcium, phosphorus, potassium and magnesium, and macrominerals such as zinc, copper, manganese, iron and cobalt [6,18,22]. By consuming 175ml of kefir, approximately 20% of the daily need of calcium and phosphorus can be met while this rate is 14% for vitamin B12, 19% for vitamin B2 and 5% for magnesium [23]. Since kefir contains less lactose compared to milk, it is a good dietary product for individuals with lactose intolerance [22].

0.3. Antimicrobial and Anti-inflammatory Effect

Certain antimicrobial substances and lactic acid produced by the microbial flora constituting kefir grains inhibit the reproduction of pathogenic microorganisms within this ecosystem [24]. In a previous study, it was shown that kefir could accelerate the healing process of burns with its strong antibacterial properties [25]. The polysaccharide in kefir has anti-inflammatory activity [26]. In another study stating that kefir had an anti-inflammatory effect, it was reported that kefir also had an antibacterial effect against pathogens such as salmonella enteritidis, staphylococcus aureus and e.coli [14,27]. With regard to its antimicrobial effect, kefir was reported to have a larger bacteriostatic effect on gram-negative bacteria and a larger bactericidal effect on gram-positive bacteria [28]. Additionally, in-vitro studies have shown that the lactobacilli and other beneficial microorganisms in kefir inhibited the ability of the harmful microorganisms in the environment to cause damage [29,30]. It has also been shown that kefir had antimicrobial activity against various types of pathogenic bacteria and fungi [26,31,32].

0.4. Effects on the Immune System

The regulatory effect of kefir on the immune mechanism has been shown in both human studies and animal experiments [18,33]. It was revealed that kefir could stimulate innate immune responses against pathogens [34]. After the intake of lactic acid bacteria in kefir, immune activities were observed in humans and various animals, and it was stated that lactic acid bacteria increased non-specific resistance to infections or strengthened specific immune reactions [35]. The lactic acid, antibiotics and various bactericides in kefir influence the degradation of pathogens and the inhibition of their reproduction [36]. Kefir is also influential in the protection of organisms against the negative effects of radiation and the reparation of the immune system [38].

0.5. Antitumoral Effects

In a previous study revealing the antioxidant properties of kefir, it was shown that kefir reduced lipid peroxidation and positively affected the antioxidant parameters in the carbon tetrachloride toxicity generated in mice [38]. Previous studies have shown that kefir had antineoplastic activity [35]. Kefir, which includes rich and beneficial properties in terms of health, demonstrates antioxidative, antimicrobial and anticarcinogenic activity with different health benefits [18,39]. In a previous study on the antitumoral effects of kefir, 0.5 ml of kefir was given to mice with transplanted fusiform cancer cells every day for 20 days through intraperitoneal injection and a significant reduction in tumor size was observed. It was also determined that kefir was influential in the elimination of tumoral necrosis [35]. Furukawa et al. examined the effects of the soluble and insoluble polysaccharide fractions of kefir grains on Lewis lung carcinoma and B16 melanoma cells in mice. It was reported that the soluble fraction was protective against metastases while the insoluble fraction inhibited melanoma metastasis [40].

0.6. The Use of Kefir in Burns

It is reported that prebiotic products reinforce the immune system, accelerate the healing process and reduce inflammation following the accumulation of lymphocyte in the wound area [41;42]. Additionally, the polysaccharide in kefir contributes to the wound healing process with anti-inflammatory activity [26]. In a previous study, it was revealed that the topical application of kefir could prevent infection in burn wounds and accelerate the healing process [25]. Huseini et al. (2012) observed that lactic acid, acetic acid, polysaccharides and other chemicals in kefir are significant factors for the healing process of wounds and that the wounds treated with kefir were significantly less severe compared to the control, base gel and silver sulfadiazine dressing groups [26]. In the study conducted by Kamila et al. on rats, it was shown that kefir had better wound-healing activity compared to treatment with clostebol-neomycin [43]. Similarly, Rodrigues et al. (2005) reported that rats treated with kefir healed faster compared to those included in clostebol-neomycin treatment on infected wounds [32].

0.7. Hypocholesterolemic Effect

Probiotic bacteria provide the inhibition of pathogenic microorganisms, increase the digestibility of food, reinforce the immune system, lower blood cholesterol levels and increase the absorption of prebiotics [44]. It was reported that the addition of kefir, which is a fermented milk product, to high-cholesterol diets significantly reduced levels of total serum cholesterol and phospholipid in mice [45]. In certain studies, a decrease was

observed in the total serum cholesterol and phospholipid levels of mice fed with a high-cholesterol diet supplemented with kefir and it was concluded that other biological indicators such as high-density lipoprotein (HDL) and serum triglyceride were not affected by kefir consumption [14]. In another study, the hypocholesterolemic effects of kefir made from sheep, cow and goat milk were compared and it was observed that sheep milk produced better results compared to cow and goat milk [18]. In animal experiments conducted with fermented dairy products and kefir, a significant reduction was observed in the serum levels of total cholesterol, low-density lipoproteins (LDL) and triglycerides [46,47]. In addition to the cholesterol-lowering effect and antihypertensive ability of kefir, kefiran was also shown to improve cholesterol and blood pressure levels [48,49]. It was determined that the supplementation of kefiran reduced serum total cholesterol, serum LDL cholesterol, serum triglycerides, liver cholesterol, and liver triglycerides in spontaneous hypertensive and stroke-prone rats fed with a high-fat diet [50].

1. Conclusion

The tendency to consume healthy products has been gradually increasing around the world. The close relationship between health and nutrition has led to the intensification of studies on the evaluation of nutrients in terms of health. The demand for functional and natural foods is constantly increasing due to high-cost health expenditures related to diabetes, heart disease, cancer and age-associated diseases in particular. In addition to the nutritional values of foods, it is also of great importance that they are healthy and safe. Milk and dairy products have been used as highly nutritious animal products in all periods since the inception of humanity. The consumption of kefir, which is defined as a functional product due to its health benefits, increases in parallel with this.

It is observed that fermented dairy beverages have acquired a different position as commonly consumed products that are considered to be important in terms of health and nutrition as a result of the increasing tendency to prefer natural foods and probiotic products in recent years. It is also observed that the milk companies dominating the global market will continue to produce these types of products in the future and have been conducting researches towards marketing them.

References

1. Ender, G., Karagözlü, C., Yerlikaya, O., Akbulut, N., (2006), Dünyada ve Türkiye’de tüketimi artan fermente süt içecekleri. *Türkiye Bolu 9. Gıda Kongresi*, 149-152.
2. Gürsoy, O., Kınık, Ö., (2006), Türkiye’de fonksiyonel süt ürünleri pazarı: Gerçekler, beklentiler, öneriler. *Türkiye Bolu 9. Gıda Kongresi*, 123-4.
3. Servin, AL., (2004), Antagonistic activities of lactobacilli and bifidobacteria against microbial pathogens, *FEMS Microbiology Reviews*, 28(4): 405-40.
4. Corthésy, B., Gaskins, HR., Mercenier, A., (2007), Cross-talk between probiotic bacteria and the host immune system, *Journal of Nutrition*, 137(3-2): 781S-90S.
5. Özyurt, VH., Ötleş, S., (2014), Prebiyotikler: Metabolizma için önemli bir gıda bileşeni. *Akademik Gıda*, 12(1): 115-123
6. Otles, S., Cagindi, O., (2003), Kefir: A Probiotic Dairy-Composition, Nutritional and Therapeutic Aspects. *Pakistan Journal of Nutrition*, 2 (2): 54-9.
7. Garofalo, C., Osimani, A., Milanovic, V., Aquilanti, L., De Filippis, F., Stellato, G., et al., (2015), Bacteria and yeast microbiota in milk kefir grains from different Italian regions. *Food Microbiol*, 49: 123-133.
8. Prado, MR., Blandon, ML., Vandenberghe, LPS., Rodrigues, CC., Guillermo, R., Thomaz-Soccol, VT. et al., (2015), Milk kefir: composition, microbial cultures, biological activities, and related products. *Front Microbiol*, 6: 1-12.
9. Mainville, I., Robert, N., Lee, B., Farnworth, ER., (2006), Polyphasic character- ization of the lactic acid bacteria in kefir. *Syst Appl Micro*, 29(1): 59-68.
10. Fontán, MCG., Martínez, S., Franco, I., Carballo, J., (2006), Microbiological and chemical changes during the manufacture of Kefir made from cows’ milk, using a commercial starter culture. *International Dairy Journal*, 16: 762-7.
11. Beshkova, DM., Simova, ED., Simov, ZI., Frengova, GI., Spasov, ZN., (2002), Pure Cultures for Making kefir. *Food Microbiology*, 19: 537-44.
12. Kowalczyk, M., Kolakowski P., Radziwill-Bienkowska JM., Szmytkowska, A., Bardowski, J., (2011), Cascade cell lyses and DNA extraction for identification of genes and microorganisms in kefir grains. *J dairy Res*, 79: 26-32.
13. Kwak, HS., Park, SK., Kim, DS., (1996), Biostabilization of kefir with a nonlactose-fermenting yeast. *J Dairy Scien*, 79(6), 937-42.
14. John, SM., Deeseenthum, S., (2015), Properties and benefits of kefir

- A review. Songklanakarin. *J Sci Technol*, 37(3): 275-82.
15. Dertli, E., Con, AH., (2017), Microbial diversity of traditional kefir grains and their role on kefir aroma. *LWT - Food Science and Technology*, 85: 151-7 .
 16. Walsh, AM., Crispie, F., Kilcawley, K., O'Sullivan, O., O'Sullivan, MG., Claesson, MJ., et al., (2016), Microbial succession and flavor production in the fermented dairy beverage kefir. *mSystems* 4 : 1(5).
 17. Wszolek, M., Tamime, A., Muir, D. and Barclay, M., (2001), Properties of kefir made in Scotland and Poland using bovine, caprine and ovine milk with different starter cultures. *LWT- Food Science and Technology*, 34: 251-61.
 18. Ahmed, Z., Wang, Y., Ahmad, A., ve ark., (2013), Kefir and health: a contemporary perspective. *Critical Reviews in Food Science and Nutrition*, 53: 422-34.
 19. Arslan, S., (2015), Chemical, microbiological and nutritional characteristics of kefir. *Journal of Food*, 13(3): 340-5.
 20. K ro lu,  ., Bakır, E., Uluda , G., K ro lu, S., (2015), Kefir ve Sa lık. *KS  Do a Bil Dergisi*, 18(1): 26-30.
 21. Rosa, DD., Dias, MS., Grze kowiak, LM., ve ark., (2017), Milk Kefir. *Nutrition Research Reviews*, 30(1): 82-96.
 22. Esmek, EM., G zeler, N., (2015), Kefir ve Kefir Kullanılarak Yapılan Bazı  r nler. *Harran Tarım ve Gıda Bilimleri Dergisi*, 19(4): 250-8.
 23. Felix, ASH., (2016), A Review About Probiotic Foods: Kefir, Kimchi and Kombucha. *Journal of Food Process Technology*. 7(11): 635-6.
 24. Lopitz-Otsoa, F., Rementeria, A., Elgue abal, N., Garaziar, J., (2006), Kefir: A symbiotic yeast-bacteria community with alleged healthy capabilities. *Revista Iberoamericana de Micologia*, 23: 67-74.
 25. Yildiz, SC., Demir, C., Cengiz, M., Ayhanci, A., (2019), Protective properties of kefir on burn wounds of mice that were infected with *S. aureus*, *P. auroginasa* and *E. coli*. *Cell Mol Biol*, 30; 65(7): 60-5.
 26. Huseini, HF., Rahimzadeh, G., Fazeli, MR., Mehrazma, M., Salehi, M., (2012), Evaluation of wound healing activities of kefir products. *Burns*, 38(5): 719-23.
 27. Guzel-Seydim, ZB., Kok-Tas, T., Grene, AK., Seydim, AC., (2011), Review: Functional Properties of Kefir. *Critical Reviews in Food Science and Nutrition*, 51: 261-8.
 28. Czamanski, RT., Greco, DP., Wiest, JM., 2004, Evaluation of antibiotic activity in filtrates of traditional kefir. *Higiene Alimentar*, 18 (124): 75-7.
 29. Kakisu, EJ., Abraham, AG., Perez, PF., De Antoni, GL., (2007), Inhibition of *Bacillus cereus* in milk fermented with kefir grains. *Journal of Food Protection*, 70(11): 2613-6.
 30. Kakisu, E., Abraham, AG., Farinati, CT., Ibarra, C., De Antoni, GL.,

- (2013), *Lactobacillus plantarum* isolated from kefir protects vero cells from cytotoxicity by type-II shiga toxin from *Escherichia coli* O157: H7. *Journal of dairy research*, 80(01): 64-71.
31. Yüksekdağ, ZN., Beyatlı, Y., Aslım, B., (2004), Determination of some characteristics coccoid forms of lactic acid bacteria isolated from Turkish kefirs with natural probiotic. *Lebensmittel-Wissenschaft und -Technologie*, 37: 663-7.
 32. Rodrigues, KL., Caputo, LR., Carvalho, JC., Evangelista, J., Schneedorf, JM., (2005), Antimicrobial and healing activity of kefir and kefiran extract. *International Journal of Antimicrobial Agents*, 25: 404-8.
 33. Hacıoğlu, G., Kurt, G., (2012), Tüketicilerin fonksiyonel gıdalara yönelik farkındalığı, kabulü ve tutumları: İzmir İli Örneği. *Business and Economics Research Journal*, 3(1): 161-71.
 34. Koutinas, A., Athanasiadis, I., Bekatorou, A., Psarianos, C., Kanellaki, M., Agouridis, N., (2007), Kefir-yeast technology: industrial scale-up of alcoholic fermentation of whey, promoted by raisin extracts, using kefir-yeast granular biomass. *Enzyme and Microbial Technology*, 41: 576-82.
 35. Cevikbas, A., Yemni, E., Ezzedenn, FW., Yardimici, T., (1994), Antitumoural antibacterial and antifungal activities of kefir and kefir grain. *Phytotherapy Research*, 8: 78-82.
 36. Çakır-Topdemir, P., Meriç, Ş., Çakır, Ç., Topdemir, T., (2010), Kefir ve özellikleri. 1. Uluslar arası Adryatik'ten Kafkaslar'a Geleneksel Gıdalar Sempozyumu, 15-17 Nisan, Tekirdağ, 305.
 37. Güngör Ö., (2007), Meyve suyu ilaveli kefirin depolama süresince özelliklerinin belirlenmesi, Doktora Tezi, Afyon Kocatepe Üniversitesi, Fen Bilimleri Enstitüsü, Afyon.
 38. Güven, A., Gülmez, M., (2003), The effect of kefir on the activities of GSH-Px, GST, CAT, GSH and LPO levels in carbon tetrachloride-induced mice tissues. *J Vet Med B Infect Dis Vet Public Health*, 50(8): 412-6.
 39. Elsayed, EA., Farooq, M., Dailin, D., El-Enshasy, HA., Othman, NZ., Malek, R., Danial, E., Wadaan, M., (2017), In vitro and in vivo biological screening of kefir polysaccharide produced by *Lactobacillus kefirifaciens*. *Biomedical Research*, 28 (2): 594-600.
 40. Furukawa, N., Matsuoka, A., Takahashi, T., Yamanaka, Y., (2000), Anti-metastatic effect of Kefir grain components on Lewis lung carcinoma and highly metastatic B16 melanoma in mice. *J Agric Sci*, 45: 62-70.
 41. Atalan, G., Demirkan, I., Yaman, H., Cina, M., (2003), Effect of topical kefir application on open wound healing on in vivo study. *Kafkas Univ Vet Fak Derg*, 9(1): 43-7.

42. Witthuhn, RC., Schoeman, T., Britz, TJ., (2005), Characterization of the microbial population at different stages of kefir production and kefir grains mass cultivation. *Int Dairy J*, 15: 383-9.
43. Kamila, LR., Lucelia, RGC., Jose, CTC., Joao, E., Jose, MS., (2005), Antimicrobial and healing activity of kefir and kefir extract. *International Journal of Antimicrobial Agents*, 25: 404-8.
44. Sezen, AG., (2013), Prebiyotik, Probiyotik ve Sinbiyotiklerin İnsan ve Hayvan Sağlığı Üzerine Etkileri. *Atatürk Üniversitesi Vet Bil Derg*, 8(3): 248-58.
45. Tamai, Y., Yashimitsu, N., Watanabe, Y., Kuwarbano, Y., Nagai, S., (1996), Effects of milk fermented by culturing with various lactic acid bacteria and a yeast on serum cholesterol level in rats. *J Ferment Bioeng*, 81: 181-2.
46. Beena, A., Prasad, V., (1997), Effect of yogurt and bifidus yogurt fortified with skim milk powder, condensed whey and lactose-hydrolysed condensed whey on serum cholesterol and triacylglycerol levels in rats. *Journal of Dairy Research*, 64(03): 453-7.
47. Wang, Y., Xu, N., Xi, A., Ahmed, Z., Zhang, B. and Bai, X., (2009), Effects of *Lactobacillus plantarum* MA2 isolated from Tibet kefir on lipid metabolism and intestinal microflora of rats fed on high-cholesterol diet. *Applied Microbiology and Biotechnology*, 84(2): 341-7.
48. Seppo, L., Kerojoki, O., Suomalainen, T., Korpela, R., (2002), The effect of a *Lactobacillus helveticus* LBK-16 H fermented milk on hypertension - a pilot study on humans. *Milchwissen*, 57: 124-7.
49. Sipola, M., Finckenberg, P., Korpela, R., Vapaatalo, H., Nurminen, M., (2002), Effect of long-term intake of milk products on blood pressure in hypertensive rats. *Journal of Dairy Research*, 69: 103-11.
50. Maeda, H., Zhu, X., Suzuki, S., Suzuki, K. and Kitamura, S., (2004), Structural characterization and biological activities of an exopolysaccharide kefir produced by *Lactobacillus kefirifaciens* WT-2BT. *Journal of agricultural and food chemistry*, 52(17): 5533-8.



Chapter 6

EFFECT OF DIFFERENT PRE-TREATMENTS ON SEED GERMINATION OF SALVIA FRUTICOSA MILL., SATUREJA THYMBRA L. AND THYMBRA SPICATA L.

Ummahan ÖZ'

1 Dr., Department of Plant and Animal Production, Alaşehir Vocational School, Manisa Celal Bayar University, ummahanoz48@gmail.com

1. Introduction

Plants have been used since ancient times for healing purposes. Plants belonging to Lamiaceae family are used in traditional treatment because of the essential oils and it contains about 200 genera and 3000 species all over the world (Seçmen et al., 2011; Güner, 2014). The genus such as *Mentha* L., *Origanum* L., *Salvia* L., *Satureja* L., *Thymbra* L. that belonging to Lamiaceae are mostly used as a source of essential oil (Cinbilgel & Kurt, 2019). *Salvia* L. is one of the largest genus of this family (Mesquita et al., 2019). The genus, which spreads naturally in the temperate, subtropical and tropical regions of the Northern and Southern hemispheres in the world, contains nearly 1000 species. There are 97 species and 109 taxa in Turkey (Karık & Sağlam, 2018; Sharifi-Rad et al., 2018). Among them, *Salvia fruticosa* Mill. is a perennial plant, endemic to the eastern Mediterranean basin (Duletić-Laušević et al., 2018). *S. fruticosa* which is the most collected and used in domestic consumption and exported, is also called Anatolian sage (Sönmez et al., 2019). In folk medicine, it is used in the treatment of different diseases. The infusion prepared from the leaves of *S. fruticosa* is used in nausea, stomachache, cold, flu and throat infections. The decoction prepared using the leaves has effects against asthma, whooping cough, diarrhea and stomachache (Tuzlacı, 2006). Essential oil of *S. fruticosa* is widely used as a mouthwash due to its antiseptic properties (Katar et al., 2019).

Although they are systematically different plant species, many plants are called “thyme” because of thymol and carvacrol contents (Özyazıcı & Kevseroğlu, 2019). *Thymus* L., *Origanum* L., *Coridothymus* Reichb. fil., *Thymbra* L. and *Satureja* L. are named as thyme (Hayta & Arabacı, 2011). The genus of *Thymbra* L. consist of four species which is called *Thymbra calostachya* (Rech.f.) Rech.f, *Thymbra capitata* (L.) Cav., *Thymbra sintesii* Bornm.&Azn., *Thymbra spicata* L. in the Mediterranean region (Stefanaki et al., 2018). Among them, *Thymbra spicata* is a widespread species in Thrace, Aegean, Western and Southeastern Anatolia, coast of Mediterranean in Turkey (Bozdemir, 2019). *T. spicata* is used in the treatment of skin disorders, cold, gastrointestinal disorders, hyperglycemia, insomnia, ophthalmia, sterility, toothache, arteriosclerosis, blood toxicity and hypercholesterolemia. In addition, this species has antitussive, sedative, analgesic, antirheumatic and antihypertensive effect (Sadikoğlu & Özhatay, 2019; Kirkan et al., 2019). It is effective against to several pathogens such as soil-borne plant pathogens, fungi infecting stored products, human pathogens etc. due to the carvacrol and thymol it contains (Rizzo et al., 2020). Essential oil of *T. spicata* consists of major chemical components such as carvacrol, thymol, α -terpinene, γ -terpinene, β -myrcene, p-cymene, thujene, β -caryophyllene (Karpiński, 2020). *Satureja* L. is an important

genus of the Lamiaceae family and it spreads in the Middle East, the Mediterranean, Europe, West Asia, North Africa, the Canary Islands and South America (Paşa et al., 2019). This genus comprises about 200 species and 40 of them are located in Turkey (Usanmaz Bozhüyük&Kordali, 2019). *Satureja thymbra* L. is an aromatic plant, endemic to the Mediterranean region (Kirkan et al., 2019). *S. thymbra* has economic and medicinal value due to the essential oil it contains. Essential oil of *S. thymbra* has main chemical components such as thymol, α -terpinene, γ -terpinene, p-cymene, carvacrol, carvacrol methyl ether, β -caryophyllene, caryophyllene oxide (Karpiński, 2020). *S. thymbra* has antimicrobial, antioxidant, insecticidal, antiviral, anticeptive/analgesic genotoxic, anti-inflammatory, herbicidal, acaricidal, insect repellent, antiplasmodial, ovidicial and antidiabetic effects (Tepe & Cilkiz, 2016). In addition to this, it is used to treatment of blood toxicity, paralysis, cough, nephropathy, indigestion, muscle cramp, nausea, diarrhea and infectious diseases (Kirkan et al., 2019; Sarropoulou and Maloupa, 2019). This species is also effective against to HSV-1 and hepatitis B virus (Bekut et al., 2018).

Medicinal and aromatic plants are used in many fields such as food, cosmetic, textile, medicine and agriculture (Göktaş & Gıdık, 2019). The export of medicinal and aromatic plants is about \$ 303,6 million in Turkey. In export, thyme, opium poppy, laurel, tea, anise, cumin, sage, black seed, lavender, mahaleb, red pepper and herbal teas are in the first rank. Especially, Turkey has an important position in export of thyme, leaf of laurel and opium poppy in the world (Aslan and Karakuş, 2019). While thyme production was 15 895 tonnes in 2018, it increased to 17 965 tonnes in 2019. Furthermore, sage (*Salvia*) production was 1 233 tonnes in 2019 (Anonymous, 2019). The plants which most collected as thyme in Turkey are belonging to the genus of *Origanum* (Baydar, 2019). *Origanum onites* L. has the highest proportion (about 80%) in our country's thyme export (Bozdemir, 2019). Cultivation of *O. onites* is carried out in Denizli province. Species of thyme like *Thymbra capitata* (L.) Cav., *T. spicata*, *Satureja cuneifolia* Ten., *S. thymbra* are mostly consumed in local markets as spices and tea (Baydar, 2019). Furthermore, this species are harvested from nature. Cultivation of species that grow even in more difficult conditions such as *S. thymbra* and *T. spicata* will increase the amount of thyme production and more economic gain.

Many medicinal and aromatic plants are successfully produced with seeds. The thyme is mostly cultivated with seed. Sage is produced by planting seeds with high germination rate, seedlings obtained from seeds planted in seedling starter trays and rooted shoot cuttings (Baydar, 2019). Seed germination consists of many biochemical and physiological processes. There are many factors that affect germination. The most important

of these is seed viability. Although the seed is viable, germination does not sometimes occur due to the dormancy. The mucilaginous layer found in the seed coat causes dormancy in Lamiaceae family and this physiological event is seen in *Salvia* (Sönmez, 2019). Seed age is an important factor in the germination of *S. thymbra*. The germination percentage of old seeds is higher than fresh. This is due to the evaporation of essential oils on walnut-type fruits. The essential oil in the calyx that surrounding the seeds strongly prevents germination, consequently the substance causes dormancy in seed germination (Tahiroğlu, 2016). Furthermore, the germination rate of *T. spicata* is also very low (Hayta & Arabacı, 2011).

The aim of research was to investigate the effects of some applications on germination rate of *Salvia fruticosa*, *Satureja thymbra* and *Thymbra spicata* and encourage the cultivation of *S. thymbra* and *T. spicata* which are not cultivated much.

2. Material and methods

2.1. Seed collection

Germination experiments were carried out with the seeds of *S. fruticosa*, *S. thymbra* and *T. spicata*. Ripe fruits of 3 plant species were collected from their natural habitats in Muğla- Milas, southwestern Turkey in July 2019. Seeds were removed from fruiting calyxes by hand and stored paper envelopes under +4°C in RH conditions until the experiment was conducted.

2.2. Seed germination experiment

This experiment was conducted under laboratory conditions at the Department of Herbal and Animal Production, Manisa Celal Bayar University, Turkey in November 2019. The temperature and relative humidity were recorded 20.8 – 25.5°C and 31-50% respectively during the experiment. Before starting the experiments, seeds with similar features were separated and surface-sterilized in 1% sodium hypochlorite solution for 5 minutes subsequently rinsed with deionized water and dried at room temperature. Germination test were conducted in petri dishes and all treatments were consisted of 3 replicates per treatment with 10 seeds. After the pre-treatments (Table 1), seeds were placed on double layer moistened filter paper discs in 9 cm diameter petri dishes. During the experiments, filter papers were moistened with distilled water when necessary. The experiments were observed for 21 days. When the radicle length reached 2 mm, the seeds were considered germinated and germinated seeds were recorded on daily basis.

2.3. Pre-treatments on the germination of *S. fruticosa*

In this experiment, 27 pre-soaking treatments were applied and 810 seeds were used in total. These pretreatments were these respectively; soaking in different concentrations (1000, 1500 and 2000 ppm) of GA_3 (24 hours) and KNO_3 (0.1%, 0.2%, 0.4% ; 24 hours), soaking in H_2O_2 (10%) for different times (5, 10 and 20 minutes) and combined applications of GA_3 , KNO_3 and H_2O_2 (Table 1). The control included no pre-soaking treatment.

2.4. Pre-treatments on the germination of *S. thymbra* and *T. spicata*

This experiment was conducted to evaluate the effects of different gibberellic acid concentrations, heat-cold shocks and combined applications (Table 1). Petri dishes were exposed to different temperatures (60°C, 80°C and 100°C) for 5 minutes in an incubator and kept in RH (-20°C) for 5, 10 and 20 minutes. Furthermore, seeds were soaking in different GA_3 concentration (10 ppm, 50 ppm and 100 ppm) for 24 hours. In addition to this, the control included no pre-treatment.

2.5. Statistical analysis

Germination percentage was calculated after 7 and 21 days by the following formula (Rahman et al., 2020):

Germination percentage = (Number of seeds germinated / Total number of seeds) \times 100

The data that obtained as a result of the study were subjected to analysis of variance with the TARIST statistical analysis program (Açıkgöz et al., 1994) according to the randomized block design with three replications and the least significant difference (LSD) test was applied to determine the significance level of the differences between the applications. The differences were considered statistically significant at $p \leq 0.05$.

Table 1: Different pre-treatments in *S. fruticosa*, *S. thymbra* and *T. spicata*.

T (no)	Applied pre-treatments and application times	
	<i>S. fruticosa</i>	<i>S. thymbra</i> and <i>T. spicata</i>
	1000 ppm GA ₃ (24 h)	60°C (5 ms)
	1500 ppm GA ₃ (24 h)	80°C (5 ms)
	2000 ppm GA ₃ (24 h)	100°C (5 ms)
	0.1% KNO ₃ (24 h)	- 20°C (5 ms)
	0.2% KNO ₃ (24 h)	- 20°C (10 ms)
	0.4% KNO ₃ (24 h)	- 20°C (20 ms)
	10% H ₂ O ₂ (5 ms)	10 ppm GA ₃ (24 h)
1	10% H ₂ O ₂ (10 ms)	50 ppm GA ₃ (24 h)
2	10% H ₂ O ₂ (20 ms)	100 ppm GA ₃ (24 h)
3	10% H ₂ O ₂ (5 ms) a.t.1000 ppm GA ₃ (24 h)	60°C (5 ms) a.t.10 ppm GA ₃ (24 h)
4	10% H ₂ O ₂ (5 ms) a.t.1500 ppm GA ₃ (24 h)	60°C (5 ms) a.t. 50 ppm GA ₃ (24 h)
5	10% H ₂ O ₂ (5 ms) a.t.2000 ppm GA ₃ (24 h)	60°C (5 ms) a.t. 100 ppm GA ₃ (24 h)
6	10% H ₂ O ₂ (10 ms) a.t.1000 ppm GA ₃ (24 h)	80°C (5 ms) a.t. 10 ppm GA ₃ (24 h)
7	10%H ₂ O ₂ (10 ms) a.t.1500 ppm GA ₃ (24 h)	80°C (5 ms) a.t. 50 ppm GA ₃ (24 h)
8	10% H ₂ O ₂ (10 ms) a.t.2000 ppm GA ₃ (24 h)	80°C (5 ms) a.t. 100 ppm GA ₃ (24 h)
9	10%H ₂ O ₂ (20 ms) a.t.1000 ppm GA ₃ (24 h)	100°C (5 ms) a.t. 10 ppm GA ₃ (24 h)
10	10% H ₂ O ₂ (20 ms) a.t.1500 ppm GA ₃ (24 h)	100°C (5 ms) a.t.50 ppm GA ₃ (24 h)
11	10%H ₂ O ₂ (20 ms) a.t.2000 ppm GA ₃ (24 h)	100°C (5 ms) a.t. 100 ppm GA ₃ (24 h)
12	10% H ₂ O ₂ (5 ms) a.t. 0.1 % KNO ₃ (24 h)	- 20°C (5 ms) a.t.10 ppm GA ₃ (24 h)
13	10% H ₂ O ₂ (5 ms) a.t. 0.2 % KNO ₃ (24 h)	- 20°C (5 ms) a.t. 50 ppm GA ₃ (24 h)
14	10% H ₂ O ₂ (5 ms) a.t. 0.4 % KNO ₃ (24 h)	- 20°C (5 ms) a.t. 100 ppm GA ₃ (24 h)
15	10% H ₂ O ₂ (10 ms) a.t. 0.1 % KNO ₃ (24 h)	- 20°C (10 ms) a.t. 10 ppm GA ₃ (24 h)
16	10% H ₂ O ₂ (10 ms) a.t. 0.2 % KNO ₃ (24 h)	- 20°C (10 ms) a.t. 50 ppm GA ₃ (24 h)
17	10% H ₂ O ₂ (10 ms) a.t. 0.4 % KNO ₃ (24 h)	- 20°C (10 ms) a.t. 100 ppm GA ₃ (24 h)
18	10% H ₂ O ₂ (20 ms) a.t. 0.1 % KNO ₃ (24 h)	- 20°C (20 ms) a.t. 10 ppm GA ₃ (24 h)
19	10% H ₂ O ₂ (20 ms) a.t. 0.2 % KNO ₃ (24 h)	- 20°C (20 ms) a.t. 50 ppm GA ₃ (24 h)
20	10% H ₂ O ₂ (20 ms) a.t. 0.4 % KNO ₃ (24 h)	- 20°C (20 ms) a.t. 100 ppm GA ₃ (24 h)
21	CONTROL	CONTROL

Abbreviations. a.t.: and then, h: hours, ms : minutes, t: treatment

3. Results and discussion

3.1. Effect of different treatments to germination in *S. fruticosa*

27 different pre-treatments were tested and whether they are statistically significant ($p \leq 0.05$) or not are indicated in Tables 2 -6. On the 7th day, the maximum germination percentage (30%) was obtained from T₃. It was observed that the germination percentage increases with increasing gibberellic acid doses unless used with other applications. On the 21st day, the best germination percentage (40%) was achieved at T₁₉. Doses of 0.1 - 1% potassium nitrate have a positive effect on germination (Er & Başalma, 2014). Furthermore, at the end of the twenty-first day, 30% germination was obtained in the T₃, T₆ and T₁₃. It was observed that when only GA₃ and only KNO₃ were applied, increasing the dose increased germination but when applied with 10% H₂O₂, it decreased the germination percentage. When GA₃ and H₂O₂ are applied together, they should be kept in 10% H₂O₂ for 10 minutes and 1000 ppm GA₃ should be used but when KNO₃ and H₂O₂ are used together, they should be kept in H₂O₂ for 5 minutes and then 0.1%KNO₃ should be tried. Furthermore, the germination percentage decreased as the waiting time and KNO₃ dose increased. It was determined that 5 minutes of waiting is sufficient when 10% H₂O₂ is applied only and excessive waiting time has adverse effects. In the control, germination rate was determined as 10% on both the 7th and 21st days because of the seed coat dormancy (Sönmez et al., 2019). Gibberellic acid breaks dormancy and increases germination percentage (Shu et al., 2015). It has been determined that gibberellic acid has a positive effect on germination in germination studies of this species (Özcan et al., 2014; Sönmez et al., 2019). The most important feature of gibberellic acid is that it increases the division, elongation and permeability of the cells. It also enables the production of other hydrolytic enzymes such as alpha amylase, protease and ribonuclease in seed. The enzymes break down the starch and the formed glucose is carried into the embryo, the water potential decreases and the seed gets more water. The radicle emerges from the seed coat and germination reaches its peak (Fletcher and Sopher, 2000; Hopkins & Hüner, 2004). It was observed that different applications are effective on the germination rate. The first germination was detected on the 4th day in T₁₂ and germination was observed earlier than control. Although H₂O₂ application alone did not accelerate germination, its use with GA₃ increased the germination rate.

3.2. Effect of different treatments to germination in *T.spicata* and *S.thymbra*

27 different pre-treatments were applied per species and whether they are statistically significant ($p \leq 0.05$) or not are indicated in Tables 7-11.

On the 7th day, the highest germination percentage (90%) was observed on T₂₀ and it was also determined that 80% germination at T₁₂, T₁₅ and T₂₇ in *S.thymbra*. The lowest germination percentage (10%) was obtained from T₁ and T₅. On the 21st day, the maximum germination rate (90%) was recorded in T₁₃ and T₂₀. Heat shock causes morphological changes in the seed and facilitates the entry of water into the seed so the probability of germination increases (Kazancı and Tavşanoğlu, 2019). In this study, only hot and cold applications did not increase germination, better results were observed when these applications were applied together with gibberellic acid. The minimum germination percentage (50%) was obtained in T₂, T₃ and T₄. Different temperature applications alone did not produce remarkable results compared to the control. In addition to these, 20% germination on the 7th day and 60% germination on the 21st day were determined in the control. In a study by Çatav et al. (2012), 12.4% germination was observed in control. In another study conducted by Çatav et al. (2014), the seeds were kept in distilled water for 24 hours in control, then placed in an culture media containing 0.7% agar and waited for 7 weeks. As a result, $47 \pm 4.4\%$ germination was determined in the control. In this study, 60% germination was observed after 21 days in the control. These results show that seed quality and maturity are important in germination. Furthermore, at the end of the twenty-first day, 80% germination was recorded at T₇, T₁₀, T₁₂, T₁₅ and T₂₇. When gibberellic acid was applied alone and with heat shocks, it was determined that the best GA₃ dose was 10 ppm and no dose increase was required. In waiting applications at 100 ppm GA₃ at -20°C, the percentage of germination increased as the waiting time increased and better results were obtained. The first germination was observed on the 4th day in all treatments of *S. thymbra* except T₁, T₂, T₃, T₄, T₅, T₆ and control. It has been determined that all applications except for only cold and only hot applications increase germination rate. The first germination in control was obtained on the 6th day. 20% germination was observed on the 6th day in the control. However, the highest germination percentage (90%) was reached on the 6th day in T₂₀. As a result, when the best applications observed in this study are tried, there is no need to wait for the germination result 21 days.

On the 7th day of the experiment in *T. spicata* the highest germination (30%) was determined in T₁₃, T₂₂, T₂₄ and T₂₆. When germination is attempted at 80°C and -20°C, 10 ppm GA₃ is sufficient, no need to increase the dose. On the 21st day, the highest germination rate (90%) was observed in T₂₄ and the lowest germination was obtained in T₃ and T₄. Furthermore, at the end of the twenty-first day, 80% germination was recorded at T₁₇ and T₂₃. It was observed that only the heat and cold shocks had no effect on the germination of the species and the application with GA₃ increased

germination. The best result in heat shocks treatments was obtained at T₁₇. In addition, the best result was obtained at T₂₄ in cold shock applications. It is reported that the application of different doses of GA₃ with cold application breaks dormancy and increases germination (Karakurt et al., 2010) and similar results were obtained in present study. It was observed that the percentage of germination increased at -20°C, as the percentage of germination generally increased. In the control, 10% germination on the 7th day and 30% germination on the 21st day were determined. In the study carried out by Hayta and Arabacı (2011), 16 different pre- treatments were applied to the *T. spicata* and the best result was obtained in the control (36%). In addition to these, the first germination was observed on the 2nd day in T₁₇ and T₁₈. The first germination in control was obtained on the 7th day. All applications, except only hot-cold applications and control, provided early seed germination.

Table 2: The effect of soaking in different GA₃ concentrations to germination percentage.

Treatments		Germination (%)
D	7	16.67
	21	18.33
p < 0.05		ns
Do (ppm)	1000	10.00 b
	1500	12.50 b
	2000	30.00 a
p < 0.05		*
D × Do ₁		10.00
		10.00
p < 0.05		ns
D × Do ₂		10.00 b
		15.00 a
p < 0.05		*
D × Do ₃		30.00
		30.00
p < 0.05		ns
Do × D ₁		10.00 b
		10.00 b
		30.00 a
p < 0.05		*
Do × D ₂		10.00 c
		15.00 b
		30.00 a
p < 0.05		*

Abbreviations. D: Day, Do: Dose, ns: non significant, *: significance at p < 0.05

Table 3: *The effect of soaking in different KNO_3 concentrations to germination percentage.*

Treatments		Germination (%)
D	7	10.00 b
	21	15.00 a
p < 0.05		*
Do (%)	0.1	12.50
	0.2	10.00
	0.4	15.00
p < 0.05		ns
D × Do ₁		10.00 15.00
p < 0.05		ns
D × Do ₂		10.00 10.00
p < 0.05		ns
D × Do ₃		10.00 b 20.00 a
p < 0.05		*
Do × D ₁		10.00 10.00 10.00
p < 0.05		ns
Do × D ₂		15.00 ab 10.00 b 20.00 a
p < 0.05		*

Abbreviations. D: Day, Do: Dose, ns: non significant, *: significance at $p < 0.05$

Table 4: *The effect of different soaking times in 10% H_2O_2 to germination percentage.*

Treatments		Germination (%)
D	7	10.00 b
	21	13.33 a
p < 0.05		*
Tm (min)	5	12.50
	10	12.50
	20	10.00
p < 0.05		ns
D × Tm ₁		10.00 15.00
p < 0.05		ns

$D \times Tm_2$	10.00
	15.00
$p < 0.05$	ns
$D \times Tm_3$	10.00
	10.00
$p < 0.05$	ns
$Tm \times D_1$	10.00
	10.00
	10.00
$p < 0.05$	ns
$Tm \times D_2$	15.00
	15.00
	10.00
$p < 0.05$	ns

Abbreviations. D: Day, Tm: Time, ns: non significant, *: significance at $p < 0.05$

Table 5: The effects of combined treatments (different soaking times in 10% H_2O_2 and then soaking in different GA_3 concentrations) to germination percentage.

Treatments		Germination (%)
D	7	10.00 b
	21	14.44 a
$p < 0.05$		*
Tm (min)	5	12.78 a
	10	13.89 a
	20	10.00 b
$p < 0.05$		*
$D \times Tm_1$		10.00 b
		15.56 a
$p < 0.05$		*
$D \times Tm_2$		10.00 b
		17.78 a
$p < 0.05$		*
$D \times Tm_3$		10.00
		10.00
$p < 0.05$		ns
$Tm \times D_1$		10.00
		10.00
		10.00
$p < 0.05$		ns

Tm × D ₂		15.56 a 17.78 a 10.00 b
p < 0.05		*
Do (ppm)	1000	13.89 a
	1500	11.67 ab
	2000	11.11 b
p < 0.05		*
D × Do ₁		10.00 b 17.78 a
p < 0.05		*
D × Do ₂		10.00 13.33
p < 0.05		ns
D × Do ₃		10.00 12.22
p < 0.05		ns
Do × D ₁		10.00 10.00 10.00
p < 0.05		ns
Do × D ₂		17.78 a 13.33 b 12.22 b
p < 0.05		*
Tm × Do ₁		13.33 b 18.33 a 10.00 b
p < 0.05		*
Tm × Do ₂		11.67 13.33 10.00
p < 0.05		ns
Tm × Do ₃		13.33 10.00 10.00
p < 0.05		ns
Do × Tm ₁		13.33 11.67 13.33

$p < 0.05$	ns
$D \times Tm_2$	18.33 a 13.33 b 10.00 b
$p < 0.05$	ns
$Do \times Tm_3$	10.00 10.00 10.00
$p < 0.05$	ns
$D \times Tm_1 \times Do_1$	10.00 b 16.67 a
$p < 0.05$	*
$D \times Tm_1 \times Do_2$	10.00 13.33
$p < 0.05$	ns
$D \times Tm_1 \times Do_3$	10.00 b 16.67 a
$p < 0.05$	*
$D \times Tm_2 \times Do_1$	10.00 b 26.67 a
$p < 0.05$	*
$D \times Tm_2 \times Do_2$	10.00 b 16.67 a
$p < 0.05$	*
$D \times Tm_2 \times Do_3$	10.00 10.00
$p < 0.05$	ns
$D \times Tm_3 \times Do_1$	10.00 10.00
$p < 0.05$	ns
$D \times Tm_3 \times Do_2$	10.00 10.00
$p < 0.05$	ns
$D \times Tm_3 \times Do_3$	10.00 10.00
$p < 0.05$	ns
$Tm \times D_1 \times Do_1$	10.00 10.00 10.00

p < 0.05	ns
Tm × D ₁ × Do ₂	10.00
	10.00
	10.00
p < 0.05	ns
Tm × D ₁ × Do ₃	10.00
	10.00
	10.00
p < 0.05	ns
Tm × D ₂ × Do ₁	16.67 b
	26.67 a
	10.00 c
p < 0.05	*
Tm × D ₂ × Do ₂	13.33 ab
	16.67 a
	10.00 b
p < 0.05	*
Tm × D ₂ × Do ₃	16.67 a
	10.00 b
	10.00 b
p < 0.05	ns
Do × D ₁ × Tm ₁	10.00
	10.00
	10.00
p < 0.05	ns
Do × D ₁ × Tm ₂	10.00
	10.00
	10.00
p < 0.05	ns
Do × D ₁ × Tm ₃	10.00
	10.00
	10.00
p < 0.05	ns
Do × D ₂ × Tm ₁	16.67
	13.33
	16.67
p < 0.05	ns

$Do \times D_2 \times Tm_2$	26.67 a 16.67 b 10.00 c
$p < 0.05$	*
$Do \times D_2 \times Tm_3$	10.00 10.00 10.00
$p < 0.05$	ns

Abbreviations. D: Day, Do: Dose, Tm: Time, ns: non significant, *: significance at $p < 0.05$

Table 6: The effects of combined treatments (different soaking times in 10% H_2O_2 and then soaking in different KNO_3 concentrations) to germination percentage.

Treatments		Germination (%)
D	7	12.22
	21	11.20
$p < 0.05$		ns
Tm (min)	5	11.67
	10	10.00
	20	13.75
$p < 0.05$		ns
$D \times Tm_1$		10.00 13.33
$p < 0.05$		ns
$D \times Tm_2$		10.00 10.00
$p < 0.05$		ns
$D \times Tm_3$		16.67 a 10.00 b
$p < 0.05$		*
$Tm \times D_1$		10.00 b 10.00 b 16.67 a
$p < 0.05$		*
$Tm \times D_2$		13.33 10.00 10.00
$p < 0.05$		ns
Dose (%)	0.1	11.67
	0.2	10.00
	0.4	13.53

p < 0.05	ns
D × Do ₁	10.00
	13.33
p < 0.05	ns
D × Do ₂	10.00
	10.00
p < 0.05	ns
D × Do ₃	16.67 a
	10.00 b
p < 0.05	*
Do × D ₁	10.00 b
	10.00 b
	16.67 a
p < 0.05	*
Do × D ₂	13.33
	10.00
	10.00
p < 0.05	ns
Tm × Do ₁	15.00
	10.00
	10.00
p < 0.05	ns
Tm × Do ₂	10.00
	10.00
	10.00
p < 0.05	ns
Tm × Do ₃	10.00 b
	10.00 b
	22.00 a
p < 0.05	*
Do × Tm ₁	15.00
	10.00
	10.00
p < 0.05	ns
Do × Tm ₂	10.00
	10.00
	10.00
p < 0.05	ns

$Do \times Tm_3$	10.00 b 10.00 b 22.00 a
$p < 0.05$	*
$D \times Tm_1 \times Do_1$	10.00 b 20.00 a
$p < 0.05$	*
$D \times Tm_1 \times Do_2$	10.00 10.00
$p < 0.05$	ns
$D \times Tm_1 \times Do_3$	10.00 10.00
$p < 0.05$	ns
$D \times Tm_2 \times Do_1$	10.00 10.00
$p < 0.05$	ns
$D \times Tm_2 \times Do_2$	10.00 10.00
$p < 0.05$	ns
$D \times Tm_2 \times Do_3$	10.00 10.00
$p < 0.05$	ns
$D \times Tm_3 \times Do_1$	10.00 10.00
$p < 0.05$	ns
$D \times Tm_3 \times Do_2$	10.00 10.00
$p < 0.05$	ns
$D \times Tm_3 \times Do_3$	30.00 a 10.00 b
$p < 0.05$	*
$D \times Tm_1 \times Do_1$	10.00 10.00 10.00
$p < 0.05$	ns
$Tm \times D_1 \times Do_2$	10.00 10.00 10.00
$p < 0.05$	ns

$Tm \times D_1 \times Do_3$	10.00 b 10.00 b 30.00 a
$p < 0.05$	*
$Tm \times D_2 \times Do_1$	20.00 a 10.00 b 10.00 b
$p < 0.05$	*
$Tm \times D_2 \times Do_2$	10.00 10.00 10.00
$p < 0.05$	ns
$Tm \times D_2 \times Do_3$	10.00 10.00 10.00
$p < 0.05$	ns
$Do \times D_1 \times Tm_1$	10.00 10.00 10.00
$p < 0.05$	ns
$Do \times D_1 \times Tm_2$	10.00 10.00 10.00
$p < 0.05$	ns
$Do \times D_1 \times Tm_3$	10.00 b 10.00 b 30.00 a
$p < 0.05$	*
$Do \times D_2 \times Tm_1$	20.00 a 10.00 b 10.00 b
$p < 0.05$	*
$Do \times D_2 \times Tm_2$	10.00 10.00 10.00
$p < 0.05$	ns
$Do \times D_2 \times Tm_3$	10.00 10.00 10.00
$p < 0.05$	ns

Abbreviations. D: Day, Do: Dose, Tm: Time, ns: non significant, *: significance at $p < 0.05$

Table 7: The effect of heat shocks for 5 minutes on the germination percentage.

Treatments		<i>Thymbra spicata</i> Germination (%)	<i>Satureja thymbra</i> Germination (%)
D	7 21	10.00 b 18.33 a	18.33 b 42.22 a
p < 0.05		*	*
T (°C)	60 80 100	15.00 17.50 10.00	31.67 32.50 26.67
p < 0.05		ns	ns
D × T ₁		10.00 20.00	10.00 b 53.33 a
p < 0.05		ns	*
D × T ₂		10.00 b 25.00 a	25.00 40.00
p < 0.05		*	ns
D × T ₃		10.00 10.00	20,00 33,33
p < 0.05		ns	ns
T × D ₁		10.00 10.00 10.00	10,00 25,00 20,00
p < 0.05		ns	ns
T × D ₂		20.00 ab 25.00 a 10.00 b	53,33 40,00 33,33
p < 0.05		*	ns

Abbreviations. D: Day, T: Temperature, ns: non significant, * : significance at p < 0.05

Table 8: The effect of different waiting times at - 20 °C on germination percentage.

Treatments		<i>Thymbra spicata</i> Germination (%)	<i>Satureja thymbra</i> Germination (%)
D	7 21	10.00 13.33	16.67 b 52.22 a
p < 0.05		ns	*
T _m (min)	5 10 20	10.00 13.33 11.67	33.33 ab 31.67 b 38.33 a
p < 0.05		ns	*
D × T _m ₁		10.00 10.00	16.67 b 50.00 a
p < 0.05		ns	*
D × T _m ₂		10.00 b 16.67 a	10.00 b 53.33 a
p < 0.05		*	*
D × T _m ₃		10.00 13.33	23.33 b 53.33 a

p < 0.05	ns	*
Tm × D ₁	10.00	16.67 ab
	10.00	10.00 b
	10.00	23.33 a
p < 0.05	ns	*
Tm × D ₂	10.00 b	50.00
	16.67 a	53.33
	13.33 ab	53.33
p < 0.05	*	ns

Abbreviations. D: Day,, Tm: Time, ns: non significant, *: significance at $p < 0.05$

Table 9: The effect of soaking in 24 hours at different GA₃ concentrations to germination percentage.

Treatments		<i>Thymbra spicata</i> Germination (%)	<i>Satureja thymbra</i> Germination (%)
D	7	11.67 b	53.33
	21	40.00 a	52.22
p < 0.05		*	ns
Do(ppm)	10	28.33	45.00
	50	23.33	53.33
	100	25.83	60.00
p < 0.05		ns	ns
D × Do ₁		10.00 b	50.00
		46.67 a	40.00
p < 0.05		*	ns
D × Do ₂		10.00 b	53.33
		36.67 a	53.33
p < 0.05		*	ns
D × Do ₃		15.00	63.33
		36.67	56.67
p < 0.05		ns	ns
Do × D ₁		10.00	50.00
		10.00	53.33
		10.00	56.67
p < 0.05		ns	ns
Do × D ₂		46.67	40.00
		36.67	53.33
		36.67	63.33
p < 0.05		ns	ns

Abbreviations. D: Day, Do: Dose, ns: non significant, *: significance at $p < 0.05$

Table 10: The effects of combined treatments (different heat shocks for 5 minutes and then soaking in 24 hours at different GA_3 concentrations) on germination.

Treatments		<i>Thymbra spicata</i> Germination (%)	<i>Satureja thymbra</i> Germination (%)
D	7 21	13.15 b 46.48 a	47.04 54.82
p < 0.05		*	ns
T (°C)	60 80 100	23.33 b 33.06 a 33.06 a	53.33 53.33 46.11
p < 0.05		*	ns
D × T ₁		11.67 b 35.00 a	48.89 57.78
p < 0.05		*	ns
D × T ₂		13.89 b 52.22 a	50.00 56.67
p < 0.05		*	ns
D × T ₃		13.89 b 52.22 a	42.22 50.00
p < 0.05		*	ns
T × D ₁		11.67 13.89 13.89	48.89 50.00 42.22
p < 0.05		ns	ns
T × D ₂		35.00 b 52.22 a 52.22 a	57.78 56.67 50.00
p < 0.05		*	ns
Do(ppm)	10 50 100	29.72 33.33 26.39	51.67 ab 41.67 b 59.44 a
p < 0.05		ns	*
D × Do ₁		13.89 b 45.56 a	43.33 60.00
p < 0.05		*	ns
D × Do ₂		15.56 b 51.11 a	41.11 42.22
p < 0.05		*	ns
D × Do ₃		10.00 b 42.78 a	56.67 62.22
p < 0.05		*	ns
Do × D ₁		13.89 15.56 10.00	43.33 41.11 56.67
p < 0.05		ns	ns
Do × D ₂		45.56 51.11 42.78	60.00 42.22 62.22
p < 0.05		ns	ns

$T \times Do_1$	21.67 b 36.67 a 30.83 ab	48.33 ab 68.33 a 38.33 b
$p < 0.05$	*	*
$T \times Do_2$	25.83 b 30.83 ab 43.33 a	40.00 43.33 41.67
$p < 0.05$	*	ns
$T \times Do_3$	22.50 31.67 25.00	71.67 48.33 58.33
$p < 0.05$	ns	ns
$Do \times T_1$	21.67 25.83 22.50	48.33 ab 40.00 b 71.67 a
$p < 0.05$	ns	*
$Do \times T_2$	36.67 30.83 31.67	68.33 43.33 48.33
$p < 0.05$	ns	ns
$Do \times T_3$	30.83 ab 43.33 a 25.00 b	38.33 41.67 58.33
$p < 0.05$	*	ns
$D \times T_1 \times Do_1$	10.00 b 33.33 a	36.67 60.00
$p < 0.05$	*	ns
$D \times T_1 \times Do_2$	15.00 b 36.67 a	40.00 40.00
$p < 0.05$	*	ns
$D \times T_1 \times Do_3$	10.00 b 35.00 a	70.00 73.00
$p < 0.05$	*	ns
$D \times T_2 \times Do_1$	16.67 b 56.67 a	60.00 76.67
$p < 0.05$	*	ns
$D \times T_2 \times Do_2$	15.00 b 46.67 a	43.33 43.33
$p < 0.05$	*	ns
$D \times T_2 \times Do_3$	10.00 b 53.33 a	46.67 50.00
$p < 0.05$	*	ns
$D \times T_3 \times Do_1$	15.00 b 46.67 a	33.33 43.33
$p < 0.05$	*	ns
$D \times T_3 \times Do_2$	16.67 b 70.00 a	40.00 43.33
$p < 0.05$	*	ns
$D \times T_3 \times Do_3$	10.00 b 40.00 a	53.33 63.33
$p < 0.05$	*	ns

$T \times D_1 \times Do_1$	10.00 16.67 15.00	36.67 60.00 33.33
$p < 0.05$	ns	ns
$T \times D_1 \times Do_2$	15.00 15.00 16.67	40.00 43.33 40.00
$p < 0.05$	ns	ns
$T \times D_1 \times Do_3$	10.00 10.00 10.00	70.00 46.67 53.33
$p < 0.05$	ns	ns
$T \times D_2 \times Do_1$	33.33 b 56.67 a 46.67 ab	36.67 60.00 33.33
$p < 0.05$	*	ns
$T \times D_2 \times Do_2$	36.67 b 46.67 b 70.00 a	40.00 43.33 40.00
$p < 0.05$	*	ns
$T \times D_2 \times Do_3$	35.00 53.33 40.00	73.33 50.00 63.33
$p < 0.05$	ns	ns
$Do \times D_1 \times T_1$	10.00 15.00 10.00	36.67 40.00 70.00
$p < 0.05$	ns	ns
$Do \times D_1 \times T_2$	16.67 15.00 10.00	60.00 43.33 46.67
$p < 0.05$	ns	ns
$Do \times D_1 \times T_3$	15.00 16.67 10.00	33.33 40.00 53.33
$p < 0.05$	ns	ns
$Do \times D_2 \times T_1$	33.33 36.67 35.00	60.00 40.00 73.33
$p < 0.05$	ns	ns
$Do \times D_2 \times T_2$	56.67 46.67 53.33	76.67 43.33 50.00
$p < 0.05$	ns	ns
$Do \times D_2 \times T_3$	46.67 b 70.00 a 40.00 b	43.33 43.33 63.33
$p < 0.05$	*	ns

Abbreviations. D: Day, Do: Dose, T: Temperature, ns: non significant, *:significance at $p < 0.05$

Table 11: The effects of combined treatments (different waiting times at - 20 °C and then soaking in 24 hours at different GA₃ concentrations) on germination.

Treatments		<i>Thymbra spicata</i> Germination (%)	<i>Satureja thymbra</i> Germination (%)
D	7	16.48 b	45.56
	21	43.33 a	51.11
p < 0.05		*	ns
Tm (min)	5	26.39	48.89
	10	30.56	45.00
	20	32.78	51.11
p < 0.05		ns	ns
D × Tm ₁		15.00 b 37.78 a	45.56 52.22
p < 0.05		*	ns
D × Tm ₂		16.67 b 44.44 a	42.22 47.78
p < 0.05		*	ns
D × Tm ₃		17.78 b 47.78 a	48.89 53.33
p < 0.05		*	ns
Tm × D ₁		15.00 16.67 17.78	45.56 42.22 48.89
p < 0.05		ns	ns
Tm × D ₂		37.78 44.44 47.78	52.22 47.78 53.33
p < 0.05		ns	ns
Do(ppm)	10	30.00	50.00
	50	30.83	51.11
	100	28.89	43.89
p < 0.05		ns	ns
D × Do ₁		15.56 b 44.44 a	45.56 54.44
p < 0.05		*	ns
D × Do ₂		20.56 b 41.11 a	50.00 52.22
p < 0.05		*	ns
D × Do ₃		13.44 b 44.44 a	41.11 46.67
p < 0.05		*	ns
Do × D ₁		15.56 20.56 13.33	45.56 50.00 41.11
p < 0.05		ns	ns
Do × D ₂		44.44 41.11 44.44	54.44 52.22 46.67
p < 0.05		ns	ns
Tm × Do ₁		34.17 25.00 30.83	50.00 43.33 56.67

p < 0.05	ns	ns
Tm × Do ₂	25.00 35.00 32.50	50.33 55.00 40.00
p < 0.05	ns	ns
Tm × Do ₃	20.00 31.67 35.00	38.33 ab 36.67 b 56.67 a
p < 0.05	ns	*
Do × Tm ₁	34.17 25.00 20.00	50.00 ab 58.33 a 38.33 b
p < 0.05	ns	*
Do × Tm ₂	25.00 35.00 31.67	43.33 55.00 36.67
p < 0.05	ns	ns
Do × Tm ₃	30.83 32.50 35.00	56.67 40.00 56.67
p < 0.05	ns	ns
D × Tm ₁ × Do ₁	15.00 b 53.33 a	46.67 53.33
p < 0.05	*	ns
D × Tm ₁ × Do ₂	20.00 30.00	56.67 60.00
p < 0.05	ns	ns
D × Tm ₁ × Do ₃	10.00 30.00	33.33 43.33
p < 0.05	ns	ns
D × Tm ₂ × Do ₁	16.67 33.33	40.00 46.67
p < 0.05	ns	ns
D × Tm ₂ × Do ₂	16.67 b 53.33 a	53.33 56.67
p < 0.05	*	ns
D × Tm ₂ × Do ₃	16.67 b 46.67 a	33.33 40.00
p < 0.05	*	ns
D × Tm ₃ × Do ₁	15.00 b 46.67 a	50.00 63.33
p < 0.05	*	ns
D × Tm ₃ × Do ₂	25.00 40.00	40.00 40.00
p < 0.05	ns	ns
D × Tm ₃ × Do ₃	13.33 b 56.67 a	56.67 56.67
p < 0.05	*	ns
Tm × D ₁ × Do ₁	15.00 16.67 15.00	46.67 40.00 50.00

p < 0.05	ns	ns
Tm × D ₁ × Do ₂	20.00 16.67 25.00	56.67 53.33 40.00
p < 0.05	ns	ns
Tm × D ₁ × Do ₃	10.00 16.67 13.33	33.33 33.33 56.67
p < 0.05	ns	ns
Tm × D ₂ × Do ₁	53.33 33.33 46.67	53.33 46.67 63.33
p < 0.05	ns	ns
Tm × D ₂ × Do ₂	30.00 53.33 40.33	60.00 56.67 40.00
p < 0.05	ns	ns
Tm × D ₂ × Do ₃	30.00 b 46.67 ab 56.67 a	43.33 40.00 56.67
p < 0.05	*	ns
Do × D ₁ × Tm ₁	15.00 20.00 10.00	46.67 56.67 33.33
p < 0.05	ns	ns
Do × D ₁ × Tm ₂	16.67 16.67 16.67	40.00 53.33 33.33
p < 0.05	ns	ns
Do × D ₁ × Tm ₃	15.00 25.00 13.33	50.00 40.00 56.67
p < 0.05	ns	ns
Do × D ₂ × Tm ₁	53.33 30.00 30.00	53.33 60.00 43.33
p < 0.05	ns	ns
Do × D ₂ × Tm ₂	33.33 53.33 46.67	46.67 56.67 40.00
p < 0.05	ns	ns
Do × D ₂ × Tm ₃	46.67 40.00 56.67	63.33 40.00 56.67
p < 0.05	ns	ns

Abbreviations. D: Day, Do: Dose, Tm: Time, ns: non significant, *:significance at p < 0.05

4. Conclusions

This study confirms that gibberellic acid breaks seed dormancy, increase germination percentage and accelerate the germination. Furthermore research results show that combination of hot and cold treatments with

gibberellic acid increases germination activity even more. The increase in temperature increases enzyme activities and thus promotes germination.

References

- Açıkgöz, N., Akbaş, M.E., Moghaddam, A., Özcan, K. (1994). *TARİST: PC 'ler için veritabanı esaslı Türkçe istatistik paketi*. I. Tarla Bitkileri Kongresi 25-29 Nisan, Bitki Islahı Bildirileri, pages: 264-267, İzmir, Turkey.
- Anonymous, (2019). Crop Production Statics. <https://biruni.tuik.gov.tr>.
- Aslan, R., Karakuş, Z. (2019). Gelenekten günümüze tıbbi ve aromatik bitkiler. *Göller Bölgesi Aylık Hakemli Ekonomi ve Kültür Dergisi Ayrıntı* 6(73): 60-66.
- Başalma, D., Er, C. (2014). *Tohum ve Tohumculuk*. Nobel Akademik Yayıncılık, Ankara, Turkey.
- Baydar, H. (2019). *Tıbbi ve Aromatik Bitkiler Bilimi ve Teknolojisi*. Nobel Akademik Yayıncılık, Ankara, Turkey.
- Bekut, M., Brkic, S., Kladar, N., Dragovic, G., Gavaric, N., Bozin, B (2018). Potential of selected Lamiaceae plants in anti(retro) viral therapy. *Pharmacological Research* 133: 301-314. doi: 10.1016/j.phrs.2017.12.016
- Bozdemir, Ç. (2019). Economic importance and usage fields of Oregano species growing in Turkey. *YYU Journal of Agricultural Science* 29(3): 583-594. doi: 10.29133/yyutbd.511777
- Cinbilgel, I. (2019). Oregano and/or marjoram: Traditional oil production and ethnomedical utilization of *Origanum* species in southern Turkey. *Journal of Herbal Medicine* 16: 100257. <https://doi.org/10.1016/j.hermed.2019.100257>
- Çatav, Ş.S., Belar, İ., Ateş, B.S., Ergan, G., Oymak, F., Ülker, E.F., Tavşanoğlu Ç. (2012). Germination response of five eastern Mediterranean woody species to smoke solutions derived from various plants. *Turkish Journal of Botany* 36(5): 480-487. doi: 10.3906/bot-1111-12
- Çatav, Ş.S., Küçükakyüz, K., Akbaş, K., Tavşanoğlu, Ç. (2014). Smoke-enhanced seed germination in Mediterranean Lamiaceae. *Seed Science Research* 24: 257-264. doi: 10.1017/S0960258514000142
- Duletic-Lausevic, S., Alimpic Aradski, A., Savikin, K., Knezevic, A., Milutinovic, M., Stevic, T., ... Marin, P.D. (2018). Composition and biological activities of Libyan *Salvia fruticosa* Mill. and *S. lanigera* Pour. extracts. *South African Journal of Botany* 117: 101-109. doi: 10.1016/sajb.2018.05.013
- Fletcher, R.A., Sopher, E.R. (2000). *Regulation of gibberelins: Is crucial for plant stress protection in Plant Growth Regulators in Agriculture*

- and Horticulture ed. A.S.Bas-ra, Food Products Press, New York.
- Göktaş, Ö., Gıdık, B. (2019). Uses of Medicinal and Aromatic Plants. *Bayburt Üniversitesi Fen Bilimleri Dergisi 2(1)* : 136-142. dergipark.gov.tr/bufbd
- Güner, A. (Ed.) (2014). *Illustrated Flora of Turkey, Vol.1*. Ali Nihat Gökyiğit Vakfı, Flora Araştırma Derneği and Türkiye İş Bankası Kültür Yayınları yayını, İstanbul, Turkey.
- Hayta, E., Arabacı, O. (2011). Determining different germination techniques on the seeds of some plant genus named as thyme. *Adnan Menderes Üniversitesi Ziraat Fakültesi Dergisi 8(1)* : 91-101.
- Hopkins, G.W., Hüner, N.P.A. (2004). *Introduction to Plant Physiology. 3rd edition*. John Wiley and Sons Inc, United States of America.
- Karakurt, H., Aslantaş, R., Eşitken, A. (2010). The environmental factors and some pre-treatments affecting on seed germination and plant growth. *Journal of Agricultural Faculty of Uludağ University 24(2)*: 115-128.
- Karpiński, T.M. (2020). Essential oils of Lamiaceae family plants as antifungals. *Biomolecules 10*: 103. doi: 10.3390/biom10010103
- Katar, D., Katar, N., Can, M. (2019). *Farklı azot dozlarının Anadolu adaçayı (Salvia triloba Mill.)'nda verim ve verim komponentleri üzerine etkisinin belirlenmesi. Pages 33- 45 in Demir, H. ed. II. International Agriculture and Forest Congress Proceeding Book. 1st ed. Asos yayınevi, Elazığ, Turkey.*
- Kazancı, D.D., Tavşanoğlu, Ç. (2019) Heat shock-stimulated germination in Mediterranean basin plants in relation to growth form, dormancy and distributional range. *Folia Geobotanica 54*: 85-98. <https://doi.org/10.1007/s12224-019-09349-0>
- Kirkan, B., Sarikurkcu, C., Amarowicz, R. (2019). Composition and antioxidant and enzyme-inhibition activities of essential oils from *Satureja thymbra* and *Thymbra spicata* var. *spicata*. *Flavour Fragrance Journal 34*: 436-442. <https://doi.org/10.1002/ffj.3522>
- Mesquita, L.S., Luz, T.R., Mesquita, J.W., Coutinho, D.F., Amaral, F.M., Ribeiro, M.N., & Malik, S. (2019). Exploring the anticancer properties of essential oils from family Lamiaceae. *Food Reviews International 35(2)*: 105-131. <https://doi.org/10.1080/87559129.2018.1467443>
- Özcan, İ.İ., Arabacı, O., Öğretmen, N.G. (2014). The determination of different germination applications on some sage species. *Turkish Journal of Agriculture-Food Science and Technology 2(5)*: 203-207.
- Özyazıcı, G., Kevseroğlu, K. (2019). Effects of ontogenic variability on yield of some labiatae family (*Mentha spicata* L., *Origanum onites* L., *Melissa officinalis* L., *Lavandula angustifolia* Mill.) plants. *Turk Journal of Agricultural Research 6(2)*: 174-185. doi: 10.19159/tutad.510877

- Paşa, C., Kılıç, T., Selvi, S., Özer Sağır, Z. (2019). Determination of essential oil ratio and essential oil components by applying different drying methods of *Satureja cuneifolia* Ten. (Lamiaceae) species. *Journal of the Institute of Science and Technology* 9(4): 2330-2335. doi: 10.21597/jist.553810
- Rahman, M.S., Chakraborty, A., Mazumdar, S., Nandi, N.C., Bhuiyan, M.N., Alauddin, S.M.,...Hossain Jakir, M. (2020). Effects of poly(vinylpyrrolidone) protected platinum nanoparticles on seed germination and growth performance of *Pisum sativum*. *Nano-Structures & Nano-Objects* 21: 100408. <https://doi.org/10.1016/j.nanoso.2019.100408>
- Rizzo, R., Verde, G., Sinacori, M., Maggi, F., Cappellacci, L., Petrelli, R., ... Benelli, G. (2020). Developing green insecticides to manage olive fruit flies? Ingestion toxicity of four essential oils in protein baits on *Bactrocera oleae*. *Industrial Crops & Products* 143: 111884. <https://doi.org/10.1016/j.indrop.2019.111884>
- Sadikoğlu, N., Ozhatay, N. (2019). Outer and inner morphological characteristics of *Satureja* and *Thymbra* taxa exported as Oregano from Turkey II. *EMU Journal of Pharmaceutical Sciences* 2(1): 13-32.
- Sarropoulou, V., Maloupa, E. (2019). In vitro propagation of *Satureja thymbra* L. (Lamiaceae) : A valuable aromatic-medicinal native plant of the Mediterranean region. *GSC Biological and Pharmaceutical Sciences* 9(2) : 9-20. <https://doi.org/10.30574/gscbps.2019.9.2.0190>
- Sharifi-Rad, M., Ozcelik, B., Altın, G., Daşkaya-Dikmen, C., Martorell, M., Ramirez- Alarcon, K., ... Sharifi-Rad, J. (2018). *Salvia* spp. plants-from farm to food applications and phytopharmacotherapy. *Trends in Food Science & Technology* 80: 242-263. <https://doi.org/10.1016/j.tifs.2018.08.008>
- Shu, K., Liu, X., Xie, Q., He, Z. (2016). Two faces of one seed: hormonal regulation of dormancy and germination. *Molecular Plant* 9: 34-45. doi: 10.1016/j.molp.2015.08.010
- Sönmez, Ç., Gökçöl, A., Şimşek Soysal, A.Ö., Bayram, E., Çelen, A.E. (2019). Research on germination and emergence performance enhancing treatments on sage (*Salvia* spp.) species. *Turkish Journal of Agriculture-Food Science and Technology* 7(3): 504-510. <https://doi.org/10.24925/turjaf.v7i3.504-510.2318>.
- Stefanaki, A., Cook, C.H., Lanaras, T., Kokkini, S. (2018). Essential oil variation of *Thymbra spicata* L. (Lamiaceae), an East Mediterranean “oregano” herb. *Biochemical Systematics and Ecology* 80: 63-69. <https://doi.org/10.1016/j.bse.2018.06.006>
- Seçmen, Ö., Gemici, Y., Görk, G., Bekat, L., Leblebici, E. (2011). *Tohumlu Bitkiler Sistematigi*. Ege Üniversitesi Yayınları, İzmir, Turkey.
- Tahiroğlu, M. (2016). *The production possibilities with seeds of thyme (Thymbra spicata L.) in Kadirli conditions*. Msc, University of Çukurova, Adana, Turkey.
- Tepe, B., Cilkiz, M. (2016). A pharmacological and phytochemical overview on *Satureja*. *Pharmaceutical Biology* 54(3): 375-412. doi: 10.3109/13880209.2015.1043560
- Tuzlacı, E. (2006). *Şifa niyetine Türkiye'nin bitkisel halk ilaçları*. Alfa Yayınları,

İstanbul, Turkey.

- Usanmaz Bozhüyük, A., Kordali, Ş. (2019). Investigation of the toxicity of ethanol extracts obtained from six different *Satureja* L. species on Colorado Potato Beetle, *Leptinotarsa decemlineata* (Say, 1824), (Coleoptera: Chrysomelidae). *Anatolian Journal of Botany* 3(1): 69-79. doi: 10.30616/ajb.623827
- Ünal, K., Sağlam, A.C. (2018). Determination of essential oil composition, total antioxidant activity, total phenolic and Flavanoid contents of Anatolian sage (*Salvia fruticosa* Mill.) populations in Marmara region. *Journal of AARI* 28(2): 37-47.



Chapter 7

THE RECENT ELECTROCHROMIC STUDIES BASED ON NICKEL OXIDE-CONDUCTING POLYMER HYBRID MATERIALS

Esin EREN¹

¹ Öğretim Görevlisi Dr , Department of Energy Technologies, Innovative Technologies Application and Research Center, Suleyman Demirel University, Department of Chemistry, Faculty of Arts and Science, Suleyman Demirel University, esineren@sdu.edu.tr

1. Introduction

Electrochromism is a reversible alteration in the optical features (color, transmittance, absorbance, reflectance) of a compound, in response to electrochemical oxidation or reduction at different potentials (Jittiarporn *et al.* 2017; Eren *et al.* 2017, 2018a). In 1932, the term ‘electrochromism’ was utilized to explain physical phenomena of Franz–Keldish and Stark’s influences (Invernale *et al.* 2009). The first electrochromic device (ECD) with tungsten trioxide (WO_3) was produced by Deb in 1969 (Deb, 1969). By the mid-1970, the electrochromic devices were being advanced for displays (Lampert, 2004). In 1978, electrochromic memory displays using small-molecule organic materials, viologen and its derivatives, were first investigated (Schoot *et al.* 1978). Since then, the term ‘electrochromic materials’ has assigned as the family of polymers and small molecules which show reversible color changes as a result of electrochemical reactions (Invernale *et al.* 2009). Electrochromic materials possess major benefits (Lampert, 2004).

- A small voltage to switch (1-5 V);
- Display specular reflection;
- Having a gray scale;
- Necessitate power only during switching;
- Display adjustable memory, up to 12-48 hours.

Electrochromic compounds and devices must be described with regard to capability for transmitting and reflecting luminous and solar radiation. These features can be familiarized via contemplating the spectra displayed in Figure 1. As seen Figure 1a, thermal radiation is managed by black-body spectra for the indicated four temperatures- multiplied via an empirical emittance less than one; obviously this radiation is at λ (wavelength) $>2 \mu\text{m}$ for normal ambient temperatures. Solar radiation impinging onto Earth’s atmosphere can be displayed via blackbody-like radiation for the Sun’s surface temperature (5505 °C) and covers $0.2 < \lambda < 3 \mu\text{m}$. At ground level, and for normal clear weather, this radiation is as displayed in Figure 1b; the sharp minima arise from molecular absorption. Luminous radiation ultimately characterized by the curve (Figure 1b). Luminous radiation lies in the range of $0.4 < \lambda < 0.7 \mu\text{m}$ and the peak is at $0.55 \mu\text{m}$. Quantitative information for luminous (lum) and solar (sol) transmittance demonstrated as T_{lum} and T_{sol} , respectively. Equation (1) can be used for calculation of $T_{\text{lum(sol)}}$, as given below (Granqvist *et al.* 2017, 2018):

$$T_{\text{lum.sol}} = \int d\lambda \phi_{\text{lum.sol}}(\lambda) T(\lambda) / \int d\lambda \phi_{\text{lum.sol}}(\lambda) \quad (1)$$

Where $T(\lambda)$ is spectral transmittance, ϕ_{lum} is the eye's spectral sensitivity and ϕ_{sol} denotes 'the air mass 1.5' solar irradiance spectrum (with the sun being 37° above the horizon) (Granqvist *et al.* 2018)

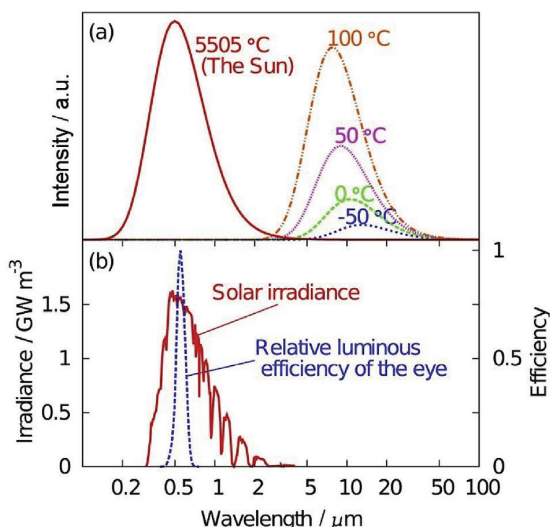


Figure 1. (a) Blackbody spectra for the shown temperatures (b) Typical solar irradiance spectrum for clear weather, and relative spectral sensitivity of a light-adapted eye (From Ref. (Granqvist *et al.* 2018)).

In general, electrochromic compounds can be divided into two major groups: **1)** inorganic materials consist of transition metals and metal oxides, prussian blue systems (Hedley *et al.* 2018), and lanthanide coordination complexes, etc. (Rowley & Mortimer, 2002) **2)** organic materials consist of viologen derivatives (1,1'-dialkyl 4,4'-bipyridinium dications) (Madasamy *et al.* 2019), TTF (tetra thiafulvalene) derivatives (Wang *et al.* 2004), TCNQ (tetra cyanoquino-dimethane) derivatives (Wang *et al.* 2013), quinones (Xu *et al.* 2013), conducting polymers such as polythiophene (PTh) (Camurlu *et al.* 2004), polyaniline (PANI) (Eren *et al.* 2018a), polypyrrole (PPy) (Camurlu *et al.* 2014), etc.

This chapter will be focussed solely on nickel oxide-conducting polymer hybrid materials for applications of electrochromic devices.

2. Electrochromic Devices (ECDs)

A schematic of the electrochromic device (ECD), represented in Figure 2, includes an active electrochromic electrode layer, a counter electrode layer, an electrolyte layer detaching the two electrodes, two transparent conductive layers using as electrical leads and the supporting substrates (Runnerstrom *et al.* 2014).

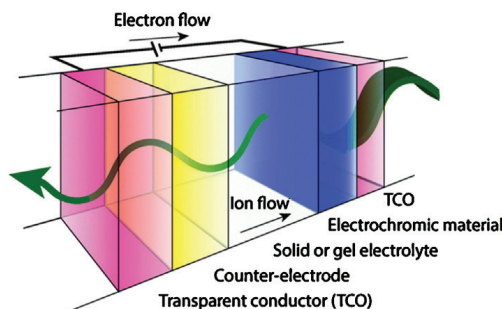


Figure 2. Generic five-layer electrochromic device design. Arrows represent transport of ions under the action of an electric field (From Ref. Runnerstrom *et al.* 2014).

Whereas the conductive electrode (such as ITO-coated glass, etc.) was used as counter electrode for single-layer-electrochromic device, the secondary electrochromic film was used as counter electrode for a complementary electrochromic device (Eren *et al.* 2018b). In the complementary ECD construction, one of electrochromic film is anodic coloring material while the other is cathodic coloring material. In such ECD device construction both electrochromic films are colored and bleached simultaneously, so the optical contrast enhances (Patel *et al.* 2017).

Recent advances in solid-state ECDs have focused onto preparing electrochromic film into a single step and low-waste procedure to reduce the environmental effect of the chemical industry (Ding *et al.* 2011). For example, an UV-curing approach merges the electrolyte and electrochromic material in one conductive substrate sandwiching between two conductive substrates such as ITO coated electrode (Ding *et al.* 2011; Invernale *et al.* 2010). As shown in Figure 3, such a single-layer “all-in-one” device is the similar as the traditional electrochromic device except for joining of electrolyte and monomer/polymer active layers into single layer. As shown in Figure 3b, the construction of such ECDs was summarized below (Ding *et al.* 2011):

- i. Fabrication of the pre-polymer electrolyte with monomer
- ii. Covering of the prepared solution onto a conductive electrode
- iii. Adding onto a second conductive electrode
- iv. Photo or thermal crosslinking to occur the gel electrolyte
- v. Implementation of an suitable potential voltage to induce polymerisation of the monomer

Recently, the hybrid-based flexible with WO_3 and PEDOT was also fabricated using uv-curable electrolyte in a single layer (Eren *et al.* 2020). As a result, uv-curing method can be acknowledged as relatively simple,

energy saving and protecting for the environment (Eren *et al.* 2020).

The working principle of the ECD is connected with ion transfer between the transparent electrical conductors. When a suitable voltage is applied to conductive electrodes, migration of ion is formed between the counter electrode and the working electrode. The electrons injected from conductive electrode then occur alternation in the optical features of the electrochromic material. Upon reversing applied potential, the ECD returns to its original state (Invernale *et al.* 2009).

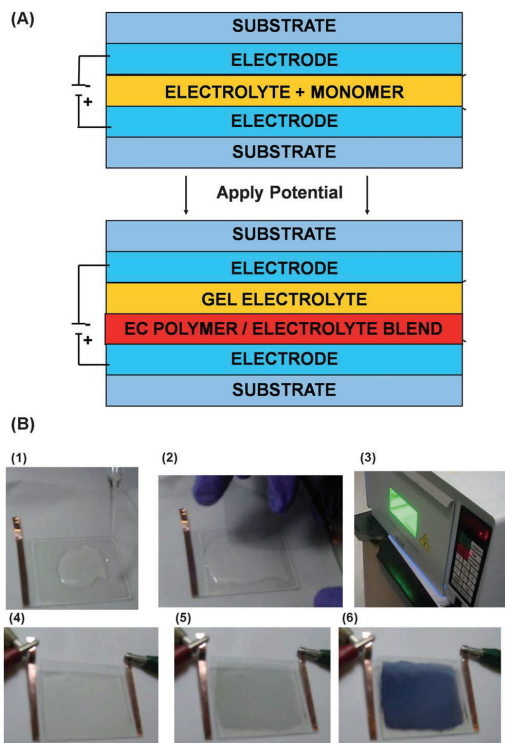


Figure 3. A) Schematic presentation of in-situ ECD structure. In the published article, SUBSTRATE= PET, ELECTRODE= ITO, and the numerous electrolyte/ monomer compositions are stated B) (1) Implement solution; (2) Put counter electrode a top; (3) UV cure; (4) implement a suitable voltage; (5) oxidized state; and (6) neutral state. (From Ref. (Ding *et al.* 2011)).

Commercialization of ECDs depends on their response time (switching time), optical contrast, coloration efficiency and durability.

Electrochromic contrast (optical contrast) is generally calculated the percent transmittance change ($\Delta\%T$) of the electrochromic material at a certain wavelength, as shown in Equation 2 (Eren *et al.* 2017):

$$\Delta T = T_{\text{bleached}} - T_{\text{colored}} \quad (2)$$

where T_{bleached} (%) and T_{colored} (%) are the transmittance of the ECD in the bleached state and coloured state, respectively. While the difference between bleached and colored state will give the highest values at certain wavelength, more accurate measurement should be also utilized (Invernale *et al.* 2009). Photopic contrast includes the whole visible spectrum weighted to the sensitivity of the human eye (Invernale *et al.* 2009). Thus, photopic contrast provides more accurate value when compared to the generally published contrast at a single wavelength (Yumin *et al.* 2019). Equation (3) was used to calculate the corresponding photopic transmittance (Yumin *et al.* 2019):

$$T_{\text{photopic}} = \frac{\int_{\lambda_{350}}^{\lambda_{850}} T(\lambda) S(\lambda) P(\lambda) d\lambda}{\int_{\lambda_{350}}^{\lambda_{850}} S(\lambda) P(\lambda) d\lambda} \quad (3)$$

where $T(\lambda)$ is the spectral transmittance of the device, $S(\lambda)$ is the normalized spectral emittance of a 6000 K blackbody and $P(\lambda)$ is the normalized spectral response of the human eye.

Switching time, which is one of the most significant factors in terms of ECD performance is described as the time needed to implement switching between the bleached and colored states. The switching time of electrochromic material is connected with some characteristics such as the electrolyte ionic conductivity, greatness of the performed potential, the film thickness, the film morphology (Thakur *et al.* 2012).

Coloration efficiency (CE) is the significant fundamental factor to evaluate the power necessity of an electrochromic compound (Thakur *et al.* 2012). The CE was calculated using the following equations (4, 5) (Eren *et al.* 2017):

$$\Delta OD = \log \frac{T_{\text{bleached}}}{T_{\text{colored}}} \quad (4)$$

$$CE = \frac{\Delta OD}{Q} \quad (5)$$

where T_{bleached} (%) and T_{colored} (%) are the transmittance of the ECD in the bleached and the colored state, respectively, OD is optical density, Q is the intercalated charge per unit area.

Stability: The device durability towards repetitive redox cycles generally confines the benefits of electrochromic materials in application area. This situation can be explained by electrochemical redox degradation due to irreversible oxidation or reduction at excessive voltages, iR damage of the electrode or the electrolyte, side reaction with water or oxygen in the device. As a result, the loss in electrochromic contrast can be obtained (Thakur *et al.* 2012).

Thus, the targeted characteristics for electrochromic device performance devices can be given a summary as below (Thakur *et al.* 2012):

- ❖ High electrochromic efficiency
- ❖ High optical modulation
- ❖ Short switching time
- ❖ High durability

2.1. Application Areas

Electrochromic materials are generally used in various fields of technology such as smart windows, smart switchable window applied in Boeing aircraft, rear-view mirrors for automobiles, electrochromic eyewear, e-papers, low cost displays (Figure 4). (Yang *et al.* 2016; Korgel (2013); Österholm *et al.* 2015). Two conductive substrates are separated via an electrolyte compound in electrochromic window. The electrochromic window is in Bright Mode under open circuit potential. In Bright mode, both working and counter electrodes are transparent to solar radiation, supplying heat and natural light to go into the room. Under the reduced voltage upto a moderate value, the window modifies to Cool mode, obstructing heat while supplying natural light to come into the room. At lower voltages, the window modifies to Dark Mode, confining the quantity of heat and natural light that go into the room (Yang *et al.* 2016; Korgel (2013)). Thus, EC smart windows are significant helpful for its aesthetics glazing to decrease glare and entering solar irradiation into the buildings, decreasing the energy consumption of air conditioning in building by 26 %, low energy consumption and a good memory effect (Eh *et al.* 2018).

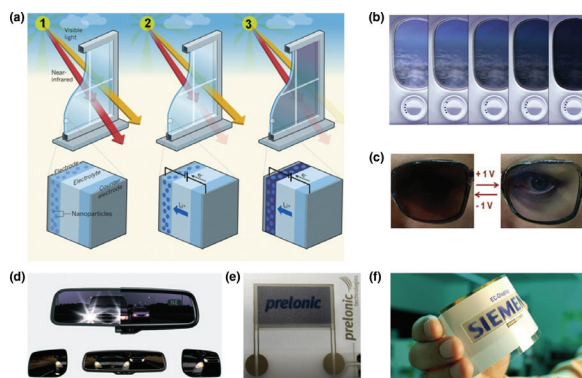


Figure 4. Applications of electrochromic devices. (a) Design of electrochromic window (b) Smart switchable window applied in Boeing aircraft produced by SmartTint (c) Photographs of the electrochromic lens (d) Automatic dimming mirror based on electrochromism produced by Gentex. Printable and flexible electrochromic displays designed by (e) Preonic Technologies and (f) Siemens (From Refs. Yang *et al.* 2016; Korgel (2013); Österholm *et al.* 2015)

3. Materials for ECD

3.1. Transition Metal Oxides

Electrochromic transition metal oxides can display several valence states upon electrochemical reduction process. Electrochromic materials can be divided into two kinds: in cathodic oxides, color change occurs upon charge insertion (electrochemical reduction process), while in anodic oxides color transition forms upon charge extraction (electrochemical oxidation process) (Patel *et al.* 2017). The widely investigated electrochromic materials are WO_3 , TiO_2 , Nb_2O_5 , MoO_3 , Ta_2O_5 (Eren *et al.* 2018a; Kiristi *et al.* 2014; Patel *et al.* 2017). The well-known anodic coloration materials are NiO , IrO_2 , Cr_2O_3 , MnO_2 , FeO_2 (Patel *et al.* 2017; Park *et al.* 2016). V_2O_5 shows both anodic and cathodic electrochromic properties based on its oxidation state (Patel *et al.* 2017; Eren *et al.* 2018b). Figure 5 displays three situations of significant for electrochromic oxides. Especially, the left side of Figure 5, for H_xWO_3 , displays an O2p band that is allocated from a split d band via an energy gap. Pure WO_3 owns a full O2p band and an empty d band, and the band is broad sufficient to render WO_3 electrochromic films of transparent. Middle side of Figure 5 belongs to anodically colouring electrochromic oxides. These electrochromic oxides can be defined as owning unoccupied t_{2g} states, and ions and electrons insertion may be formed to these filled states to the top of the band suggesting that the material shows a gap between the e_g and t_{2g} levels. The band is broad enough to give transparent color. The right side of Figure 5 displays V_2O_5 that owns both cathodic and anodic electrochromic features depending on diverse electronic structure (Granqvist *et al.* 2018).

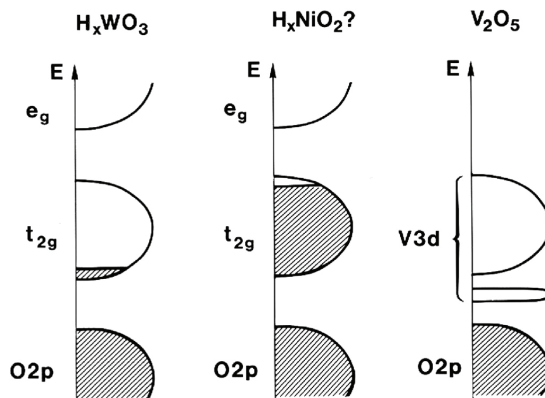
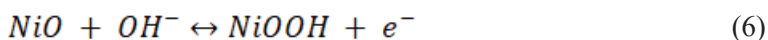


Figure 5. Schematic band structures for diverse situations of EC oxides. Shaded areas show filled states and E is energy. The pertinent chemical species are demonstrated at the top; some uncertainty prevails for the Ni-containing species (From Ref. Granqvist *et al.* 2018).

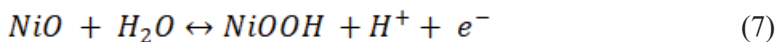
3.1.1. Nickel Oxide (NiO)

Nickel oxide (NiO) is one of the most widely studied transition metal oxide because of its high coloration efficiency, good cyclic reversibility, large dynamic range and low material cost (Cai *et al.* 2012). The conversion from a colored to a bleached state is associated with a multiple valances of Ni ions in Nickel oxide because of the alternation of Ni3d electrons (Lee *et al.* 2020).

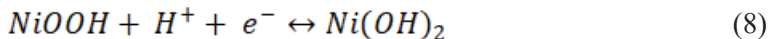
Various methods consisting of electrochemical, sputtering, vacuum deposition, thermal evaporation, spray pyrolysis, sol-gel have been used to prepare NiO-based films (Nakaoka *et al.* 2004; Avendaño *et al.* 2006). NiO-based film was used for both electrochromic and supercapacitor applications. NiO film can also be used as the potential charge storing electrochromic film (Jamdegni & Kaur, 2020). The coloration process of nickel oxide film belongs to the oxidation occurring before the oxygen evolution reaction which can be shown as the following electrochemical reaction (Cai *et al.* 2012) (6, 7):



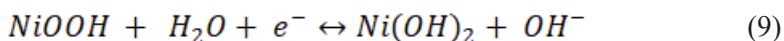
or



The bleaching process belongs to the reduction peak which can be described as the following electrochemical reactions (Cai *et al.* 2012) (8,9):



or



However, some features restrict its traditional improvement including slow response time, low electrical conductivity, poor cycling stability (Cai *et al.* 2012, Li *et al.* 2020). Recently, various studies were performed to enhance NiO electrochromic performance. Much scientific research focused on the study of adjustable crystal structure, controllable surface morphology and tunable structure of NiO, preparation of NiO-based composites (Liu *et al.* 2015, Li *et al.* 2020). One approach for its adjustable electronic structure is through doping with suitable elements that allow it to improve the optical features and the durability of NiO-based films (Li *et al.* 2020). For instance, Lee *et al.* fabricated tungsten-doped nickel oxide-based electrochromic devices with improved stability. The colored state and bleached state of ECD were displayed in Figure 6. ECD device using $Ni_{1-x}W_x$ (x: 0.024) as counter electrode and WO_3 as working electrode indicated relatively durability optical contrast with %2 loss from 100 to 1000 cycles.

Columnar nanostructure occurred gradually dense with enhancement of W content, which may lead to the decreased optical contrast and the increased durability. This situation can be explained by the reduced deep trap sites (Lee *et al.* 2020). Moreover, they produced flexible ECD using $\text{Ni}_{1-x}\text{W}_x$ (x : 0.024) as counter electrode and WO_3 as working electrode, as displayed in Figure 7. During the repetitive cycles until 1000 cycles, the prepared flexible ECD demonstrated considerable electrochromic stability with attaining optical contract of 40%. The color of flexible ECDs altered from light yellow to deep blue (Lee *et al.* 2020).

Wang *et al.* showed that the electrolyte pH owns an important influence on the NiOx films in borate electrolyte medium. In this study, pH values were selected as 7, 9, 11 to evaluate the prepared NiOx films and the corresponding electrochromic features (Wang *et al.* 2020). As seen in Figure 8a, the highest optical modulation was obtained as 87% for the nickel oxide film prepared under pH 9 medium for 2 h. The cyclic durability of the the nickel oxide film fabricated at pH 9 was performed using cyclic voltammetry measurement. As seen in Figure 8b, while the reduction peaks changed in the direction of negative potentials, the oxidation peaks changed slightly in the direction of positive potentials during the first twenty cycles. At the 40th cycle, the electrochromic film was nearly wholly peeled from the substrate. According to chronoamperometry curves, the NiO_x -9 films showed a faster response times (t_b : 5.4 s, t_c : 6.2 s), when compared with that of NiOx prepared under different pH medium (Figure 8c). Optical memory evaluation for two different states of the NiOx film prepared at pH9 was shown in Figure 8d. Although the colored NiOx film displayed a weakening of 24.2% after 5h, the weakening slowly for at least 48 h, which infers that the nickel oxide film had good optical memory for prolonged times after elimination of the powersupply (Wang *et al.* 2020).

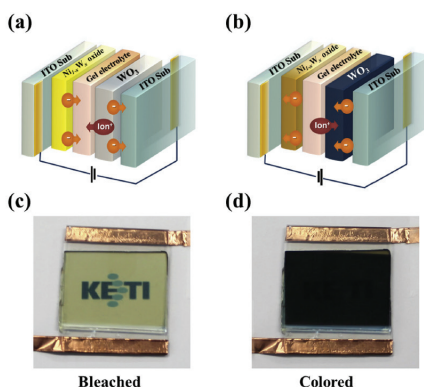


Figure 6. Schematic and optical images of ECD using $\text{Ni}_{1-x}\text{W}_x$ (x : 0.024) as counter electrode at the a), c) bleached state and b) d) colored state, respectively (From Ref. Lee *et al.* 2020).

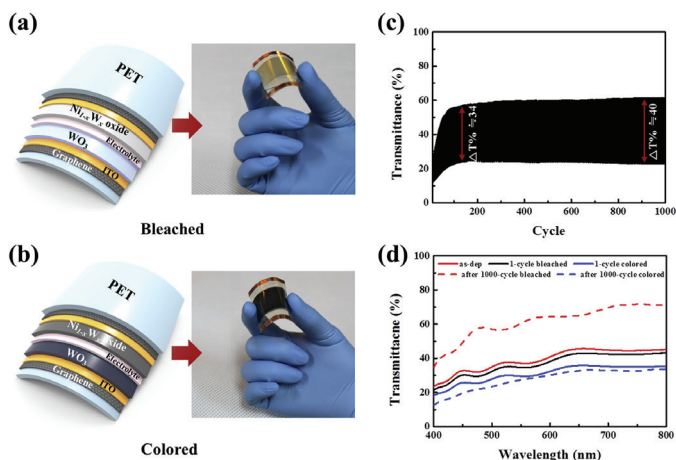


Figure 7. Schematic diagrams and optical images of flexible EC devices using *c*-ITO/graphene/PET transparent electrode at the (a) bleached state and (b) colored state. (c) In situ transmittance modulation at 550 nm upon continuous potential cycling (+1.5 ~ -1.5 V) and (d) transmittance spectra for flexible EC devices (From Ref. Lee et al. 2020).

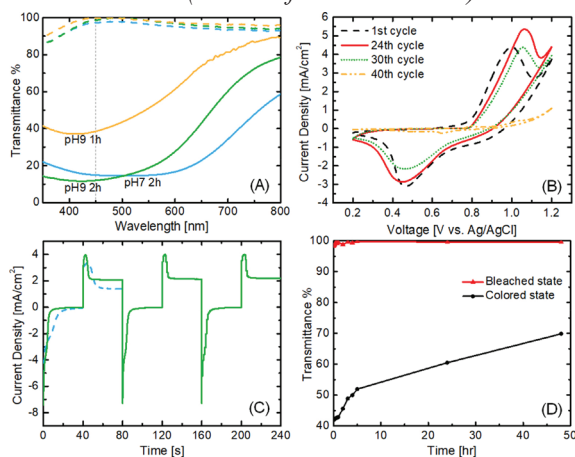


Figure 8. a) Optical transmittance spectra of the NiO_x prepared at different pH medium, b) CVs durability investigation of the NiO_x film prepared at pH9, c) chronoamperometry curves of the NiO_x films at prepared at pH7 (blue dashed line), and pH9 (green line) in 0.1 M $\text{K}_2\text{B}_4\text{O}_7$ electrolyte, d) Optical memory investigation for the bleached (red) and colored (black) states of the NiO_x film prepared at pH9 (From Ref. Wang et al. 2020).

Li et al. synthesized one-dimensional copper (Cu)-doped NiO nanofibers using electrospinning method and their electrochromic characteristics were evaluated (Li et al. 2020). $\text{Ni}_{0.97}\text{Cu}_{0.03}\text{O}$ nanofibers showed enhanced electrochromic performance, containing fast response time (t_c : 1.6 s, t_b : 0.9s), high optical contrast (73% at 550 nm), high coloration efficiency ($77.9 \text{ cm}^2\text{C}^{-1}$), good cycling stability (80% after 2000th cycles)

when compared with undoped NiO nanofibers (Figure 9). The improved electrochromic performance can be ascribed to the synergetic effect of the 1D nanostructures with the decreased granule size and superior electrical conductivity (Li *et al.* 2020).

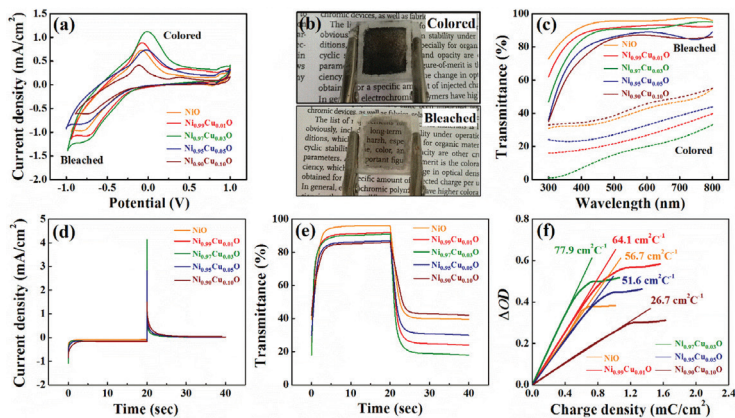


Figure 9. (a) CV curves of $\text{Ni}_{1-x}\text{Cu}_x\text{O}$ ($x = 0, 0.01, 0.03, 0.05$ and 0.1) nanofibers; (b) Digital photographs of $\text{Ni}_{0.97}\text{Cu}_{0.03}\text{O}$ nanofibers based EC device in colored state and bleached state; (c) Optical transmittance spectra of $\text{Ni}_{1-x}\text{Cu}_x\text{O}$ ($x = 0, 0.01, 0.03, 0.05$ and 0.1) nanofibers in bleached and colored states; (d) CA curves for $\text{Ni}_{1-x}\text{Cu}_x\text{O}$ ($x = 0, 0.01, 0.03, 0.05$ and 0.1) nanofibers with voltage interval from -1.0 V (20 s) to 1.0 V (20 s); (e) Corresponding transmittance of $\text{Ni}_{1-x}\text{Cu}_x\text{O}$ ($x = 0, 0.01, 0.03, 0.05$ and 0.1) nanofibers at 550 nm ; (f) Variation of optical density (ΔOD) vs. charge density for $\text{Ni}_{1-x}\text{Cu}_x\text{O}$ ($x = 0, 0.01, 0.03, 0.05$ and 0.1) nanofibers (From Ref. Li *et al.* 2020).

3.1.2. Electrochromic Nickel Oxide (NiO)-Conducting Polymer Hybrids

It is well-known that the hybrid electrochromic material can show enhanced optical features than those of individual material (Liu *et al.* 2015). The NiO/Polyaniline (PANI) composite film consisting of highly porous was successfully produced via assembling chemical bath deposition and electrochemical deposition methods, consecutively (Xia *et al.* 2008). As seen in Figure 10, the NiO/PANI film displayed a significant electrochromism with reversible various color alternations under different applied potentials. Optical modulation was calculated as up to 56% at 550 nm for NiO/PANI film (Xia *et al.* 2008).

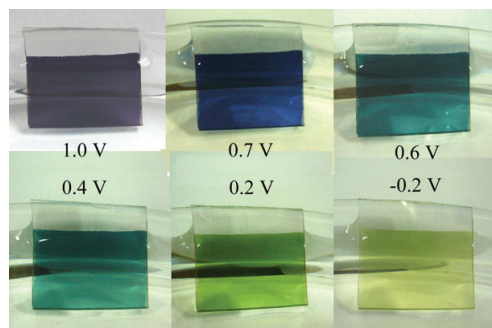
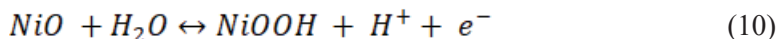
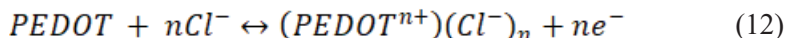
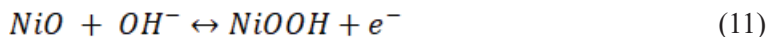


Figure 10. Photographs of a sample with a size of $2.5 \times 2.5 \text{ cm}^2$ under diverse applied voltages (From Ref. Xia *et al.* 2008).

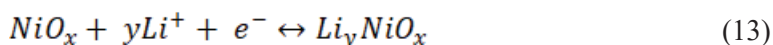
One year later, the same group prepared NiO/poly(3,4-ethylenedioxythiophene) composite thin film by the same methods mentioned preparation of NiO/PANI composite (Xia *et al.* 2009). Multicolor electrochromism having various color change containing purple, light blue brown was attained for the NiO/PEDOT composite film. Compared with the NiO film, the higher current values were obtained for NiO/PEDOT film because of higher electrochemical activity. The electrochemical processes occurred in NiO/PEDOT film can be shown by the following electrochemical reactions (Xia *et al.* 2009):



or



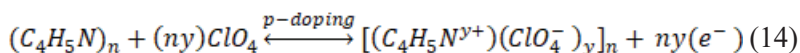
Sonavane *et al.* prepared nickel oxide/polypyrrole (NiO/PPy) thin films by using simple electrodeposition and chemical bath deposition (CBD) (Sonavane *et al.* 2010a). The NiO/PPy exhibited improved electrochromic features than their individual components. The improved situation may be explained with the chemical bonding between them. The alternation from NiO_x to Li_yNiO_y after intercalation and deintercalation of Li^+ ions results in alternation from Ni^{+3} to Ni^{+2} . Due to alternation in charge form Ni^{+2} to Ni^{+3} , the NiO film changed from transparent color to brownish gray color (Figure 11a). A simplified electrochemical reaction for NiO film was shown in Eq. 13:



Transparent Colored (Brownish gray)

Upon reduction process, PPy film became orange-yellow color and

return to black-violet under oxidization process (Figure 11b). The reaction can be shown in Eq. 14:



Insulating (Orange-yellow) Conducting (Black-violet)

As seen in Figure 11c, the color of NiO/PPy film appeared brown-yellow, black-violet under +1.5, -1.5 V applied voltages, respectively (Sonavane *et al.* 2010a).

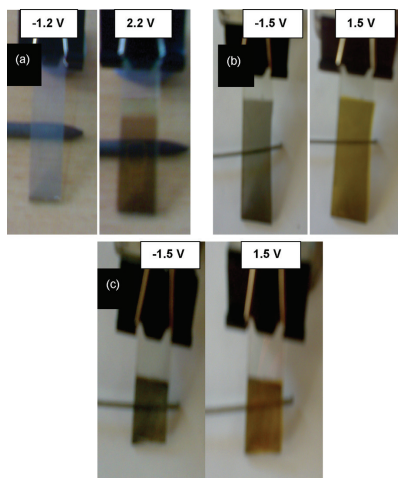


Figure 11. Photographs of a sample (a) NiO, (b) PPy and (c) NiO/PPy under diverse applied voltages (From Ref. Sonavane *et al.* 2010a).

In a different study, NiO/polyaniline (PANI) thin films were prepared using electrochemical and chemical bath deposition methods (Sonavane *et al.* 2010b). Improved electrochromic performance was obtained for NiO/PANI electrode (ΔT : 31%, CE: 85 cm²/C). NiO/PANI film showed high durability up to 1000th cycles. The multicolours including yellow, light green, violet, blue, dark green attained from the NiO/PANI electrodes are displayed in Figure 12 (Sonavane *et al.* 2010b).

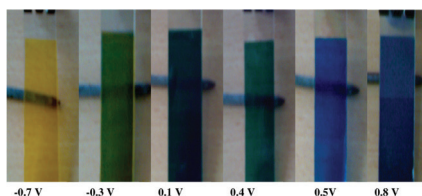


Figure 12. Photographs of a sample NiO/PANI in its coloured state under different applied potentials (From Ref. Sonavane *et al.* 2010b).

Švegl *et al.* produced electrochromic nickel oxide (Ni_(1-x)O) thin films and composite nickel oxide–polyaniline(Ni_(1-x)O–PANI) thin films via peroxo soft chemistry route (Švegl *et al.* 2012). A simple schematic of in-

interaction between $\text{Ni}_{(1-x)}\text{O}$ and PANI was displayed in Figure 13a-d. The distorted octahedral coordination of Ni^{2+} with surplus of positive charge (hole) at the grain boundary which is generated through nearby nickel vacancies is stabilized via a charge transfer (electron) from C=N double bond of quinoid (N-Q-N) structure (Figure 13a). This charge transfer generates a bipoisitive species in quinoid structure (Figure 13b) which turns to polaron (Figure 13c) and more stable bipolaron structure (Figure 13d). The resistivity of $\text{Ni}_{(1-x)}\text{O}$ structure reduced by adding PANI, which results in improved electrochromic influence in the presence of LiClO_4 -based electrolyte medium. The photopic transmittance modulations were attained as more than 65% and 70% during switching for $\text{Ni}_{(1-x)}\text{O}$ and $\text{Ni}_{(1-x)}\text{O}$ -PANI films, respectively (Švegl *et al.* 2012).

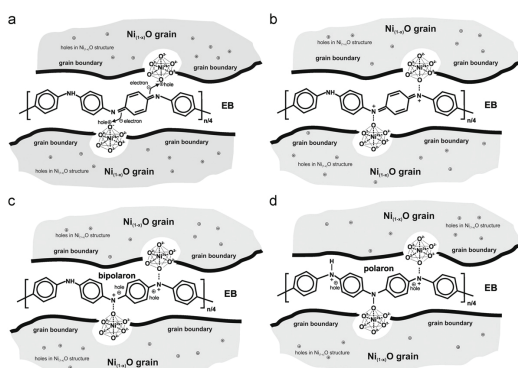


Figure 13. Simplified schematic presentation of PANI interaction with defect $\text{Ni}_{(1-x)}\text{O}$ structure. (a,b) Recombination of holes from $\text{Ni}_{(1-x)}\text{O}$ and electrons from PANI and (c,d) formation of bipolar on and polar on structure of EB, respectively (From Ref. Švegl *et al.* 2012).

Jamdegni *et al.* fabricated a NiO functionalized polyaniline (PANI) composite having color changes from a black to transparent (Figure 14) (Jamdegni *et al.* 2020). This color change can be ascribed to the combination coloration of PANI (from transparent to dark green) and NiO (from transparent to brown). Compared with PANI film, the PANI-fNiO film displayed higher optical modulation due to the synergistic additive of both the components in coloration (Figure 15) (Jamdegni *et al.* 2020).

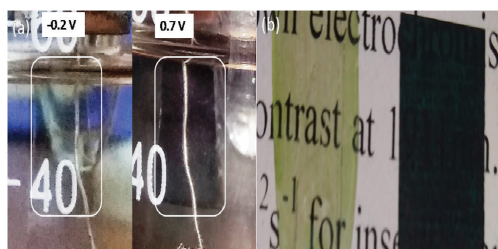


Figure 14. (a) PANI-fNiO electrode at different potentials (Pani-fNiO electrode has been displayed inside the white rectangular box) and (b) Colored and bleached state of PANI-fNiO (From Ref. Jamdegni *et al.* 2020).

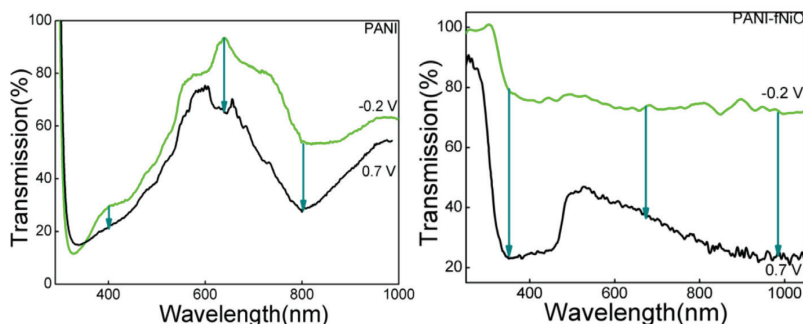


Figure 15. Transmittance spectra in colored and bleached state of (a) PANI and (b) PANI-fNiO (From Ref. Jamdegni et al. 2020).

4. Conclusion

This chapter has displayed the related to electrochromic materials with the specific interest to hybrids of nickel oxide and conjugated polymers. With the introduction of conducting polymers into NiO, the electrochromic performance can be significantly improved. Conducting polymers can be used to enhance conductivity of NiO, allowing to the improved electron transport rate, faster switching time. Thus, with such type of addition both NiO and conducting polymers synergistically favor each other's coloration and bleaching state, presenting the enhanced optical contrast. The significant contribution provided by the materials based on NiO-conducting polymers can be implemented towards the application of EC devices with high performance.

References

- Avendaño, E., Berggren, L., Niklasson, G. A., Granqvist, C. G., Azens, A. (2006) Electrochromic materials and devices: Brief survey and new data on optical absorption in tungsten oxide and nickel oxide films, *Thin Solid Films* 496 , 30 – 36.
- Cai, G.-f., Tu, J.-p., Zhang, J., Mai, Y.j., Lu, Y., Gu, C.-d., Wang, X.-l. (2012) An efficient route to a porous NiO/reduced graphene oxide hybrid film with highly improved electrochromic properties, *Nanoscale*, 2012, 4, 5724–5730.
- Camurlu, P. (2014) Polypyrrole Derivatives for Electrochromic Applications, *RSC Adv.* 4, 55832-55845.
- Camurlu, P., Cirpan, A., Toppare, L. (2004) Synthesis, characterization, and electrochromic properties of conducting poly(hexanedioic acid bis-(2-thiophen-3-yl-ethyl ester) and its copolymer with thiophene, *Synthetic Metals* 146, 91–97.
- Deb, S. K. (1969) A Novel Electrophotographic System., *Appl. Opt. Suppl.*,

- 3, 192-195, 1969.
- Ding, Y., Invernale, M. A., Mamangun, D. M. D., Kumar, A., Sotzing, G. A. (2011) A simple, low waste and versatile procedure to make polymer electrochromic devices, *J. Mater. Chem.*, 21, 11873-11878.
- Eh, A. L.-S., Tan, A. W. M., Cheng, X., Magdassi, S., Lee, P. S. (2018) Recent Advances in Flexible Electrochromic Devices: The Prerequisites, Challenges and Prospects, *Energy Technology*, 6, 33-45.
- Eren E., Aydın, M. F., Oksuz, A. U. (2020) A practical approach for generation of WO_3 -based flexible electrochromic devices, *Journal of Solid State Electrochemistry*, 24, 1057–1065.
- Eren, E. Alver C., Karaca, G. Y., Uygun, E., Oksuz, A. U. (2018a). Enhanced electrochromic performance of WO_3 hybrids using polymer plasma hybridization process. *Synthetic Metals*, 235, 115–124.
- Eren, E., Alver, C., Karaca, G. Y., Uygun, E., Oksuz, L., Oksuz, A. U. (2018b) High-Performance Flexible Complementary Electrochromic Device Based on Plasma Modified WO_3 Nano Hybrids and V_2O_5 Nanofilm with low Operation Voltages, *Electroanalysis*, 30, 2099 – 2109.
- Eren, E., Karaca, G. Y., Koc, U., Oksuz, L., Oksuz, A. U. (2017) Electrochromic characteristics of radio frequency plasma sputtered WO_3 thin films onto flexible polyethylene terephthalate substrates. *Thin Solid Films*, 634, 40–50.
- Granqvist, C. G., Niklasson, G. A. (2017) Thermochromic Oxide-Based Thin Films and Nanoparticle Composites for Energy-Efficient Glazings, *Buildings*, 7, 3.
- Granqvist, C.G., Arvizu, M.A., Bayrak Pehlivan, I., Qu, H.-Y., Wen, R.-T., Niklasson, G. A. (2018) Electrochromic materials and devices for energy efficiency and human comfort in buildings: A critical review, *Electrochimica Acta* 259 , 1170-1182.
- Hedley, L., Porteous, L., Hutson, D., Robertson, N., Johansson, J. O. (2018) Electrochromic bilayers of Prussian blue and its Cr analogue, *J. Mater. Chem. C*, 6, 512-517.
- Invernale, M. A., Acik, M., Sotzing, G. A. (2009) Thiophene-based electrochromic materials, In Book: Handbook of Thiophene-based Materials: Applications in Organic Electronics and Photonics, I. F. Perepichka, D. F. Perepichka, Ed.; John Wiley & Sons, Chapter 20, 757-782.
- Invernale, M. A., Ding, Y., Mamangun, D. M. D., Yavuz, M.S., Sotzing, G. A. (2010) Preparation of Conjugated Polymers Inside Assembled Solid-State Devices, *Adv. Mater.*, 22, 1379–1382, 2010.
- Jamdegni M., Kaur, A. (2020) Highly efficient dark to transparent electrochromic electrode with charge storing ability based on polyaniline and functionalized nickel oxide composite linked through a binding agent, *Electrochimica Acta* 331, 135359.
- Jittiarporn, P., Badilescu S., Al Sawafta, M.N., Sikong L., Truong, V.-V. (2017). Electrochromic Properties of Sol-Gel Prepared Hybrid Transition

- Metal Oxides A Short Review. *Journal of Science: Advanced Materials and Devices*, 2 (3) 286-300.
- Kiristi, M, Bozduman, F, Oksuz, A. U., Oksuz, L., Hala, A. (2014) Solid State Electrochromic Devices of Plasma Modified WO_3 Hybrids, *Ind. Eng. Chem. Res.* 53, 15917–15922.
- Korgel, B. A. (2013) *Materials Science: Composite for Smarter Windows*, *Nature*, 500, 278-9.
- Lampert C. M. (2004) Chromogenic Smart Materials, *Materials today*, 7, 28-35.
- Lee, S. J., Lee, T.G., Nahm, S., Kim, D. H., Yang, D. J., Han, S. H. (2020) Investigation of all-solid state electrochromic devices with durability enhanced tungsten-doped nickel oxide as a counter electrode, *Journal of Alloys and Compounds* 815, 152399.
- Li, Y., Cui, Y., Yao, Z., Liu, G., Shan, F. (2020) Fast electrochromic switching of electrospun Cu-doped NiO nanofibers, *Scripta Materialia* 178 , 472–476.
- Liu, Y., Jia, C., Wan, Z., Weng, X., Xie, J., Deng, L. (2015) Electrochemical and electrochromic properties of novel nanoporous $\text{NiO/V}_2\text{O}_5$ hybrid film, *Solar Energy Materials & Solar Cells* 132, 467–475.
- Madasamy, K., Velayutham, D., Suryanarayanan, V., Kathiresan, M., Ho, K.-C. (2019) Viologen based Electrochromic Materials and Devices, *J. Mater. Chem. C*, 7, 4622-4637.
- Nakaoka, K., Ueyama, J., Ogura, K. (2004) Semiconductor and electrochromic properties of electrochemically deposited nickel oxide films, *Journal of Electroanalytical Chemistry* 571, 93–99.
- Österholm, A. M., Shen, D. E., Kerszulis, J. A., Bulloch, R. H., Kuepfert, M., Dyer, A. L., Reynolds, J. R. (2015) Four Shades of Brown: Tuning of Electrochromic Polymer Blends Toward High-Contrast Eyewear, *ACS Appl. Mater. Interfaces*, 7, 1413-1421.
- Park, S.-I., Quan, Y.-J., Kim, S.-H., Kim, H., Kim, S., Chun, D.-M., Lee, C. S., Taya, M., Chu, W.-S., Ah, S.-H. (2016) *International Journal of Precision Engineering and Manufacturing-Green Technology* 3, 397-421.
- Patel, K J, Bhatt, G G, Ray, J R, Suryavanshi, P, Panchal, C J (2017) All-inorganic solid-state electrochromic devices: a review, *Journal of Solid State Electrochemistry*, 21, 337-347.
- Rowley, N. M., Mortimer R. J. (2002) New electrochromic materials, *Science Progress*, 85 (3), 243–262.
- Runnerstrom, E. L., Llordés, A., Lounis, S., Milliron, D. J. (2014) Nanostructured Electrochromic Smart Windows: Traditional Materials and NIR-selective Plasmonic Nanocrystals, *Chem. Commun.*, 50, 10555-10572.
- Schoot, C. J., Ponjee, J. J., van Dam, H. T., Van Doorn, R. A., Bolwijn, P.T. (1973) New electrochromic memory display, *Applied Physics Letters*, 23, 64-65.
- Sonavane, A. C., Inamdar, A. I., Dalavi, D. S., Desmukh, H. P., Patil, P.S.

- (2010a) Simple and rapid synthesis of NiO/PPy thin films with improved electrochromic performance, *Electrochimica Acta* 55, 2344–2351.
- Sonavane, A. C., Inamdar, A. I., Desmukh, H. P., Patil, P.S. (2010b) Multicoloured electrochromic thin films of NiO/PANI, *J. Phys. D: Appl. Phys.* 43 , 315102.
- Švegl, F., Vuk, A. S., Hajzeri, M., Perše, L. s., Orel, B. (2012) Electrochromic properties of $\text{Ni}_{(1-x)}\text{O}$ and composite $\text{Ni}_{(1-x)}\text{O}$ -polyaniline thin films prepared by the peroxo soft chemistry route, *Solar Energy Materials & Solar Cells* 99 , 14–25.
- Thakur, V. K., Ding, G., Ma, J., Lee, P. S. , Lu, X. (2012) Hybrid Materials and Polymer Electrolytes for Electrochromic Device Applications, *Adv. Mater.* 24, 4071–4096.
- Wang, C., Batsanov, A. S., Bryce, M. R. (2004) Electrochromic tetrathiafulvalene derivatives functionalised with 2,5-diaryl-1,3,4-oxadiazole chromophores, *Chem. Commun.* 2004, 578-579.
- Wang, G., Fu, X., Deng, J., Huang, X., Miao, Q. (2013) Electrochromic and spectroelectrochemical properties of novel 4,40-bipyridilium–TCNQ anion radical complexes, *Chemical Physics Letters* 579, 105–110.
- Wang, K.-H., Yoshida, M., Ikeuchi, H., Watnab, G., Lee, Y.-L., Hu, C.-C., Kawai, T. (2020) Effects of electrolyte pH on the formation of nickel oxide films and the corresponding electrochromic properties. *Journal of the Taiwan Institute of Chemical Engineers*, <https://doi.org/10.1016/j.jtice.2020.02.021>.
- Xia, X. H., Tu, J.P., Zhang, J., Huang, X. H., Wang, X. L., Zhang, W. K., Huang, H. (2009) Multicolor and fast electrochromism of nanoporous NiO/poly(3,4-ethylenedioxythiophene) composite thin film, *Electrochemistry Communications* 11, 702–705.
- Xia, X. H., Tu, J.P., Zhang, J., Wang, X.L., Zhang, W. K., Huang, H. (2008) A highly porous NiO/polyaniline composite film prepared by combining chemical bath deposition and electro-polymerization and its electrochromic performance, *Nanotechnology* 19, 465701.
- Xu, G., Zhao, J., Cui, C., Hou, Y., Kong, Y. (2013) Novel multicolored electrochromic polymers containingphenanthrene-9,10-quinone and thiophene derivatives moieties, *Electrochimica Acta* 112, 95– 103.
- Yang, P., Sun, P., Mai, W. (2016) Electrochromic energy storage devices, *Materials Today*, 19, 394-402.
- Zhu, Y., Otley, M. T., Alamer, F.A., Kumar, A., Zhang, X., Mamangun, D. M.D., Li, M., Arden, B. G., Sotzing, G. A. (2014) Electrochromic properties as a function of electrolyte on the performance of electrochromic devices consisting of a single-layer polymer, *Organic Electronics*, 15, 1378–1386, 2014.



Chapter 8

ANALYSIS OF SELF-ASSEMBLED MULTILAYERS: MONITORING AND CHARACTERIZATION

Nejla CİN¹

¹ Dr., PhD., Istanbul Technical University, Faculty of Science and Letters, Chemistry Department, cinin@itu.edu.tr

1. Introduction

Nanoscience and nanochemistry have gained extensive attraction in the current scientific research studies due to offering fabrication of promising multifunctional surfaces ranging from the medical applications (Tibbals, 2011; Costa and Mano, 2014; Ariga *et al.*, 2019) to environmental (Azzouz *et al.*, 2018) and energy technologies for every aspect of life (Hammond, 2004; D. Gianeti *et al.*, 2012). Materials in the nanometer length scale are advantageous since they possess superior physical and chemical features due to increased surface area, roughness, and area-to-volume ration (Hammond, 2004; Patel *et al.*, 2017). Taking these advantageous of nanoscaled materials, nanotechnology and nanochemistry have been utilized in conjunction with multidisciplinary approaches in order to design smart nanomaterials regarding their end-use application (Kotov, Dekdny and Fendler, 1995; Tang *et al.*, 2006; Ariga, Hill and Ji, 2007; Seyrek and Decher, 2012; Costa and Mano, 2014; Ariga *et al.*, 2019). Functional surfaces and coatings strategies enabling the production of contact lenses (Zhang, Cao, and Qi, 2020), medical implants (Mateescu *et al.*, 2015), cell encapsulation, gene transferring, tissue engineering (Boudou *et al.*, 2010; Nitta and Numata, 2013) targeted drug delivery (Cui, Li and Decher, 2016), electrical and optical sensors (Lutkenhaus and Hammond, 2007; Shahamirifard, Ghaedi and Hajati, 2018), membranes for ultrafiltration (Ball, 2018a), flame retardant surfaces (Zhang *et al.*, 2013) can be given as some of the examples of these studies.

On the other hand, it is worthy to note that variety of substances e.g., synthetic and natural polymers, inorganic particles or colloidal species are used to prepare nanomaterials all of which are different in structure, shape, stability, and functionalities (Hammond, 2004; Lynn, 2006; Tibbals, 2011; Decher, 2012; Seyrek and Decher, 2012; Ariga *et al.*, 2019). A schematic representation of the type of polymers used in nanomaterial fabrication are illustrated in Figure 1. Characteristics of the surrounding medium and the physical and chemical properties of nanomaterials have a direct influence on their durability, binding and loading capacities (Liu and Picart, 2016; Jacob *et al.*, 2018). The feature of these materials in nanometer length has to meet certain requirements regarding their utilization in the area of interest. For instance, the ones implied in the biomedical application have to provide biocompatibility to living cells without toxicity, or in case of stimuli-responsive surfaces, it is required to respond to a specific condition, e.g. pH, temperature, magnetic field or electromagnetic radiation (Sukhorukov *et al.*, 2001; Bajpai *et al.*, 2008; Delcea, Möhwald and Skirtach, 2011; Yi and Sukhorukov, 2014). Therefore, analytical instrumental techniques are of great importance to characterize the physicochemical properties of these materials with high precision and accuracy as well as monitoring

their building up process. Analytical tools and strategies are also essentially employed to understand and reveal the chemical and physical phenomena occurring behind the nanofabrication methodology (Yang, 2018). In this regard, instrumental analytic chemistry focuses on not only analysis of surfaces and interfaces of the nanomaterials but also the development of experimental methods for imaging purposes and improvement of measurement techniques in sub-angstrom scales, alongside with design of devices to construct nanomaterials with specific functionalities and/or to control their structure (Szweda, Tschopp, Felix, Decher and Lutz, 2018).

In addition, it is very well known that a significant part of the atoms comprising the nanomaterials is usually at the surface of the material (Tibbals, 2011). That is why, surface analysis and identifying the properties of these materials, and development of surface coating and functionalization strategies are the current research interest for various areas of application. Multidisciplinary areas, e.g. material sciences, physics, chemistry, biology, agriculture, food sciences, environmental technologies, and engineering sciences including electrical, mechanical, and textile are all included in the field of nanotechnology.

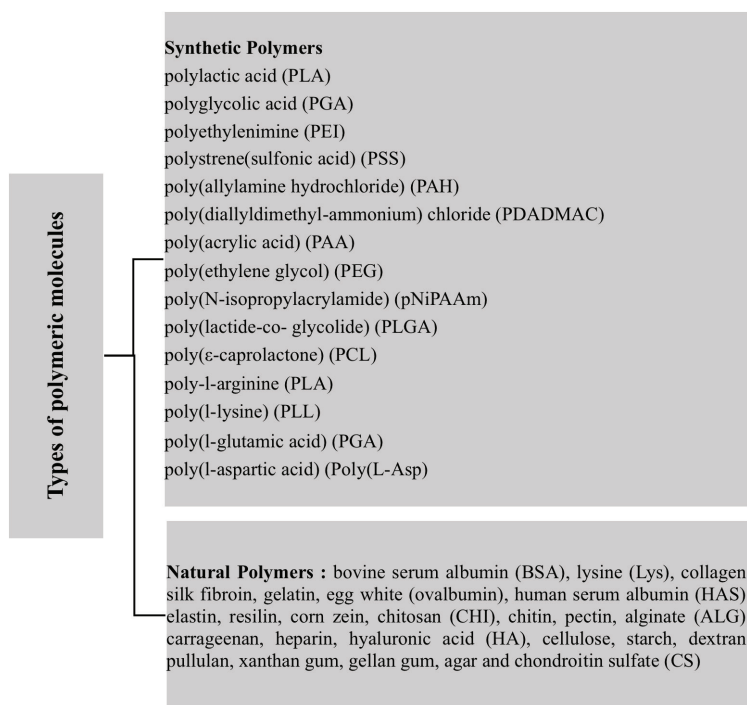


Figure 1. Types of polymeric molecules employed in nanofabrication.

During the last decade, new frontiers and progress in the nanotechnology and nanoscience let the development of surface modification and

functionalization strategies to be used in all these areas as well (Hammond, 2000; Tang *et al.*, 2006; Ariga, Hill and Ji, 2007; Lutkenhaus and Hammond, 2007; Becker, Johnston and Caruso, 2010; Ariga *et al.*, 2013; Picart, Caruso and Voegel, 2015; Richardson, Björnalm and Caruso, 2015; Richardson *et al.*, 2016a; Ball, 2018a). There are innumerable studies that have been carried out in this field and a variety of surface coating methods have been applied and reviewed in the literature (De Villiers *et al.*, 2011; Pahal *et al.*, 2017; Fuller and Köper, 2019). Among these, layer-by-layer (LbL) deposition technique emerged in the early 1990s and become one of the most popular surface coatings and functionalization techniques (Decher and Hong, 1991; Decher, Hong and Schmitt, 1992). Since then, multi-layer films produced by alternative deposition of polymeric species having complementary charged and/or functional groups has gained attraction and intensively studied (Lichter, Vliet and Rubner, 2009; Vautier *et al.*, 2011; Wu and Zhang, 2012; Denga *et al.*, 2013). Structure of LbL films provides a favorable environment for the investigation of physicochemical phenomena that occur in multilayered self-assembly and design of supramolecular materials (Schneider and Decher, 2008a; Ariga *et al.*, 2009; An, Huang and Shi, 2018; Szweda, Tschopp, Felix, Decher and Lutz, 2018). From this point, the analytical instrumental techniques for monitoring the film growth and evaluation of LbL film characteristics are of importance since they provide necessary information for a better insight to understand these physicochemical phenomena.

In this chapter, advance instrumental analysis techniques used to monitor the building up of LbL self-assemblies and to evaluate their physical and chemical properties from an analytical point of view will be summarized. Advanced analytical instrumental methods utilized in the analysis of LbL thin film surfaces regarding will be highlighted. The challenges and current limitations in the analysis of multilayered self-assemblies focusing on LbL-based nanostructures will be discussed.

2. LbL deposition and PEM films

The deposition of multilayers via sequential adsorption of colloids using oppositely charged silica particles was first demonstrated by Iler 1966 (Iler, 1966), and then this concept neglected until the early 1990s when it was adopted to alternative deposition of a polyanion and polycation leading to the formation of polyelectrolyte multilayer (PEM) films (Decher and Hong, 1991; Decher, Hong and Schmitt, 1992; Decher, 1997). Such architectures and coatings of oppositely charged polymers in a layer by layer manner first realized and demonstrated by Decher *et. al* in 1991 (Decher and Hong, 1991). Since then the method was named “layer-by-layer (LbL)” deposition and it had been appeared more than a hundred thousand

papers up to date. It has been widely utilized owing to allowing fabrication of nanoscaled materials with a well-defined architecture (Xuan *et al.*, 2006; Kim and Choi, 2007; Zhang, Chen and Zhang, 2007; Su *et al.*, 2009; Becker, Johnston and Caruso, 2010; De Villiers *et al.*, 2011; Borges and Mano, 2014; Costa and Mano, 2014). Indeed, it provides building up of thin films in tunable thicknesses and composition by inexpensive routes (Tang *et al.*, 2006; Ariga, Hill and Ji, 2007; Ariga *et al.*, 2013; Richardson, Björnmalm and Caruso, 2015; Richardson *et al.*, 2016a). Besides, it offers a wealth of potential applications due to its versatility and applicability using a vast number of layered components, such as organic or inorganic polymers, proteins, viruses, cells, colloids, quantum dots (QDs), or complexes (Caruso, Caruso and Möhwald, 1998; Aliev *et al.*, 1999; Fischer and Laschewsky, 2000; Vuillaume *et al.*, 2003; Yoo *et al.*, 2006; Jewell and Lynn, 2008; Kozlovskaya *et al.*, 2011; De Saint-Aubin *et al.*, 2012; Liang *et al.*, 2012; Moraes *et al.*, 2013; Zhang and Sun, 2015). Drug delivery systems (Lynn, 2006; Becker, Johnston and Caruso, 2010; Cui, Li and Decher, 2016; Jacob *et al.*, 2018), diagnosis (Boudou *et al.*, 2010; Liu and Picart, 2016), biomimetics, cell encapsulation and tissue engineering (Tang *et al.*, 2006; Detzel, Larkin and Rajagopalan, 2011; Zhang, Xing and Li, 2018; Liu *et al.*, 2019), medical implants (Kerdjoudj *et al.*, 2008; Mateescu *et al.*, 2015), inject printing (Andres and Kotov, 2010; Ajiro *et al.*, 2015), fuel cell and sensors, micro-batteries (Lee *et al.*, 2010), hydrophobic and flame-retardant surfaces prepared by LbL approach can be given just to illustrate the application area of LbL.

In the LbL deposition method, traditionally, oppositely charged polyelectrolytes are deposited alternatively on a charged surface yielding polyelectrolyte multilayer (PEM) films in the nanometer scale (Decher and Hong, 1991; Decher, Hong and Schmitt, 1992; Decher, 1997) (Figure 2). It allows the deposition of various number of materials on any type of substrate as long as either a charge reversal for electrostatic attraction or interaction between the primary layer and initial layer material e.g. charge transfer, hydrogen bonding, host-guest interaction, or covalent bonding, are fulfilled (Cochin and Laschewsky, 1999; Dubas and Schlenoff, 1999; Ladam *et al.*, 2000; Sukhishvili and Granick, 2002; Boulmedais *et al.*, 2003; Quinn *et al.*, 2007; Seo *et al.*, 2009; Bernsmann *et al.*, 2010; Kozlovskaya *et al.*, 2011; An, Huang and Shi, 2018; Ball, 2018b). The versatility and simplicity of LbL deposition techniques lies in its applicability on any platforms in any structure, shape, and size, such as planary, flat, spherical, or rodlike in the forms of lipids, capsules, fibers (Caruso, Caruso and Möhwald, 1998; Donath *et al.*, 1998; Volodkin *et al.*, 2007; De Geest *et al.*, 2009; Richardson, Björnmalm and Caruso, 2015; Richardson *et al.*, 2016a)

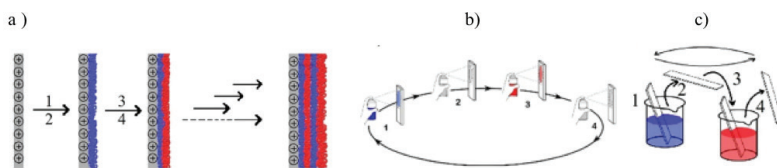


Figure 2. a) Schematic illustration of an electrostatically driven LbL assembly on a planar substrate using oppositely charged polyions, b) LbL-spraying (Decher and Hong, 1991; Decher and Schlenoff, 2012) (c) immersive LbL. 1 and 3: sequential adsorption steps of individual polyions, 2 and 4: washing/drying (Decher and Hong, 1991, Izquierdo *et al* 2005).

The main phenomenon behind the LbL methodology, mechanism of multilayer film growth and its distinct characteristics, parameters effecting the LbL deposition; such as concentration of constituents, ionic strength, pH, washing and drying steps, and temperature, and LbL technologies, e.g. spraying, immersive, spin-assisted LbL either manually or by automatic systems have been extensively studied and reported (Dubas and Schlenoff, 1999; Hammond, 2000; Boulmedais *et al.*, 2003; Lynn, 2006; Tang *et al.*, 2006; Ariga, Hill and Ji, 2007; Lichter, Vliet and Rubner, 2009; Su *et al.*, 2009; Boudou *et al.*, 2010; Cini *et al.*, 2010; Vautier *et al.*, 2011; Laachachi *et al.*, 2012; Ball *et al.*, 2012; Cini *et al.*, 2012; Decher and Schlenoff, 2012; Ariga *et al.*, 2013; Borges and Mano, 2014; Costa and Mano, 2014; Richardson, Björnalm and Caruso, 2015; Szweda, Tschopp, Felix, Decher and Lutz, 2018).

As the subject of LbL methodology and its area of application is a quite broad concept unto itself and the fundamentals of LbL methodology with the exception of the concept are extensively covered by current and ongoing studies, the basics of the LbL technique and properties of LbL films will not be discussed here. Although the proof of the principles behind this concept is already demonstrated, well-accepted, adjusting and revealing of the mechanical properties of these films are still challenging and it has some limitations (Tang *et al.*, 2006; Borges and Mano, 2014). For instance, it is difficult to characterize the LbL films in which the covalent crosslinking is the main driving force (Seo *et al.*, 2009; An, Huang and Shi, 2018; Ball, 2018b).

It is worthy to note that not only quantitative analysis but also qualitative analysis necessarily performed in order to a comprehensive understanding of the interactions in the nanometer scale in a more specific way. Isolation of proteins in a core-shell structure can be achieved by isotope labeling and label-free quantification (Wasdo *et al.*, 2008) which can be qualitatively visualized around the nanoparticles by confocal fluorescence microscopy in live-cell imaging (Kantawong *et al.*, 2009). However, extensive characterization methods through advanced analytical techniques

are still required in order to describe how the size and charge of nanoparticle regulate the formation of these core-shelled structures under *in-vivo* conditions (Wasdo *et al.*, 2008; Kantawong *et al.*, 2009; Cai *et al.*, 2013; Barui *et al.*, 2020).

In this context, the role analytical instrumental techniques that are applicable for monitoring the film formation and evaluation of LbL film characteristics regarding the substrate type and film geometries are of importance. Herein, section 3., the most commonly used instrumental techniques providing an overall description of the film growth, surface morphologies, thicknesses, and composition regarding the substrate types and film fabrication mediums will be addressed.

3. Instrumental Analytic Methods in LbL Self-Assembled Films: Overview

The instrumental analytic techniques used for evaluation of the LbL films are mainly spectroscopic, chromatographic, microscopic, and electrochemical methods, as well as light scattering and refractometry. (Kujawa *et al.*, 2005; Halthur, Claesson and Elofsson, 2006; Ariga, Hill and Ji, 2007; Seyrek and Decher, 2012; Ariga *et al.*, 2013; Richardson, Björnmalm and Caruso, 2015; Richardson *et al.*, 2016a). It is a fact that characterization methods are strongly dependent on the substrate material, being either flat or nonflat. In addition, certain analytical techniques require specific materials and film properties to be applied (Surfaces, 2016). In this section, the most commonly used analytical tools in LbL technology for monitoring the film growth, analyzing the film internal structure and composition, imaging, revealing the morphological properties and stability, and determination of adsorption kinetic of layers will be summarized. In addition, the general principles of several selected advanced instrumental methods as being relatively new techniques will be provided. The provided references are given to provide a clear understanding of the instrumental analysis techniques appropriate for LbL films without priority.

3.1 Monitoring the film growth and composition

In general, regular film growth and layer build up can be monitored either change in optical absorbance or film thickness. Ellipsometry (ex situ or in situ), Surface Plasmon Resonance Spectroscopy (SPR), Scanning Angle Reflectometry (SAR) Optical Waveguide Light-mode Spectroscopy (OWLS), Small-angle X-Ray (XRR) or Neutron Reflectivity (NR), Small-angle X-ray scattering (SAXS), Impinging Jet Reflectometry and Dual-Polarization Interferometry (DPI) are some optical techniques used to measure the film thickness on flat substrates (Decher and Schmitt, 1992; Schmitt *et al.*, 1993; Caruso *et al.*, 1997; Lösche *et al.*, 1998; Picart *et*

al., 2001; Swann *et al.*, 2004; Kujawa *et al.*, 2005; Halthur, Claesson and Elofsson, 2006; Ariga, Hill and Ji, 2007; Ariga *et al.*, 2013). On the other hand, light scattering techniques, e.g. Dynamic Light Scattering (DLS) (Schneider and Decher, 2008b), flow cytometry (Gunawan *et al.*, 2014), and microscopy (Kujawa *et al.*, 2005) can be applied for monitoring the building up of core-shell type LbL systems and PEMs on colloidal substrates. In addition to size measurements, charge reversal after each deposition is detected by zeta potential measurements (Ladam *et al.*, 2000; Sukhorukov *et al.*, 2004; Irigoyen *et al.*, 2009). However, depending on the substrate type and film components consisting of specific adsorption bands Ultraviolet (UV), UV-visible (UV-vis) Spectrophotometry (Laschewsky *et al.*, 1997; Richert *et al.*, 2004) and Fourier transform Infrared Spectroscopy (FTIR) (Stockton and Rubner, 1997; Wang *et al.*, 1997; Caruso *et al.*, 1998; Schwinté *et al.*, 2001; Lawrie *et al.*, 2007) can be employed for monitoring the film growth and determining the film composition and its structural properties. It should be noted that a quartz glass substrate is required for UV-Vis spectroscopy analysis if the sample is not in particulate form. An increase in the absorption is observed relative to the adsorbed amount of component in each layer. In case of FTIR (*ex-situ* or *in-situ*), the film growth is monitored through the chemical composition of the film via either reflection absorption (RAS) or attenuated total reflection (ATR) modes depending on the type of substrate (Schwinté *et al.*, 2001; Richardson *et al.*, 2016a). In addition to these techniques, Nuclear Magnetic Resonance (NMR) (Smith *et al.*, 2004; Vaca Chávez and Schönhoff, 2007), X-ray photoelectron spectroscopy (XPS) (Caruso *et al.*, 1997; Lawrie *et al.*, 2007) and Circular dichroism (CD) spectrometry have been used to study the film composition (Boulmedais *et al.*, 2003). Among these techniques, NMR enables the determination of LbL film growing on colloidal particles in terms of composition, diffusion, and hydration properties, but the details of these concepts will not be discussed in this chapter.

3.2. Imaging, morphology, interfacial diffusion, and stability

Microscopic techniques including Scanning Electron Microscopy (SEM), Transmission Electron Microscopy (TEM) (Gracio *et al.*, 2013), Atomic Force Microscope (AFM) (either dried or in solution), Scanning Probe Microscopy (SPM) are used to study the morphology and imaging of the multilayers (Caruso *et al.*, 1998; Kujawa *et al.*, 2005). Confocal laser scanning microscopy (CLSM) in which the materials of interest are labeled with fluorescent dyes has been applied to visualize the particulate form of films and monitor the diffusion of layers as well (Picart *et al.*, 2002; Mertz *et al.*, 2007). Importantly, it should be noted that due to the requirement of an electron transparent sample for TEM measurements, it is not convenient for imaging of a multilayer film as is. Nonetheless, vis-

ualizing the cross-section of the film is possible if the film should be cut into thin slides. Regarding that, TEM is appropriate only if the LbL film growing is on a particulate substrate or nanotubes, or if it is a hollow capsule of core-shelled form. On the other hand, SEM requiring a conductive sample, it is applicable if the LbL films deposited on a conductive material unless the film itself displays no conductivity. However, both SEM and TEM are applicable for nonflat or curved surfaces. In fact, XRR is also appropriate to investigate the roughness and density of the LbL films as well as thickness determination. Although it has limited use due to a lack of information on molecular conformation within the film matrix, it provides useful data to understand the structural differences regarding stratification. NR also helps to resolve the internal structure of the LbL films. Interfacial roughness and polymer interpenetration can be revealed by this technique (Kharlampieva *et al.*, 2008; Félix *et al.*, 2009). Composition profiles of the films can be precisely obtained by NR since it allows the measurement of thickness along with z-direction normal to the interface on a length scale of up to 500nm with a resolution of about 0.2nm. Besides, measurements in the liquid state, such as High Pressure Liquid Chromatography (HPLC), could be useful to determine the chemical stability and nano-encapsulation efficiency especially in case of drug entrapment (Kabary *et al.*, 2018).

Moreover, Differential Interference Contrast (DIC) (Richardson *et al.*, 2013) microscopy is used to study visualizing the LbL capsules of about larger than 500nm with high interference contrast (Richardson *et al.*, 2016b). Apart from these methods, contact angle measurements are useful to study the roughness of LbL films. Profilometry has been used as an analytical tool for the mechanical measurement of LbL film thickness (Lutkenhaus *et al.*, 2007). Furthermore, electrochemical methods, e.g. cyclic voltammetry (CV) (Yoshida *et al.*, 2014) in the case of conductive films having redox potential and electrochemical impedance spectroscopy (Lutkenhaus *et al.*, 2007) are used as analytical tools in LbL science and technology. In electrochemical impedance spectroscopy, in-plane and cross-plane ion transportation are measured via conductivity. Comparison of in-plane and cross-plane ion transfer speed gives knowledge on material properties of the films regarding orientation, e.g. isotropic or anisotropic film structure.

3.3. Kinetics of adsorption

A simple quartz crystal microbalance (QCM) device was first introduced by Kunitake, Lvov and Ariga for *in-situ* investigations of LbL assembling processes (Lvov, Ariga and Kunitake, 1994; Lvov *et al.*, 1995). It allows the quantification of the film mass in the nanogram level with great precision over a QCM cell. In this method, adsorption rate and amount

of adsorbed material hence adsorption kinetic are obtained. However, it should be noted that the overall mass detected in an *in situ* QCM includes not only the mass of adsorbed layer but also the water associated with the multilayers or substrate (Seyrek and Decher, 2012). Nevertheless, reliable qualitative analysis is provided by this method. OWLS and SPR can be also used for studies of adsorption kinetic as well as for determining the dielectric constant, thickness, and anisotropy.

3.4. In situ characterization

Depending on the end-use application of the LbL PEMs, the composition of the films is often very complicated and combination of several analytical tools are imperatively employed for characterization and monitoring of the LbL deposits (Halthur, Claesson and Elofsson, 2006; Ariga, Hill and Ji, 2007; Ariga *et al.*, 2013; Richardson, Björnmalm and Caruso, 2015; Richardson *et al.*, 2016b). Utilizing *in situ* instrumental analytic techniques together with other analytical tools are typical examples of these applications, such as Scanning Tunneling Microscopy (STM) (Zajac *et al.*, 1994), *in situ* ellipsometry, QCM-D, DPI, and AFM (Bao, Mahurin and Dai, 2004; Goulet *et al.*, 2005; Lee *et al.*, 2010; Li *et al.*, 2012). Not limited to the aforementioned instrumental analytic methods, Surface-Enhanced Raman Scattering (SERS) has been used to study the adsorption of layers in LbL films (Caruso *et al.*, 1998; Goulet *et al.*, 2005; Hansen, Fellingham and Russell, 2011; Peng *et al.*, 2013). Principles of all of these techniques can be found elsewhere while some representative examples are referred to in this chapter. However, the general principles of SPR, XPS, CD, and representative examples for SERS and DPI as being a relatively new technique will be given in detail in section 3.5.

3.5. Miscellaneous Instrumental Techniques

3.5.1. Surface Plasmon Resonance Spectroscopy (SPR)

The principles of SPR is based on the charge density oscillation phenomenon at the interface of two media with a dielectric constant of opposite signs (Kujawa *et al.*, 2005; Ferreira, Mendes and Kubota, 2010). Upon interaction of light having a specific wavelength with an AuNP, the free electrons in the metal oscillate collectively. When the incoming light has the same wavevector with the oscillating conduction electrons, the incoming energy is absorbed into the plasmon wave and, hence resonance occurs. Typically, dielectric properties of AuNPs changes in the case of a polymer layer is added on to the surface of AuNPs. As a result of that change in dielectric properties, the SPR peak is shifted. As each layer added the peak wavelength is decreases and dielectric properties change. It is a conven-

ient technique to study air-dried LbL films likewise ellipsometry, and it is, therefore used to investigate the effect of pH or polymer molecular weight on film growth.

3.5.2.X-ray photoelectron spectroscopy (XPS)

In XPS, the energy levels of photoelectrons in a spectrum with a series of photoelectron peaks having characteristic binding energies for each element are determined, hence chemical composition of a surface is obtained using these peak areas. Chemical bonding information by shifts in peaks and binding energies due to changes in the chemical state of the emitting atom are also provided, enabling the multilayers to be monitored for chemical reactions (Caruso *et al.*, 1997; Liu *et al.*, 2015)

3.5.3. Circular dichroism (CD) spectrometry

This technique is appropriate for the determination of the structure of chiral molecules. The differential absorption of right- and left-circularly polarized light is determined and an accurate determination of secondary the film structure displaying chirality, (e.g. proteins, polypeptides, polysaccharides, chiral dyes) within LbL film matrix is fulfilled. CD indeed provides information on both the content and conformation of the molecules. Therefore, it is applicable to study the conformational changes within the film structure during film growth upon any conditional changes, e.g. ionic strength, pH, and temperature.

3.5.6. Surface-Enhanced Raman Scattering (SERS) in LbL film analysis

In SERS, measurement of large increases in Raman scattering cross-sections of molecules adsorbed at the surfaces of nanoscale metallic particles is provided, hence it enables the characterization of LbL thin films incorporating metallic nanoparticles (Ariga, Hill and Ji, 2007; Lee *et al.*, 2010; Li *et al.*, 2012). For instance, the utilization of LbL films dendrimer and colloidal Ag particles was proposed as an excellent substrate for SERS measurements by Aroca and co-workers (Goulet *et al.*, 2005). Similarly, thin layers of TiO_2 on a silver island film substrate prepared by the LbL surfaces sol-gel approach serving as a unique SERS substrate to monitor the adsorption of several molecules on dielectric titania surfaces was demonstrated by Bao *et. al* (Bao, Mahurin and Dai, 2004). An improvement in the stability of SERS substrates was reported due to the protection capability of TiO_2 to silver islands from oxidation and aggregation. Electromagnetic enhancement at distances within the LbL film matrix let these films having chemically selective external layers to be utilized as sensors for specific analytes (Ariga, Hill and Ji, 2007).

3.5.7. Dual-Polarization Interferometry (DPI) in LbL film analysis

DPI enables the measurement of changes both in thickness and refractive index of the deposited layers *in situ* (Swann *et al.*, 2004). The principle of this technique based on the effect of surface adsorption on the decreasing wave field emitted from the sensing waveguide, so that a change in the light traveling through the reference and propagating through the sensing waveguide occurs. The shift in the fringe pattern in the far-field is observed as a result of this change and it is alternatively and continuously recorded for both horizontally and vertically polarized light. The combination of both polarizations enables a solution of thickness and refractive index. Upon comparison, an excellent agreement has been observed between the masses detected by ellipsometry (Ariga, Hill and Ji, 2007). Analysis of PGA/PLL LbL films immobilized with matrix derivate protein was performed using DPI as well as *in situ* ellipsometry and QCM-D by Elofsson and coworkers (Halthur, Claesson and Elofsson, 2006).

4. Challenges and Concluding Remarks

In this chapter, several selected advanced instrumental methods applied in characterization LbL films are summarized. Instrumental analysis techniques used to monitor the building up of LbL self-assemblies and to evaluate their physical and chemical properties from an analytical point of view are exemplified. It is attempted to give representative studies to provide a clear understanding of the instrumental analysis techniques appropriate for LbL films without any intention on the emphasis of their priority. Instrumental analytic chemistry focuses on not only the analysis of surfaces and interfaces of the nanomaterials but also the development of experimental methods for imaging purposes and improvement of measurement techniques in sub-angstrom scales, alongside with design of devices to construct nanomaterials with specific functionalities and/or to control their structure. Analytical tools and strategies are of importance for understanding and revealing the chemical and physical phenomena occurring behind the nanofabrication methodology as well. It is worthy to note that not only quantitative analysis but also qualitative analysis necessarily performed in order to a comprehensive understanding of the interactions in the nanometer scale in a more specific way. Although the proof of the principles behind LbL methodology is already demonstrated, well-accepted, and despite its wide applicability, adjusting and revealing the mechanical properties of these films are still challenging and it has some limitations. For instance, it remains difficult to characterize the film if the covalent crosslinking is the main driving force in the film construction. Besides, extensive characterization methods through advanced analytical techniques

are still required in order to describe how the size and charge of nanoparticle regulate the formation of these core-shelled structures under *in-vivo* conditions. The design of multifunctional nanomaterials requires collaborative work between various areas of science and engineering technologies in all of which the utilization of instrumental analytical tools is inevitable.

REFERENCES

- Ajiro, H., Kuroda, A., Kan, K. and Akashi, M. (2015) *Langmuir*, 31, 10583–10589.
- Aliev, F. G., Correa-Duarte, M. A., Mamedov, A., Ostrander, J. W., Giersig, M., Liz-Marzán, L. M. and Kotov, N. A. (1999) *Advanced Materials*, 11(12), 1006–1010.
- An, Q., Huang, T. and Shi, F. (2018) *Chemical Society Reviews*, 47(13), 5061–5098.
- Andres, C. M. and Kotov, N. A. (2010) *J. Am. Chem. Soc.*, 132, 14496–14502.
- Ariga, K., Hill, J. P. and Ji, Q. (2007) *Physical Chemistry Chemical Physics*, 9(19), 2319–2340.
- Ariga, K., Ji, Q., Hill, J. P., Kawazoe, N. and Chen, G. (2009) *Expert Opinion on Biological Therapy*, 9(3), 307–320.
- Ariga, K., Nishikawa, M., Mori, T., Takeya, J., Shrestha, L. K. and Hill, J. P. (2019) *Science and Technology of Advanced Materials*. Taylor & Francis, 20(1), 51–95.
- Ariga, K., Wu, K. C.-W., Ji, Q., Yonamine, Y., Rydzek, G., Hill, J. P. and Yamauchi, Y. (2013) *Chemistry Letters*, 43(1), 36–68.
- Azzouz, A., Kailasa, S. K., Lee, S. S., J. Rascón, A., Ballesteros, E., Zhang, M. and Kim, K. H. (2018) *TrAC - Trends in Analytical Chemistry*, 108, 347–369.
- Bajpai, A. K., Shukla, S. K., Bhanu, S. and Kankane, S. (2008) *Progress in Polymer Science (Oxford)*, 33(11), 1088–1118.
- Ball, V. (2018a) in *Ball, V. (ed.) Self-Assembly Processes at Interfaces Multiscale Phenomena, Interface Science and Technology, V. 21*. Chapter 9. Industrial Applications of Self-assembly at Interfaces. Elsevier Ltd., 427–434.
- Ball, V. (2018b) in *Ball, V. (ed.) Self-Assembly Processes at Interfaces Multiscale Phenomena, Interface Science and Technology, V. 21*. Chapter 6. Using Covalent Chemistry: Grafting on and Grafting From Surfaces. Elsevier Ltd., 333–365.
- Ball, V., Laachachi, A., Toniazzo, V. and Ruch, D. (2012) *Journal of Colloid and Interface Science*. Elsevier Inc., 366(1), 96–104.
- Bao, L., Mahurin, S. M. and Dai, S. (2004) *Analytical Chemistry*, 76(15), 4531–4536.
- Barui, A. K., Oh, J. Y., Jana, B., Kim, C. and Ryu, J. (2020) *Advanced*

Therapeutics, 3(1), 1900124.

- Becker, A. L., Johnston, A. P. R. and Caruso, F. (2010) *Small*, 6(17), 1836–1852.
- Bernsmann, F., Frisch, B., Ringwald, C. and Ball, V. (2010) *Journal of Colloid and Interface Science*. Elsevier Inc., 344(1), 54–60.
- Borges, J. and Mano, J. F. (2014) *Chemical Reviews*, 114(18), 8883–8942.
- Boudou, T., Crouzier, T., Ren, K., Blin, G. and Picart, C. (2010) *Advanced Materials*, 22(4), 441–467.
- Boulmedais, F., Ball, V., Schwinte, P., Frisch, B., Schaaf, P. and Voegel, J. C. (2003) *Langmuir*, 19(2), 440–445.
- Cai, X., Ramalingam, R., Wong, H. S., Cheng, J., Ajuh, P., Cheng, S. H. and Lam, Y. W. (2013) *Nanomedicine: Nanotechnology, Biology, and Medicine*. Elsevier Inc., 9(5), 583–593.
- Caruso, F., Caruso, R. A. and Möhwald, H. (1998) *Science*, 282, 1111–1114.
- Caruso, F., Furlong, D. N., Ariga, K., Ichinose, I. and Kunitake, T. (1998) *Langmuir*, 14(16), 4559–4565.
- Caruso, F., Niikura, K., Furlong, D. N. and Okahata, Y. (1997) *Langmuir*, 13(13), 3422–3426.
- Cini, N., Tulun, T., Blanck, C., Toniazzo, V., Ruch, D., Decher, G. and Ball, V. (2012) *Physical Chemistry Chemical Physics*, 14(9), 3048.
- Cini, N., Tulun, T., Decher, G., Ball, V., (2010) *J. Am. Chem. Soc.*, 132, 8264–8265.
- Cochin, D. and Laschewsky, A. (1999) *Macromolecular Chemistry and Physics*, 200(3), 609–615.
- Costa, R. R., and Mano, J. F. (2014) *Chemical Society Reviews*, 43(10), 3453–3479.
- Cui, W., Li, J. and Decher, G. (2016) *Advanced Materials*, 28(6), 1302–1311.
- D. Gianeti, M., A. L. Wagemaker, T., C. Seixas, V. and M.B.G. Maia Campos, P. (2012) *Current Nanoscience*, 8(4), 526–534.
- Decher, G. (1997) *Science*, 277(5330), 1232–1237.
- Decher, G. and Schlenoff, J. B. (ed.). (2012) *Multilayer Thin Films: Sequential Assembly of Nanocomposite Materials*, 2nd edition. Wiley-VCH.
- Decher, G. (2012) in *Decher, G., Schlenoff, J. B. (ed.). Multilayer Thin Films: Sequential Assembly of Nanocomposite Materials*, 2nd edition. Layer-by-Layer Assembly (Putting Molecules to Work). Wiley-VCH, 1–21.
- Decher, G. and Schmitt, J. (1992) *Progr. Colloid Polym. Sci.*, 89, 160–164.
- Decher, G. and Hong, J. -D (1991) *Makromolekulare Chemie. Macromolecular Symposia*, 46(1), 321–327.
- Decher, G., Hong, J. -D., and Schmitt, J. (1992) *Thin Solid Films*, (210–

- 211), 831–835.
- De Geest, B. G., De Koker, S., Sukhorukov, G. B., Kreft, O., Parak, W. J., Skirtach, A. G., Demeester, J., *et al.* (2009) *Soft Matter*, 5(2), 282–291.
- Delcea, M., Möhwald, H. and Skirtach, A. G. (2011) *Advanced Drug Delivery Reviews*. Elsevier B.V., 63(9), 730–747.
- Denga, Z. J., Morton, S. W., Ben-Akiva, E., Dreaden, E. C., E.Shopsowitz, K. and Hammond, P. T. (2013) *ACS Nano*, 7(11), 1–23.
- De Saint-Aubin, C., Hemmerlé, J., Boulmedais, F., Vallat, M. F., Nardin, M. and Schaaf, P. (2012) *Langmuir*, 28(23), 8681–8691.
- Detzel, C. J., Larkin, A. L. and Rajagopalan, P. (2011) *Tissue Engineering - Part B: Reviews*, 17(2), 101–113.
- De Villiers, M. M., Otto, D. P., Strydom, S. J. and Lvov, Y. M. (2011) *Advanced Drug Delivery Reviews*. Elsevier B.V., 63(9), 701–715.
- Donath, E., Sukhorukov, G. B., Caruso, F., Davis, S. A. and Möhwald, H. (1998) *Oxford Economic Papers*, 50(4), 534–562.
- Dubas, S. T. and Schlenoff, J. B. (1999) *Macromolecules*, 32(24), 8153–8160.
- Félix, O., Zheng, Z., Cousin, F. and Decher, G. (2009) *Comptes Rendus Chimie*, 12(1–2), 225–234.
- Ferreira, D. C. M., Mendes, R. K. and Kubota, L. T. (2010) *Journal of the Brazilian Chemical Society*, 21(9), 1648–1655.
- Fischer, P. and Laschewsky, A. (2000) *Macromolecules*, 33(3), 1100–1102.
- Fuller, M. A. and Köper, I. (2019) *Nano Convergence*. Springer Singapore, 6(1).
- Goulet, P. J. G., Dos Santos, D. S., Alvarez-Puebla, R. A., Oliveira, O. N. and Aroca, R. F. (2005) *Langmuir*, 21(12), 5576–5581.
- Gracio, J. D. A., Singh, Â. M. K., Ruch, D., Buehler, M. J. and Al, C. E. T. (2013) *ACS Nano*, (2), 1524–1532.
- Gunawan, S. T., Liang, K., Such, G. K., Johnston, A. P. R., Leung, M. K. M., Cui, J. and Caruso, F. (2014) *Small*, 10(20), 4080–4086.
- Halthur, T. J., Claesson, P. M. and Elofsson, U. M. (2006) *Langmuir*, 22(26), 11065–11071.
- Hammond, P. T. (2000) *Current Opinion in Colloid and Interface Science*, 4, 430–442.
- Hammond, P. T. (2004) *Advanced Materials*, 16(15 SPEC. ISS.), 1271–1293.
- Hansen, L. D., Fellingham, G. W. and Russell, D. J. (2011) *Analytical Biochemistry*. Elsevier Inc., 409(2), 220–229.
- Iler, R. K. (1966) *J. Colloid Interface Sci*, 21, 569–594.
- Irigoyen, J., Moya, S. E., Iturri, J. J., Llarena, I., Azzaroni, O. and Donath, E. (2009) *Langmuir*, 25(6), 3374–3380.
- Izquierdo, A., Ono, S. S., Voegel, J.-C., Schaaf, P., Decher, G. (2005) *Langmuir*, 21, 7558–7567.

- Jacob, J., Haponiuk, J. T., Thomas, S. and Gopi, S. (2018) *Materials Today Chemistry*, 9, 43–55.
- Jewell, C. M. and Lynn, D. M. (2008), 60, 979–999.
- Kabary, D. M., Helmy, M. W., Elkhodairy, K. A., Fang, J. Y. and Elzoghby, A. O. (2018) *Colloids and Surfaces B: Biointerfaces*. Elsevier B.V., 169, 183–194.
- Kantawong, F., Burgess, K. E. V., Jayawardena, K., Hart, A., Burchmore, R. J., Gadegaard, N., Oreffo, R. O. C., *et al.* (2009) *Biomaterials*. Elsevier Ltd, 30(27), 4723–4731.
- Kerdjoudj, H., Berthelemy, N., Rinckenbach, S., Kearney-Schwartz, A., Montagne, K., Schaaf, P., Lacolley, P., *et al.* (2008) *Journal of the American College of Cardiology*, 52(19), 1589–1597.
- Kharlampieva, E., Kozlovskaya, V., Ankner, J. F. and Sukhishvili, S. A. (2008) *Langmuir*, 24(20), 11346–11349.
- Kim, B. S. and Choi, J. W. (2007) *Biotechnology and Bioprocess Engineering*, 12(4), 323–332.
- Kotov, N. A., Dekdny, I. and Fendler, J. H. (1995) *Journal of Physical Chemistry*, (99), 13065–13069.
- Kozlovskaya, V., Harbaugh, S., Drachuk, I., Shchepelina, O., Kelley-Loughnane, N., Stone, M. and Tsukruk, V. V. (2011) *Soft Matter*, 7(6), 2364–2372.
- Kujawa, P., Moraille, P., Sanchez, J., Badia, A. and Winnik, F. M. (2005) *J. Am. Chem. Soc.*, 127, 9224–9234.
- Laachachi, A., Toniazzo, V., Ruch, D., Apaydin, K. and Ball, V. (2012) *Biointerphases*, 7(1), 59.
- Ladam, G., Schaad, P., Voegel, J. C., Schaaf, P., Decher, G. and Cuisinier, F. (2000) *Langmuir*, 16(3), 1249–1255.
- Laschewsky, A., Wischerhoff, E., Bertrand, P. and Delcorte, A. (1997) *Macromolecular Chemistry and Physics*, 198(10), 3239–3253.
- Lawrie, G., Keen, I., Drew, B., Chandler-Temple, A., Rintoul, L., Fredericks, P. and Grøndahl, L. (2007) *Biomacromolecules*, 8(8), 2533–2541.
- Lee, S. W., Yabuuchi, N., M.Gallant, B., Chen, S., Kim, B.-S., Hammond, P. T. and Shao-Horn, Y. (2010) *Nat. Nanotechnol.* 2010, 5, 531., 5, 531–537.
- Li, Y., Chen, S., Wu, M. and Sun, J. (2012) *Advanced Materials*, 24(33), 4578–4582.
- Liang, R., Xu, S., Yan, D., Shi, W., Tian, R., Yan, H., Wei, M., *et al.* (2012) *Advanced Functional Materials*, 22(23), 4940–4948.
- Lichter, J. A., Vliet, K. J. Van and Rubner, M. F. (2009), 8573–8586.
- Liu, T., Wang, Y., Zhong, W., Li, B., Mequanint, K., Luo, G. and Xing, M. (2019) *Advanced Healthcare Materials*, 8(1), 1–16.
- Liu, X., Leng, C., Yu, L., He, K., Brown, L. J., Chen, Z., Cho, J., *et al.* (2015) *Angewandte Chemie - International Edition*, 54(16), 4851–

4856.

- Liu, X. Q. and Picart, C. (2016) *Advanced Materials*, 28(6), 1295–1301.
- Lösche, M., Schmitt, J., Decher, G., Bouwman, W. G. and Kjaer, K. (1998) *Macromolecules*, 31(25), 8893–8906.
- Lutkenhaus, J. L. and Hammond, P. T. (2007) *Soft Matter*, 3(7), 804–816.
- Lutkenhaus, J. L., Olivetti, E. A., Verploegen, E. A., Cord, B. M., Sadoway, D. R. and Hammond, P. T. (2007) *Langmuir*, 23(16), 8515–8521.
- Lvov, Y., Ariga, K. and Kunitake, T. (1994) *Chemistry Letters*, 2323–2326.
- Lvov, Y., Ariga, K., Kunitake, T. and Ichinose, I. (1995) *Journal of the American Chemical Society*, 117(22), 6117–6123.
- Lynn, D. M. (2006) *Soft Matter*, 2(4), 269–273.
- Mateescu, M., Baixe, S., Garnier, T., Jierry, L., Ball, V., Haikel, Y., Metz-Boutigue, M. H., *et al.* (2015) *PLoS ONE*, 10(12), 1–13.
- Mertz, D., Hemmerlé, J., Boulmedais, F., Voegel, J. C., Lavalley, P. and Schaaf, P. (2007) *Soft Matter*, 3(11), 1413–1420.
- Moraes, M. L., Lima, L. R., Silva, R. R., Cavicchioli, M. and Ribeiro, S. J. L. (2013) *Langmuir*, 29(11), 3829–3834.
- Nitta, S. K. and Numata, K. (2013) *International Journal of Molecular Sciences*, 14(1), 1629–1654.
- Pahal, S., Gakhar, R., Raichur, A. M. and Varma, M. M. (2017) *IET Nanobiotechnology*, 11(8), 903–908.
- Patel, S., Singh, D., Srivastava, S., Singh, M., Shah, K., Nandini Chauhan, D. and Chauhan, N. S. (2017) *Advances in Pharmacology and Pharmacy*, 5(3), 31–43.
- Peng, Y., Li, L., Mu, X. and Guo, L. (2013) *Sensors and Actuators, B: Chemical*. Elsevier B.V., 177, 818–825.
- Picart, C., Caruso, F. and Voegel, J.-C. (2015). *Layer-by-Layer Films for Biomedical Applications*; Wiley-VCH.
- Picart, C., Lavalley, P., Hubert, P., Cuisinier, F. J. G., Decher, G., Schaaf, P. and Voegel, J. C. (2001) *Langmuir*, 17(23), 7414–7424.
- Picart, C., Mutterer, J., Richert, L., Luo, Y., Prestwich, G. D., Schaaf, P., Voegel, J. C., *et al.* (2002) *Proceedings of the National Academy of Sciences of the United States of America*, 99(20), 12531–12535.
- Quinn, J. F., Johnston, A. P. R., Such, G. K., Zelikin, A. N. and Caruso, F. (2007) *Chemical Society Reviews*, 36(5), 707–718.
- Richardson, J. J., Björnmalm, M. and Caruso, F. (2015) *Science*, 348(6233).
- Richardson, J. J., Cui, J., Björnmalm, M., Braunger, J. A., Ejima, H. and Caruso, F. (2016a) *Chemical Reviews*, 116(23), 14828–14867.
- Richardson, J. J., Cui, J., Björnmalm, M., Braunger, J. A., Ejima, H. and Caruso, F. (2016b) *Chemical Reviews*, 116(23), 14828–14867.
- Richardson, J. J., Liang, K., Kempe, K., Ejima, H., Cui, J. and Caruso, F. (2013) *Advanced Materials*, 25(47), 6874–6878.
- Richert, L., Boulmedais, F., Lavalley, P., Mutterer, J., Ferreux, E., Decher,

- G., Schaaf, P., *et al.* (2004) *Biomacromolecules*, 5(2), 284–294.
- Schmitt, J., Grünewald, T., Decher, G., Pershan, P. S., Kjaer, K. and Lösche, M. (1993) *Macromolecules*, 26(25), 7058–7063.
- Schneider, G. and Decher, G. (2008a) *Langmuir*, 24(5), 1778–1789.
- Schneider, G. and Decher, G. (2008b) *Langmuir*, 24(5), 1778–1789.
- Schwinté, P., Voegel, J. C., Picart, C., Haikel, Y., Schaaf, P. and Szalontai, B. (2001) *Journal of Physical Chemistry B*, 105(47), 11906–11916.
- Seo, J., Jochum, F., Theato, P., Lang, T., Schattling, P., Char, K. and Nilles, K. (2009) *Langmuir*, 26(3), 1830–1836.
- Seyrek, E. and Decher, G. (2012) *Polymer Science: A Comprehensive Reference, 10 Volume Set*. Elsevier B.V.
- Shahamirifard, S. A., Ghaedi, M. and Hajati, S. (2018) *Sensors and Actuators, B: Chemical*. Elsevier B.V., 259, 20–29.
- Smith, R. N., McCormick, M., Barrett, C. J., Reven, L. and Spiess, H. W. (2004) *Macromolecules*, 37(13), 4830–4838.
- Stockton, W. B. and Rubner, M. F. (1997) *Macromolecules*, 30(9), 2717–2725.
- Su, X., Kim, B., Kim, S. R., Hammond, P. T. and Irvine, D. J. (2009) *ACS Nano*, 3(11), 3719–3729.
- Sukhishvili, S. A. and Granick, S. (2002) *Macromolecules*, 35(1), 301–310.
- Sukhorukov, G. B., Antipov, A. A., Voigt, A., Donath, E. and Möhwald, H. (2001) *Macromol. Rapid Commun*, 22, 44–46.
- Sukhorukov, G. B., Volodkin, D. V., Günther, A. M., Petrov, A. I., Shenoy, D. B. and Möhwald, H. (2004) *Journal of Materials Chemistry*, 14(14), 2073–2081.
- Surfaces, A. (2016) *Monographs in Supramolecular Chemistry*.
- Swann, M. J., Peel, L. L., Carrington, S. and Freeman, N. J. (2004) *Analytical Biochemistry*, 329(2), 190–198.
- Szweda, R., Tschopp, M., Felix, O., Decher, G. and Lutz, J.-F. (2018) *Angewandte Chemie*, 130(48), 16043–16047.
- Szweda, R., Tschopp, M., Felix, O., Decher, G. and Lutz, J. F. (2018) *Angewandte Chemie - International Edition*, 57(48), 15817–15821.
- Tang, Z., Wang, Y., Podsiadlo, P. and Kotov, N. A. (2006) *Advanced Materials*, 18(24), 3203–3224.
- Tibbals, H. F. (2011) *Perspectives in Nanotechnology*. New York, NY, USA: CRC Press, Taylor & Francis Group.
- Vaca Chávez, F. and Schönhoff, M. (2007) *J. Chem. Phys.*, 126, 104705.
- Vautier, D., Lavalle, P., Voegel, J.-C., Senger, B., Ball, V. and Schaaf, P. (2011) *Advanced Materials*, 23(10), 1191–1221.
- Volodkin, D., Möhwald, H., Voegel, J. C. and Ball, V. (2007) *Journal of Controlled Release*, 117(1), 111–120.
- Vuillaume, P. Y., Glinel, K., Jonas, A. M. and Laschewsky, A. (2003) *Chemistry of Materials*, 15(19), 3625–3631.

- Wang, L., Wang, Z., Zhang, X., Shen, J., Chi, L. and Fuchs, H. (1997) *Macromolecular Rapid Communications*, 18(6), 509–514.
- Wasdo, S. C., Barber, D. S., Denslow, N. D., Powers, K. W., Palazuelos, M., Jr., S. M. S., Moudgil, B. M., *et al.* (2008) *Int. J. Nanotechnol.*, 5(1), 92–115.
- Wu, G. and Zhang, X. (2012) *Decher, G., Schlenoff, J. B. (ed.). Multilayer Thin Films: Sequential Assembly of Nanocomposite Materials, 2nd edition. Layer-by-Layer Assembly: From Conventional to Unconventional Methods. Wiley-VCH.*, 43–67.
- Xuan, Z., Tang, Y., Li, X., Liu, Y. and Luo, F. (2006) *Biochemical Engineering Journal*, 31(2), 160–164.
- Yang, R. (2018). Boca Raton: CRC Press.
- Yi, Q. and Sukhorukov, G. B. (2014) *Advances in Colloid and Interface Science*. Elsevier B.V., 207(1), 280–289.
- Yoo, P. J., Nam, K. T., Qi, J., Lee, S. K., Park, J., Belcher, A. M. and Hammond, P. T. (2006) *Nature Materials*, 5(3), 234–240.
- Yoshida, K., Hasebe, Y., Takahashi, S., Sato, K. and Anzai, J. I. (2014) *Materials Science and Engineering C*. Elsevier B.V., 34(1), 384–392.
- Zajac, G. W., Gallas, J. M., Cheng, J., Eisner, M., Moss, S. C. and Alvarado-Swaigood, A. E. (1994) *Biochim. Biophys. Acta*, 1199(3), 271–278.
- Zhang, S., Xing, M. and Li, B. (2018) *International Journal of Molecular Sciences*, 19(6).
- Zhang, T., Yan, H., Peng, M., Wang, L., Ding, H. and Fang, Z. (2013) *Nanoscale*, 5(7), 3013–3021.
- Zhang, X., Cao, X. and Qi, P. (2020) *Journal of Biomaterials Science, Polymer Edition*. Taylor & Francis, 31(4), 549–560.
- Zhang, X., Chen, H. and Zhang, H. (2007) *Chemical Communications*, (14), 1395–1405.
- Zhang, Y. and Sun, J. (2015) *ACS Nano*, 9(7), 7124–7132.



Chapter 9

WHAT PURPOSE DO THE GREAT MATHEMATICAL PROBLEMS SERVE?

Güzide ŞENEL¹

¹ Dr. Öğr. Üyesi, Amasya Üniversitesi, g.senel@amasya.edu.tr

1. Introduction

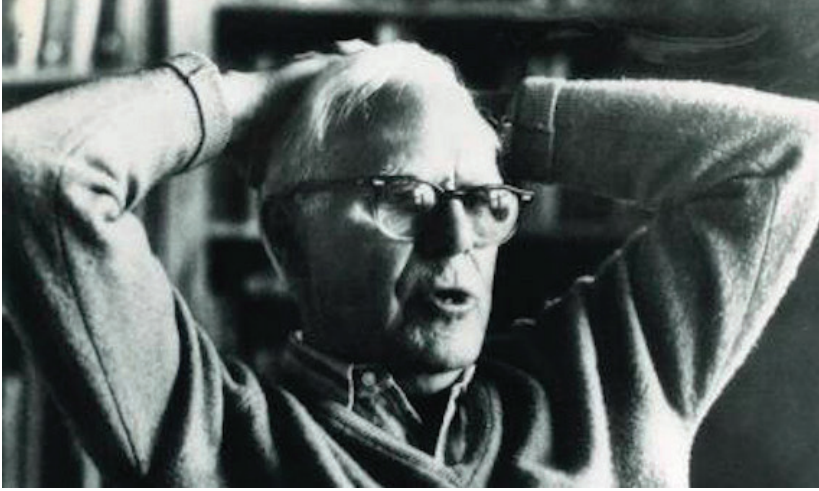
Throughout history, the eccentric mathematicians have popular appeal. For proving this allegation, the mathematicians; George Dantzig, John Nash, Grigori Perelman, Henri Poincaré can be given. Now, the historical development will be presented in consideration of the studies made before, that are given in the references. Also, I should note that this is a compilation work that's main works are given in the references.

George Dantzig, who died in 2005, regarded as the father of linear programming and known for his contributions in statistics, computer science and economic analysis. Let's have a goosey at the history of this mathematician: "In 1939, a mathematics student, George Dantzig, at the University of California, Berkeley (USA) arrived late for class. Before the end of the lesson, he wrote in his notebook the two problems that the professor had written on the blackboard, assuming that they were the assigned homework. The student took a few days to deliver the solutions, since the task was more difficult than usual. A few weeks later, on a Sunday at 8 am, the student and his wife were awakened by the sound of someone banging on the door of their house. It was the professor, in a state of great excitement; those mathematical formulations written on the blackboard were not exercises for the class, but rather two famous problems of statistics that nobody had been able to solve, until then." Russian mathematician Grigori Perelman, who solved the Poincaré Conjecture only to reject the Fields Medal and the prize of one million dollars offered by the Clay Mathematics Institute. The hypothesis proposed by Henri Poincaré in 1904 says that, "just as a rubber band around a sphere can shrink until it is reduced to a single point without detaching from the surface, the same applies to a hypersphere in four dimensions; and this, in turn, does not occur with a donut-shaped body." The Poincaré Conjecture is the only solved one of the seven Millennium Problems, each within the specified prize, a million dollar, by the Clay Institute. According to Devlin, the solutions to some of these problems could have practical implications. Devlin clarifies that this is not the case for the greatest enigmas of mathematics; the key does not lie in "knowing what the answers are," but rather in "the method of solution in which one would hope to find many benefits for humanity." "Usually, knowing the answer to whatever mathematical problem has no value other than that of curiosity," says the expert. "Mathematicians actually have very little interest in the specific answer to a question. Rather, the interest lies in how one reaches that answer." We underline that the aforementioned results in solutions of math tricks all rely on blowing your mind.

2. Mathematical Games

A mathematical game is a game whose rules, strategies and out-

comes are defined by clear mathematical parameters. Generally, mathematical games need not be conceptually sophisticated to involve deeper computational background materials. One of the most popular mathematician and science writer, with interests in mathematical games was Martin Gardner (October 21, 1914 – May 22, 2010).



Martin Gardner

Gardner was best known for creating and sustaining interest in recreational mathematics—and by extension, mathematics in general—throughout the latter half of the 20th century, principally through his “Mathematical Games” columns. Over a period of 24 years (January 1957 – December 1980), Martin Gardner wrote 288 successive monthly “Mathematical Games” columns for *Scientific American* magazine. During the next 7½ years, through June 1986, Gardner wrote 9 more columns, bringing his total to 297, as other authors wrote most of the “Mathematical Games” columns. Gardner, as recounted in his book *Mathematics for fun* (1988), hoped that readers could “resist the temptation to look up the answer before they sincerely tried to solve the problem.” And whether they found the right answer or not, he wished that “they were happy for having been confused.” In the view of Gardner’s assessments, some mathematical tricks will be obtained in the following section.

3. Mathematical Tricks

In this section, 10 Math tricks are presented that will blow your mind. These simple math tricks can help you perform calculations more quickly and easily. They also come in handy if you want to impress your teacher, parents, or friends. Also, the solutions generalize by exploiting some general facts seemingly overlooked by the aforementioned authors.

1. Multiplying by 6

If you multiply 6 by an even number, the answer will end with the same digit. The number in the ten's place will be half of the number in the one's place.

Example: $6 \times 4 = 24$.

2. The Answer Is 2

1. Think of a number.
2. Multiply it by 3.
3. Add 6.
4. Divide this number by 3.
5. Subtract the number from Step 1 from the answer in Step 4.

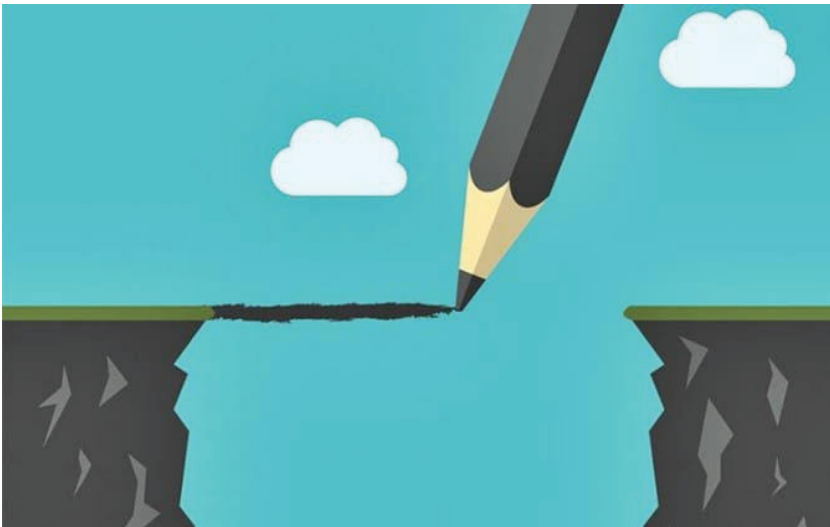
The answer is 2.

3. Same Three-Digit Number

1. Think of any three-digit number in which each of the digits is the same. Examples include 333, 666, 777, and 999.

2. Add up the digits.
3. Divide the three-digit number by the answer in Step 2.

The answer is 37.



4. Six Digits Become Three

1. Take any three-digit number and write it twice to make a six-digit number. Examples include 371371 or 552552.

2. Divide the number by 7.

3. Divide it by 11.

4. Divide it by 13.

The order in which you do the division is unimportant!

The answer is the three-digit number.

Examples: 371371 gives you 371 or 552552 gives you 552.

1. A related trick is to take any three-digit number.

2. Multiply it by 7, 11, and 13.

The result will be a six-digit number that repeats the three-digit number.

Example: 456 becomes 456456.

5. The 11 Rule

This is a quick way to multiply two-digit numbers by 11 in your head.

1. Separate the two digits in your mind.

2. Add the two digits together.

3. Place the number from Step 2 between the two digits. If the number from Step 2 is greater than 9, put the one's digit in the space and carry the ten's digit.

Examples: $72 \times 11 = 792$.

$57 \times 11 = 5 _ 7$, but $5 + 7 = 12$, so put 2 in the space and add the 1 to the 5 to get 627.

6. Memorizing Pi

To remember the first seven digits of pi, count the number of letters in each word of the sentence:

"How I wish I could calculate pi."

This becomes 3.141592.

7. Contains the Digits 1, 2, 4, 5, 7, 8

1. Select a number from 1 to 6.

2. Multiply the number by 9.

3. Multiply it by 111.
4. Multiply it by 1001.
5. Divide the answer by 7.

The number will contain the digits 1, 2, 4, 5, 7, and 8.

Example: The number 6 yields the answer 714285.

8. Multiply Large Numbers in Your Head

To easily multiply two double-digit numbers, use their distance from 100 to simplify the math:

1. Subtract each number from 100.
2. Add these values together.
3. 100 minus this number is the first part of the answer.
4. Multiply the digits from Step 1 to get the second part of the answer.

9. Super Simple Divisibility Rules

You've got 210 pieces of pizza and want to know whether or not you can split them evenly within your group. Rather than whip out the calculator, use these simple shortcuts to do the math in your head:

- Divisible by 2 if the last digit is a multiple of 2 (210).
- Divisible by 3 if the sum of the digits is divisible by 3 (522 because the digits add up to 9, which is divisible by 3).
- Divisible by 4 if the last two digits are divisible by 4 (2540 because 40 is divisible by 4).
- Divisible by 5 if the last digit is 0 or 5 (9905).
- Divisible by 6 if it passes the rules for both 2 and 3 (408).
- Divisible by 9 if the sum of the digits is divisible by 9 (6390 since $6 + 3 + 9 + 0 = 18$, which is divisible by 9).
- Divisible by 10 if the number ends in a 0 (8910).
- Divisible by 12 if the rules for divisibility by 3 and 4 apply.

Example: The 210 slices of pizza may be evenly distributed into groups of 2, 3, 6, 10.

10. Finger Multiplication Tables

Everyone knows you can count on your fingers. Did you realize you can use them for multiplication? A simple way to do the "9" multiplication

table is to place both hands in front of you with fingers and thumbs extended. To multiply 9 by a number, fold down that number finger, counting from the left.

Examples: To multiply 9 by 5, fold down the fifth finger from the left. Count fingers on either side of the "fold" to get the answer. In this case, the answer is 45.

To multiply 9 times 6, fold down the sixth finger, giving an answer of 54.

4. Declarations

Acknowledgements: The author gratefully acknowledge the comments of the editorial board which led to the improvement of this paper.

Funding: There is no source of funding for the research.

Availability of data and materials: The datasets used or analyzed during the current study are available from the corresponding author on reasonable request.

References

- Helmenstine, Anne Marie, Ph.D. "10 Math Tricks That Will Blow Your Mind." ThoughtCo, Apr. 5, 2020, [thoughtco.com/math-tricks-that-will-blow-your-mind-4154742](https://www.thoughtco.com/math-tricks-that-will-blow-your-mind-4154742).
<https://www.bbvaopenmind.com/en/science/leading-figures/martin-gardner-and-math-fun/>
- Gardner, Martin (Jan 1999). "The Asymmetric Propeller" (PDF). *The College Mathematics Journal*. 30 (1): 18-22. doi:10.2307/2687198. Archived (PDF) from the original on 2014-03-04.
<https://www.bbvaopenmind.com/en/temas/what-purpose-do-the-great-mathematical-problems-serve/>
- AMS Notices (2011): "Martin Gardner was a gem. There is absolutely no question that he, more than anyone else in the world, was responsible for turning people of all ages on to the pleasures of mathematical recreations." —Ronald L. Graham.
- Burstein, Mark, ed. (2011). *A Bouquet for the Gardner: Martin Gardner Remembered*. New York: The Lewis Carroll Society of North America. ISBN 978-0-930326-17-3.
https://en.wikipedia.org/wiki/Martin_Gardner
https://en.wikipedia.org/wiki/List_of_Martin_Gardner_Mathematical_Games_columns
https://en.wikipedia.org/wiki/Mathematical_game